# Updates on Run12 $\pi^0$ – jet $A_{LL}$

Yaping Wang (CCNU)
Zhenyu Ye (UIC)

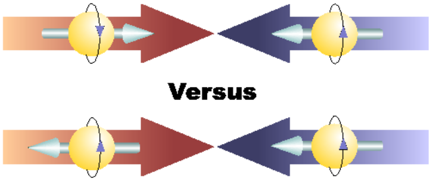

# Outline

- Asymmetry Analysis
- Asymmetry Results
- Summary and Outlook

# Asymmetry Analysis -- Dataset and Triggers

- **Dataset: 2012 pp longitudinal at √s=510 GeV**
  - Reconstructed EEMC trees location (~2.6 T): /star/u/ypwang/disk05/Run12Pi0s_EEMC
  - Reconstructed jet trees location: /star/data05/scratch/zchang/Run12Jets_new
    /star/data05/scratch/zchang/Run12Jets_new_new
  - Use Zilong's final run list (359 runs)

- **Use events in which jet triggers are fired in BEMC with a matched jet:**
  - Hardware, software and geometric trigger conditions applied
  - Triggers (threshold: JP0 5.4 GeV/c, JP1 7.3 GeV/c, JP2 14.4 GeV/c):

★If(JP2 hardware & JP2 software & geometric match JP2 & pT>14.4) JP2 triggered

★If(JP1 hardware & JP1 software & geometric match JP1 & pT>7.3) JP1 triggered

★If(JP0 hardware & JP0 software & geometric match JP0 & pT>5.4) JP0 triggered

# Asymmetry Analysis – Analysis cuts

- $\pi^0$ $p_T$: > 2.0 GeV/c
- $\pi^0$ mass: (0, 0.6)
- $\pi^0$ physics eta: (1.086, 2.0)
- Decayed photon eta: (1.11, 1.96)
- Decayed photon 1 energy: > 2.0 GeV
- Decayed photon 2 energy: > 1.5 GeV
- Preshower energy for each photon: < 40 MeV
- SMD relative energy threshold for each photon $(E_{cluster1/2u}+E_{cluster1/2v})/E_{tower1/2}$: > 0.008

- Jet $p_T$ > 5.0 GeV/c
- Jet physics eta: (-0.9, 0.9)
- Jet detector eta: (-0.7, 0.9)
- $R_t$ < 0.95
- Using Anti-$k_T$ algorithm with cone size R = 0.6
- Sum track $p_T$ > 0.5 GeV/c

✧ $\Delta\phi$ > 2.0 (azimuthal angle between a forward $\pi^0$ opposite a barrel jet)

✧ Signal $\pi^0$ mass region: (0.1, 0.2) GeV/c$^2$

**w/ all analysis cuts applied**

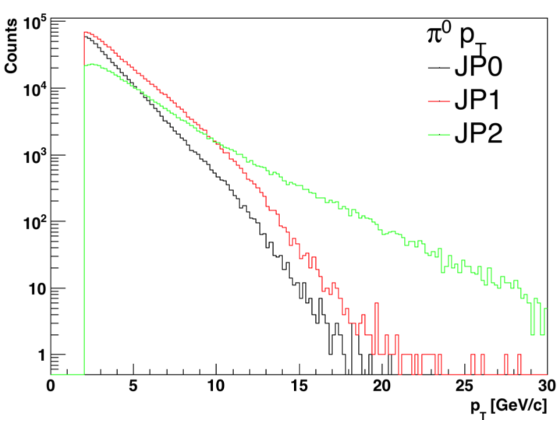


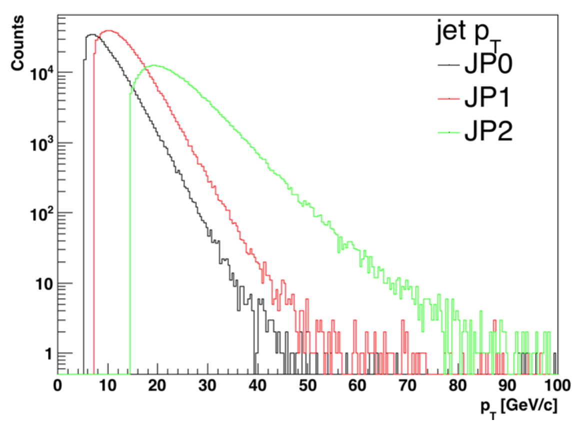


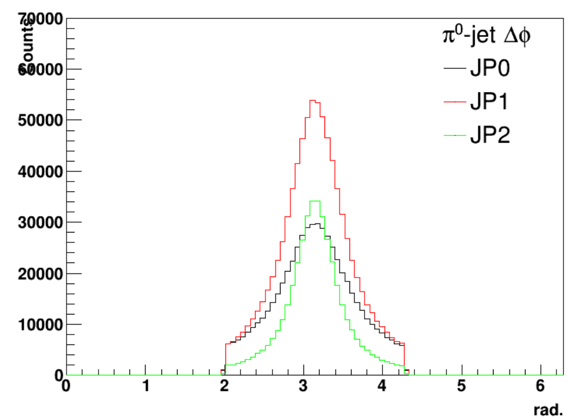

# Asymmetry Analysis -- Analysis cuts

**w/ all analysis cuts applied**

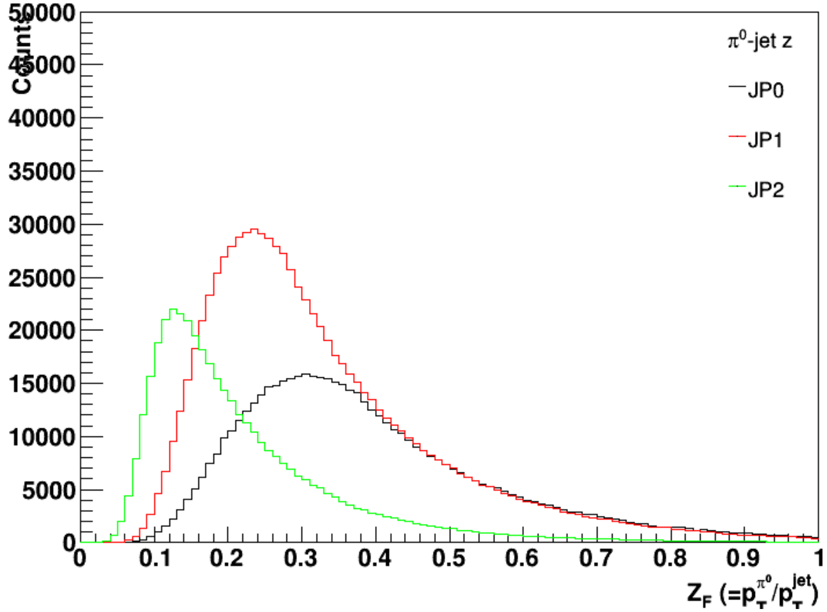


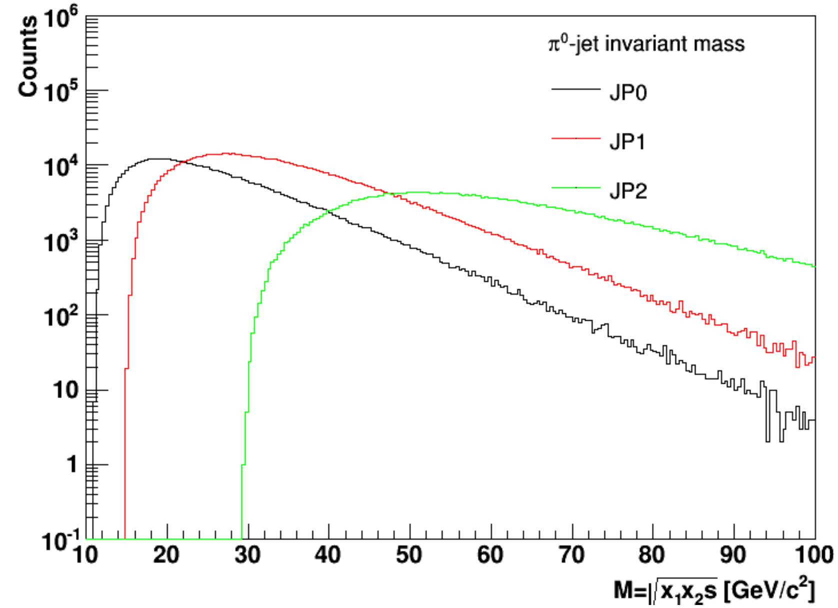


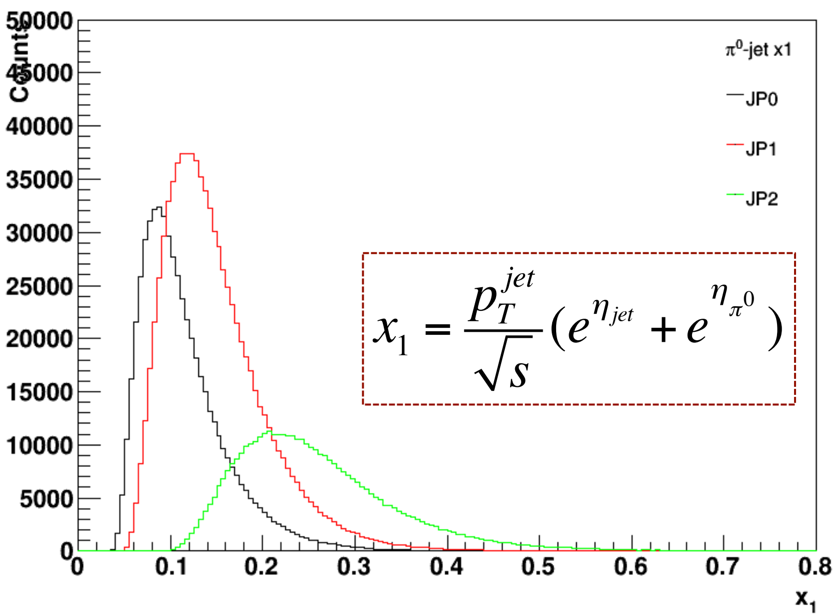


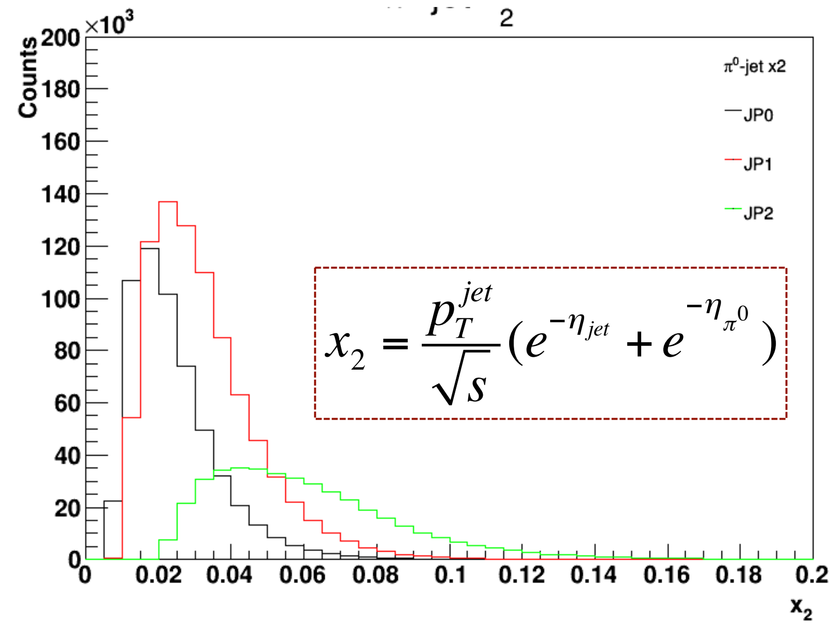

# Asymmetry Analysis -- Variable binning

```
const Int_t nPi0PTbins = 11;
const Double_t mPi0PTbins[nPi0PTbins + 1] = { 2.0, 3.0, 4.0, 5.0, 6.0, 7.0, 8.0, 9.0, 10.0, 12.0, 16.0, 25.0};

const Int_t nJetPTbins = 15; // jet pT bin 18% resolutions
const Double_t mJetPTbins[nJetPTbins + 1] = {5.0, 6.0, 7.1, 8.4, 10.0, 11.8, 13.9, 16.4, 19.4, 22.9, 27.0,
31.9, 37.6, 44.4, 52.3, 61.8};

const Int_t nPi0JetMassbins = 11;
const Double_t mPi0JetMassbins[nPi0JetMassbins+1] = {10.0, 14.0, 20.0, 24.0, 29.0, 35.0, 42.0, 50.0,
60.0, 72.0, 86.0, 100.0};

const Int_t nZFbins = 6; // zF 150% resolution
const Double_t mZFbins[nZFbins+1] = { 0.06, 0.135, 0.20, 0.30, 0.45, 0.675, 1.0};

const Int_t nXbins = 6; // x1/x2 150% resolution
const Double_t mX1bins[nXbins+1] = { 0.025, 0.070, 0.100, 0.150, 0.230, 0.35, 0.8};
const Double_t mX2bins[nXbins+1] = { 0.005, 0.015, 0.023, 0.035, 0.053, 0.08, 0.2};
```

# Asymmetry Analysis -- Statistics of $\pi^0$-jet for JP0

w/ all analysis cuts applied

**$p_T^{\pi 0}$ bin:**

| Bin | spin5 | spin6 | spin9 | spin10 |
|---|---|---|---|---|
| 0 | 63313 | 63270 | 64152 | 63660 |
| 1 | 35133 | 35220 | 35991 | 35221 |
| 2 | 19050 | 19400 | 19783 | 19491 |
| 3 | 10475 | 10531 | 10606 | 10600 |
| 4 | 5551 | 5571 | 5648 | 5473 |
| 5 | 2952 | 2999 | 2964 | 2901 |
| 6 | 1601 | 1592 | 1628 | 1513 |
| 7 | 900 | 886 | 862 | 884 |
| 8 | 768 | 671 | 731 | 697 |
| 9 | 188 | 183 | 181 | 188 |
| 10 | 12 | 9 | 6 | 7 |

**$z_F$ bin:**

| Bin | spin5 | spin6 | spin9 | spin10 |
|---|---|---|---|---|
| 0 | 1789 | 1752 | 1765 | 1809 |
| 1 | 10537 | 10643 | 10679 | 10711 |
| 2 | 34137 | 34385 | 34537 | 34105 |
| 3 | 49587 | 49743 | 50906 | 50110 |
| 4 | 30303 | 30309 | 30945 | 30296 |
| 5 | 11058 | 11026 | 11175 | 11117 |

**$p_T^{jet}$ bin:**

| Bin | spin5 | spin6 | spin9 | spin10 |
|---|---|---|---|---|
| 0 | 11843 | 11715 | 12097 | 12196 |
| 1 | 23693 | 23618 | 24178 | 23868 |
| 2 | 26775 | 26699 | 27142 | 26619 |
| 3 | 25906 | 26187 | 26680 | 26060 |
| 4 | 20149 | 20151 | 20323 | 20199 |
| 5 | 14368 | 14568 | 14626 | 14302 |
| 6 | 9009 | 9160 | 9303 | 9184 |
| 7 | 4938 | 4979 | 4878 | 4821 |
| 8 | 2144 | 2183 | 2221 | 2204 |
| 9 | 825 | 760 | 775 | 858 |
| 10 | 222 | 239 | 245 | 236 |
| 11 | 52 | 52 | 55 | 63 |
| 12 | 9 | 12 | 22 | 17 |
| 13 | 2 | 4 | 4 | 5 |
| 14 | 1 | 2 | 0 | 1 |

**$x_1$ bin:**

| Bin | spin5 | spin6 | spin9 | spin10 |
|---|---|---|---|---|
| 0 | 20167 | 20129 | 20575 | 20275 |
| 1 | 46402 | 46163 | 46972 | 46616 |
| 2 | 47959 | 48471 | 49248 | 48363 |
| 3 | 21443 | 21673 | 21769 | 21426 |
| 4 | 3739 | 3641 | 3735 | 3707 |
| 5 | 228 | 253 | 251 | 247 |

**$M_{\pi 0\text{-jet}}$ bin:**

| Bin | spin5 | spin6 | spin9 | spin10 |
|---|---|---|---|---|
| 0 | 5152 | 5110 | 5254 | 5331 |
| 1 | 39867 | 39545 | 40499 | 39981 |
| 2 | 27448 | 27425 | 28108 | 27436 |
| 3 | 25331 | 25662 | 26048 | 25566 |
| 4 | 19195 | 19347 | 19543 | 19226 |
| 5 | 12000 | 12238 | 12045 | 11960 |
| 6 | 6244 | 6387 | 6316 | 6404 |
| 7 | 3128 | 3086 | 3113 | 3095 |
| 8 | 1140 | 1080 | 1166 | 1155 |
| 9 | 340 | 321 | 353 | 366 |
| 10 | 72 | 97 | 67 | 79 |

**$x_2$ bin:**

| Bin | spin5 | spin6 | spin9 | spin10 |
|---|---|---|---|---|
| 0 | 32135 | 31911 | 32765 | 32140 |
| 1 | 45262 | 45272 | 46404 | 45806 |
| 2 | 40051 | 40407 | 40706 | 40085 |
| 3 | 17756 | 18119 | 18008 | 17865 |
| 4 | 4281 | 4161 | 4180 | 4231 |
| 5 | 453 | 460 | 487 | 505 |

**Total (5/6/9/10):**

139943 140332 142552 140635

# Asymmetry Analysis -- Statistics of $\pi^0$-jet for JP1

w/ all analysis cuts applied

**$p_T^{\pi 0}$ bin:**

| Bin | spin5 | spin6 | spin9 | spin10 |
|---|---|---|---|---|
| 0 | 78081 | 79156 | 80311 | 79306 |
| 1 | 51283 | 51716 | 52329 | 51920 |
| 2 | 30912 | 31501 | 31631 | 31628 |
| 3 | 19455 | 19361 | 19549 | 19294 |
| 4 | 11981 | 12033 | 12226 | 12041 |
| 5 | 7338 | 7453 | 7530 | 7363 |
| 6 | 4316 | 4435 | 4281 | 4327 |
| 7 | 2442 | 2540 | 2547 | 2626 |
| 8 | 2235 | 2172 | 2134 | 2235 |
| 9 | 667 | 649 | 677 | 716 |
| 10 | 26 | 38 | 45 | 33 |

**$z_F$ bin:**

| Bin | spin5 | spin6 | spin9 | spin10 |
|---|---|---|---|---|
| 0 | 7695 | 7821 | 7973 | 7888 |
| 1 | 33627 | 33994 | 34816 | 34300 |
| 2 | 68814 | 69323 | 70253 | 69639 |
| 3 | 57402 | 58349 | 58625 | 58123 |
| 4 | 29851 | 30125 | 30098 | 29873 |
| 5 | 9713 | 9766 | 9841 | 9923 |

**$p_T^{jet}$ bin:**

| Bin | spin5 | spin6 | spin9 | spin10 |
|---|---|---|---|---|
| 0 | 0 | 0 | 0 | 0 |
| 1 | 0 | 0 | 0 | 0 |
| 2 | 19996 | 20251 | 20082 | 20043 |
| 3 | 37507 | 38252 | 38192 | 38357 |
| 4 | 43207 | 43437 | 44214 | 43386 |
| 5 | 40710 | 41250 | 41816 | 41361 |
| 6 | 31887 | 32294 | 32864 | 32506 |
| 7 | 20128 | 20194 | 20474 | 20270 |
| 8 | 9826 | 9832 | 9960 | 9973 |
| 9 | 3790 | 3893 | 3957 | 3869 |
| 10 | 1209 | 1259 | 1277 | 1287 |
| 11 | 348 | 294 | 320 | 330 |
| 12 | 76 | 55 | 74 | 73 |
| 13 | 26 | 23 | 19 | 15 |
| 14 | 8 | 6 | 4 | 8 |

**$x_1$ bin:**

| Bin | spin5 | spin6 | spin9 | spin10 |
|---|---|---|---|---|
| 0 | 3620 | 3777 | 3752 | 3748 |
| 1 | 34490 | 35021 | 34931 | 34888 |
| 2 | 86966 | 88085 | 88732 | 88005 |
| 3 | 66523 | 66963 | 68211 | 67407 |
| 4 | 15806 | 15930 | 16283 | 16106 |
| 5 | 1316 | 1268 | 1347 | 1326 |

**$M_{\pi 0\text{-jet}}$ bin:**

| Bin | spin5 | spin6 | spin9 | spin10 |
|---|---|---|---|---|
| 0 | 0 | 0 | 0 | 0 |
| 1 | 10820 | 11115 | 11187 | 11099 |
| 2 | 26944 | 27210 | 27353 | 27230 |
| 3 | 42949 | 43635 | 43927 | 43703 |
| 4 | 46425 | 46829 | 47033 | 46670 |
| 5 | 36975 | 37593 | 38410 | 37976 |
| 6 | 23798 | 23920 | 24162 | 23959 |
| 7 | 13039 | 13091 | 13265 | 12999 |
| 8 | 5427 | 5360 | 5505 | 5423 |
| 9 | 1697 | 1707 | 1791 | 1806 |
| 10 | 459 | 429 | 450 | 441 |

**$x_2$ bin:**

| Bin | spin5 | spin6 | spin9 | spin10 |
|---|---|---|---|---|
| 0 | 13466 | 13653 | 13843 | 13574 |
| 1 | 50279 | 51010 | 51566 | 51427 |
| 2 | 72384 | 72972 | 73531 | 73057 |
| 3 | 52814 | 53512 | 54240 | 53576 |
| 4 | 17424 | 17585 | 17677 | 17442 |
| 5 | 2357 | 2314 | 2401 | 2408 |

**Total (5/6/9/10):**
206536 211054 213260 211489

# Asymmetry Analysis -- Statistics of $\pi^0$-jet for JP2

w/ all analysis cuts applied

**$p_T^{\pi 0}$ bin:**

| Bin | spin5 | spin6 | spin9 | spin10 |
|---|---|---|---|---|
| 0 | 27425 | 27861 | 27706 | 27527 |
| 1 | 22693 | 22565 | 22898 | 22617 |
| 2 | 15985 | 15976 | 15862 | 15759 |
| 3 | 10848 | 10925 | 10919 | 10784 |
| 4 | 7277 | 7265 | 7325 | 7336 |
| 5 | 4918 | 4963 | 4961 | 4892 |
| 6 | 3482 | 3460 | 3456 | 3390 |
| 7 | 2408 | 2340 | 2305 | 2327 |
| 8 | 2903 | 2831 | 2960 | 2864 |
| 9 | 2427 | 2373 | 2420 | 2296 |
| 10 | 1047 | 1030 | 1018 | 1030 |

**$z_F$ bin:**

| Bin | spin5 | spin6 | spin9 | spin10 |
|---|---|---|---|---|
| 0 | 28082 | 28425 | 28059 | 27944 |
| 1 | 28825 | 28931 | 29136 | 28903 |
| 2 | 23572 | 23443 | 23490 | 23329 |
| 3 | 13297 | 13363 | 13508 | 13274 |
| 4 | 5398 | 5217 | 5305 | 5124 |
| 5 | 1435 | 1430 | 1461 | 1415 |

**$p_T^{jet}$ bin:**

| Bin | spin5 | spin6 | spin9 | spin10 |
|---|---|---|---|---|
| 0 | 0 | 0 | 0 | 0 |
| 1 | 0 | 0 | 0 | 0 |
| 2 | 0 | 0 | 0 | 0 |
| 3 | 0 | 0 | 0 | 0 |
| 4 | 0 | 0 | 0 | 0 |
| 5 | 0 | 0 | 0 | 0 |
| 6 | 8777 | 9013 | 9185 | 8924 |
| 7 | 22016 | 22036 | 22308 | 21847 |
| 8 | 25776 | 25852 | 25738 | 25512 |
| 9 | 21302 | 21030 | 20792 | 20991 |
| 10 | 13357 | 13369 | 13397 | 13326 |
| 11 | 6420 | 6508 | 6537 | 6489 |
| 12 | 2594 | 2654 | 2693 | 2572 |
| 13 | 860 | 830 | 893 | 887 |
| 14 | 273 | 273 | 274 | 255 |

**$x_1$ bin:**

| Bin | spin5 | spin6 | spin9 | spin10 |
|---|---|---|---|---|
| 0 | 0 | 0 | 0 | 0 |
| 1 | 1 | 0 | 0 | 0 |
| 2 | 5528 | 5486 | 5692 | 5590 |
| 3 | 38191 | 38531 | 38792 | 38092 |
| 4 | 44133 | 43975 | 43639 | 43641 |
| 5 | 13574 | 13646 | 13747 | 13533 |

**$M_{\pi 0\text{-jet}}$ bin:**

| Bin | spin5 | spin6 | spin9 | spin10 |
|---|---|---|---|---|
| 0 | 0 | 0 | 0 | 0 |
| 1 | 0 | 0 | 0 | 0 |
| 2 | 0 | 0 | 0 | 0 |
| 3 | 0 | 0 | 0 | 0 |
| 4 | 1203 | 1282 | 1250 | 1279 |
| 5 | 8523 | 8655 | 8864 | 8537 |
| 6 | 19252 | 19345 | 19123 | 18923 |
| 7 | 25859 | 25765 | 25817 | 25710 |
| 8 | 22341 | 22159 | 22195 | 22005 |
| 9 | 13670 | 13535 | 13765 | 13687 |
| 10 | 6096 | 6268 | 6075 | 6174 |

**$x_2$ bin:**

| Bin | spin5 | spin6 | spin9 | spin10 |
|---|---|---|---|---|
| 0 | 0 | 0 | 0 | 0 |
| 1 | 772 | 824 | 781 | 772 |
| 2 | 14042 | 14375 | 14239 | 14015 |
| 3 | 31486 | 31054 | 30896 | 30726 |
| 4 | 35186 | 35109 | 35506 | 35045 |
| 5 | 19886 | 20185 | 20381 | 20214 |

**Total (5/6/9/10):**

101413 101589 101830 100822

# Asymmetry Analysis – Asymmetry definitions

## Spin pattern @ Run 12:

| Spin4 | Yellow | Blue |
|---|---|---|
| 5 | - | - |
| 6 | + | - |
| 9 | - | + |
| 10 | + | + |

## Longitudinal double spin asymmetries:

$$A_{LL} = \frac{\sum P_Y P_B[(N^{++}+N^{--})-R_3(N^{+-}+N^{-+})]}{\sum P_Y^2 P_B^2[(N^{++}+N^{--})+R_3(N^{+-}+N^{-+})]}$$

$$\delta A_{LL} = \frac{\sqrt{\sum P_Y^2 P_B^2[\delta(N^{++}+N^{--})^2+R_3^2\delta(N^{+-}+N^{-+})^2]}}{\sum P_Y^2 P_B^2[(N^{++}+N^{--})+R_3(N^{+-}+N^{-+})]}$$

## Longitudinal single-spin asymmetries:

$$A_L^Y = \frac{\sum P_Y[(N^{++}+N^{+-})-R_1(N^{--}+N^{-+})]}{\sum P_Y^2[(N^{++}+N^{+-})+R_1(N^{--}+N^{-+})]}$$

$$A_L^B = \frac{\sum P_B[(N^{++}+N^{-+})-R_2(N^{--}+N^{+-})]}{\sum P_B^2[(N^{++}+N^{-+})+R_2(N^{--}+N^{+-})]}$$

## Like-sign/Unlike-sign asymmetry:

$$A_{LL}^{ls} = \frac{\sum P_Y P_B(N^{++}-R_4 N^{--})}{\sum P_Y^2 P_B^2(N^{++}+R_4 N^{--})}$$

$$A_{LL}^{us} = \frac{\sum P_Y P_B(R_6 N^{+-}-R_5 N^{-+})}{\sum P_Y^2 P_B^2(R_6 N^{+-}+R_5 N^{-+})}$$

* Indices on the N's are for yellow beam first and for blue beam second.

# Asymmetry Analysis – Background asymmetry corrections

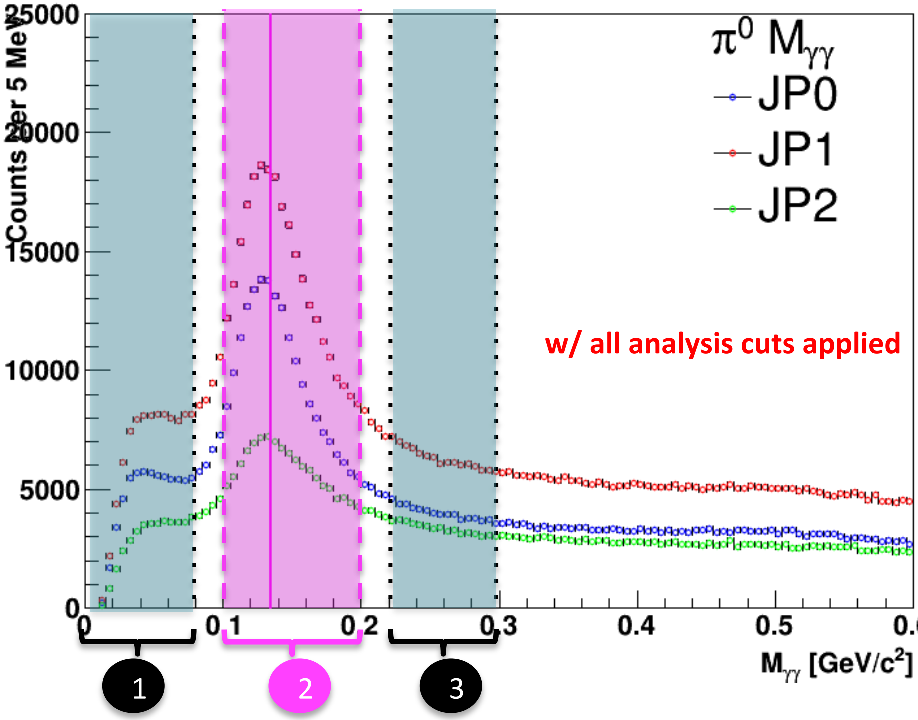


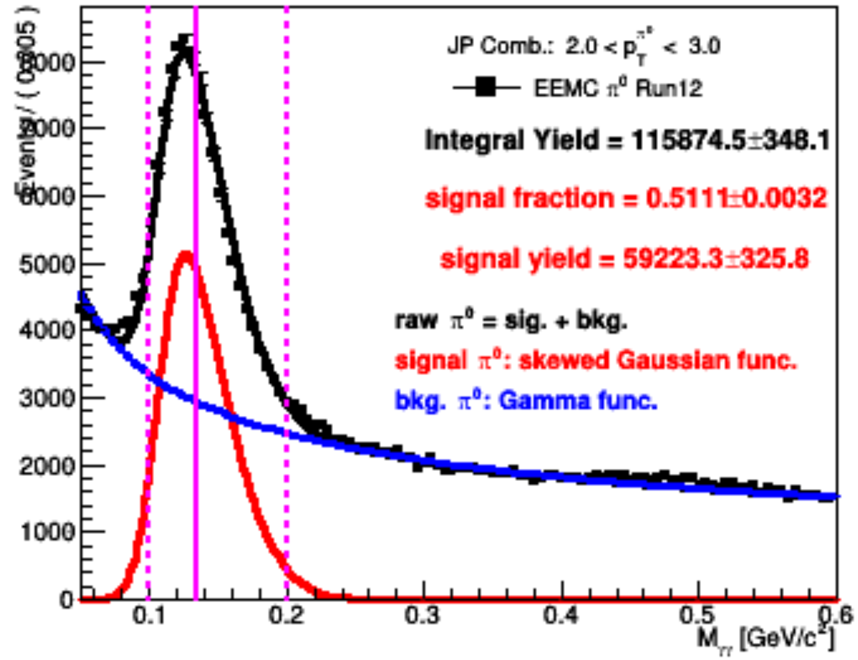


❶ Low mass region: $0 < M_{\gamma\gamma} < 0.08$

❷ Mass-peak region: $0.1 < M_{\gamma\gamma} < 0.2$

❸ High mass region: $0.22 < M_{\gamma\gamma} < 0.3$

$$A_{LL}^{S} = \frac{1}{s}\left(A_{LL}^{S+B} - (1-s)A_{LL}^{B}\right)$$

$$\delta^2 A_{LL}^{S} = \frac{\delta^2 A_{LL}^{S+B}}{s^2} + \frac{(1-s)^2}{s^2}\delta^2 A_{LL}^{B} + \left(\frac{A_{LL}^{S+B} - A_{LL}^{B}}{s^2}\right)^2 \delta^2 s$$

- The asymmetry measured in the mass-peak region, $A_{LL}^{S+B}$, mixes both the signal asymmetry, $A_{LL}^{S}$, and the asymmetry in the background components, $A_{LL}^{B}$.
- To estimate the signal fraction, ***s***, in mass-peak region, fit range was set to [0.05, 0.6] GeV/c$^2$.
- Asymmetries measured in the sideband regions (LMR and HMR) on either side of the mass peak region, are averaged to estimate the background asymmetry in the peak region.

# Asymmetry Analysis – Background asymmetry estimations

Mass dependence in the background asymmetry is studied, and no indication of the mass dependence within uncertainties is seen.

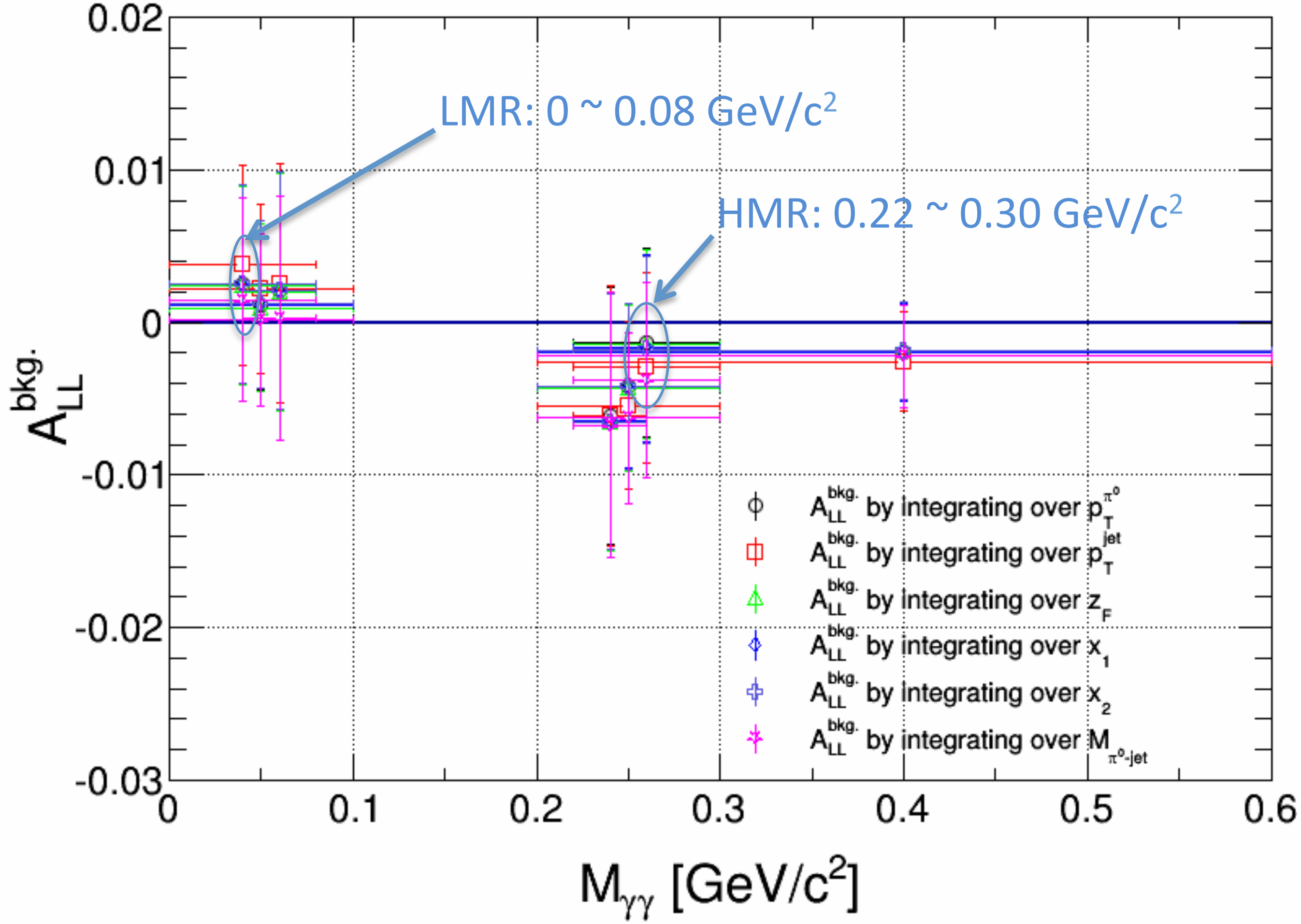


The average of the two sideband background asymmetries is used for the estimate of the background asymmetry in the peak region.

# Asymmetry Analysis – Background asymmetry estimations

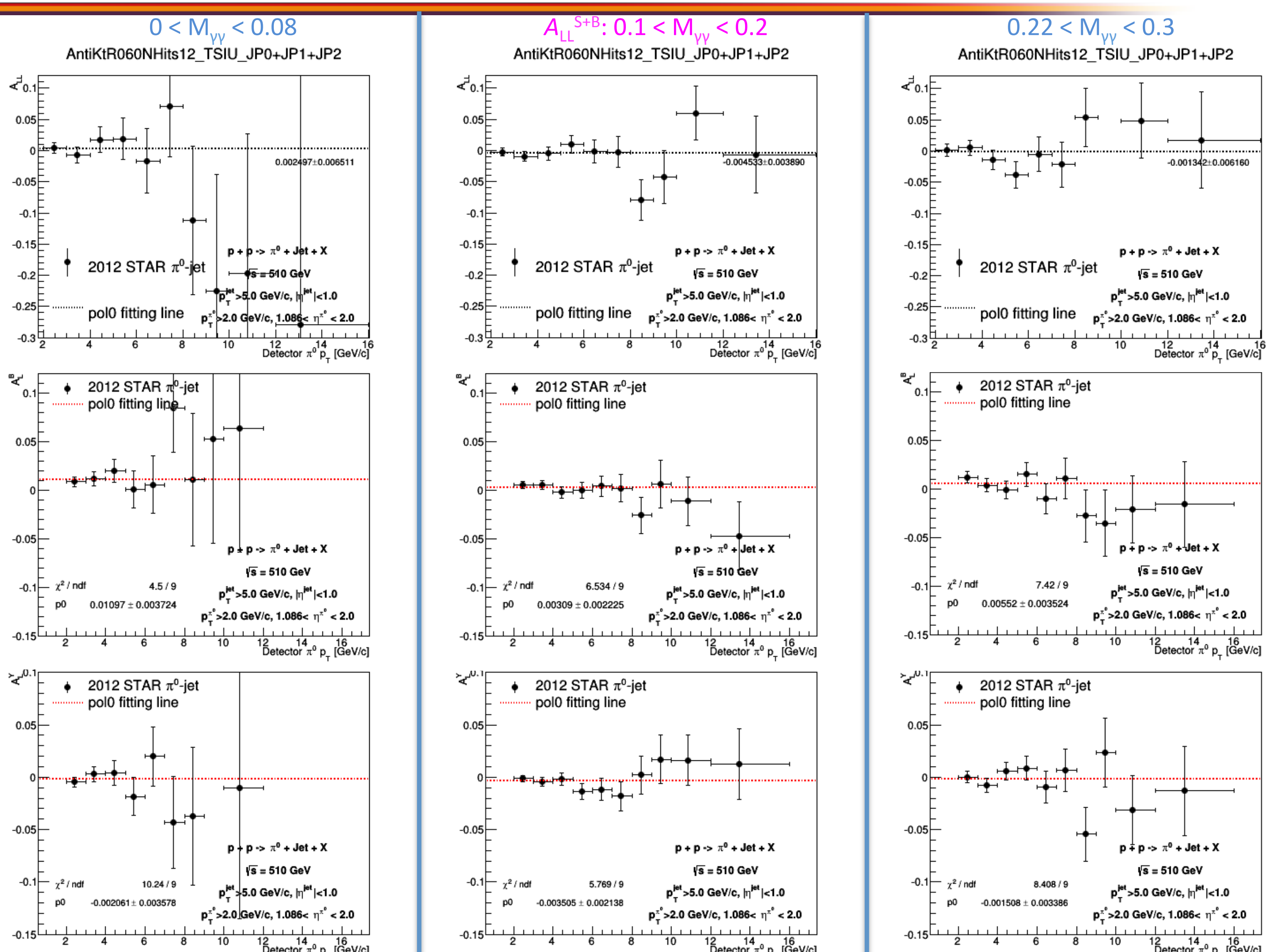


Due to limited statistics, the raw longitudinal asymmetry is computed integrating over $\pi^0$ $p_T$, jet $p_T$, $z_F$, $x_1$, $x_2$ and –jet invariant mass bins, respectively.

# Asymmetry Analysis – Background asymmetry estimations

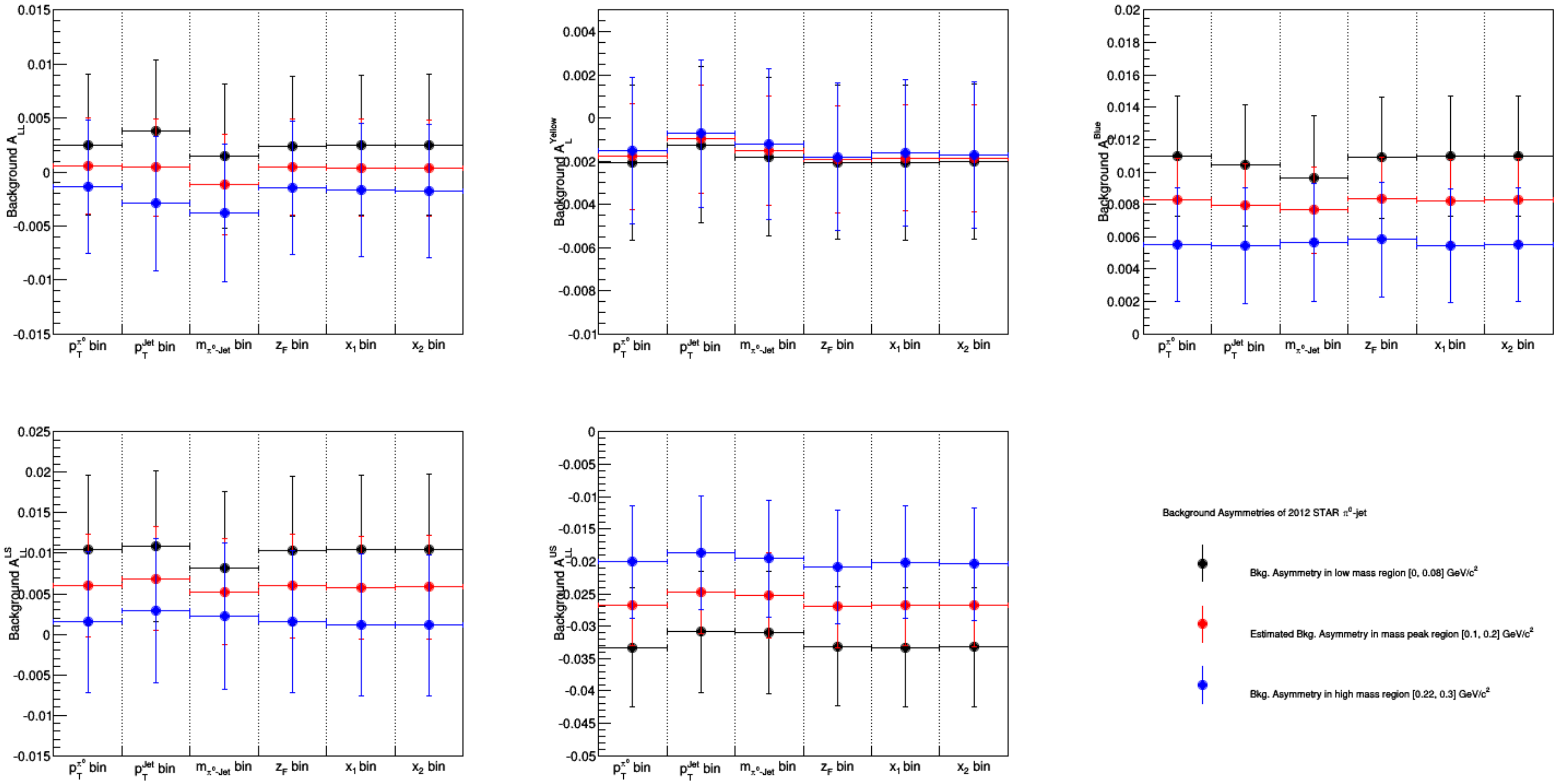


Background asymmetry, $A_{LL}^{B}$, estimate for each asymmetry type and variable bins:

| Bkg. Asym. | $p_T^{\pi 0}$ | $p_T^{jet}$ | $z_F$ | $x_1$ | $x_2$ | $M_{\pi 0\text{-jet}}$ |
|---|---|---|---|---|---|---|
| $A_{LL}$ | 0.000578±0.004481 | 0.000416±0.004530 | -0.001151±0.004619 | 0.000454±0.004488 | 0.000398±0.004479 | 0.000362±0.004479 |
| $A_L^Y$ | -0.001784±0.002463 | -0.000979±0.002490 | -0.001511±0.002538 | -0.001919±0.002467 | -0.001845±0.002462 | -0.001865±0.002462 |
| $A_L^B$ | 0.008246±0.002564 | 0.007940±0.002592 | 0.007642±0.002642 | 0.008357±0.002567 | 0.008216±0.002562 | 0.008249±0.002562 |
| $A_{LL}^{LS}$ | 0.005963±0.006355 | 0.006860±0.006424 | 0.005214±0.006551 | 0.005952±0.006364 | 0.005786±0.006351 | 0.005813±0.006351 |
| $A_{LL}^{US}$ | -0.026695±0.006338 | -0.024803±0.006407 | -0.025260±0.006530 | -0.027011±0.006347 | -0.026748±0.006334 | -0.026844±0.006335 |

# Asymmetry Analysis -- Estimate signal fraction within peak region

To check polarization status dependence of signal fraction ***s***, mass spectrum with different spin pattern combinations are compared by the fitted parameters*, including signal fraction, $\chi^2$/NDF, mass peak position and width.

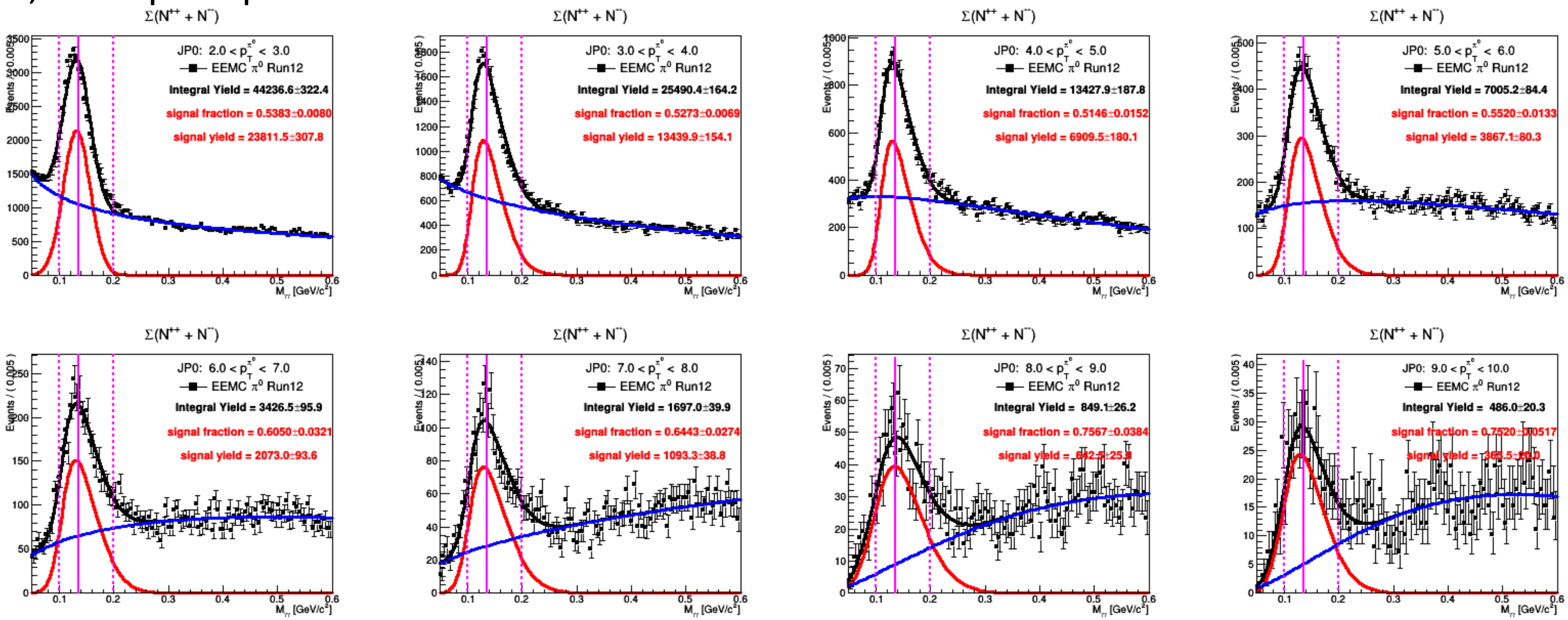


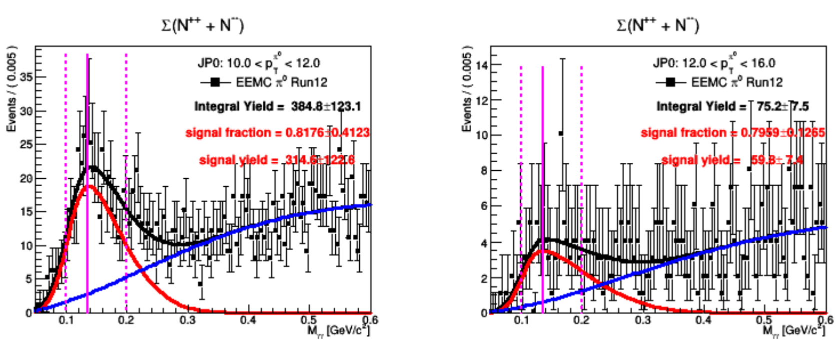


**Signal:** $k \times e^{\frac{-(x-\mu)^2}{2\sigma^2}} \times [1 + \mathrm{Erf}(\frac{a(x-\mu)}{\sqrt{2}\sigma})]$

**Background:** $A \times x^B \times e^{Cx}$

$$A_{LL} = \frac{\sum P_Y P_B \boxed{(N^{++} + N^{--})} - R_3(N^{+-} + N^{-+})]}{\sum P_Y^2 P_B^2 \boxed{(N^{++} + N^{--})} - R_3(N^{+-} + N^{-+})]}$$

**Raw Yield = Signal + Background**

* The extended likelihood formalism in RooFit

# Asymmetry Analysis -- Estimate signal fraction within peak region

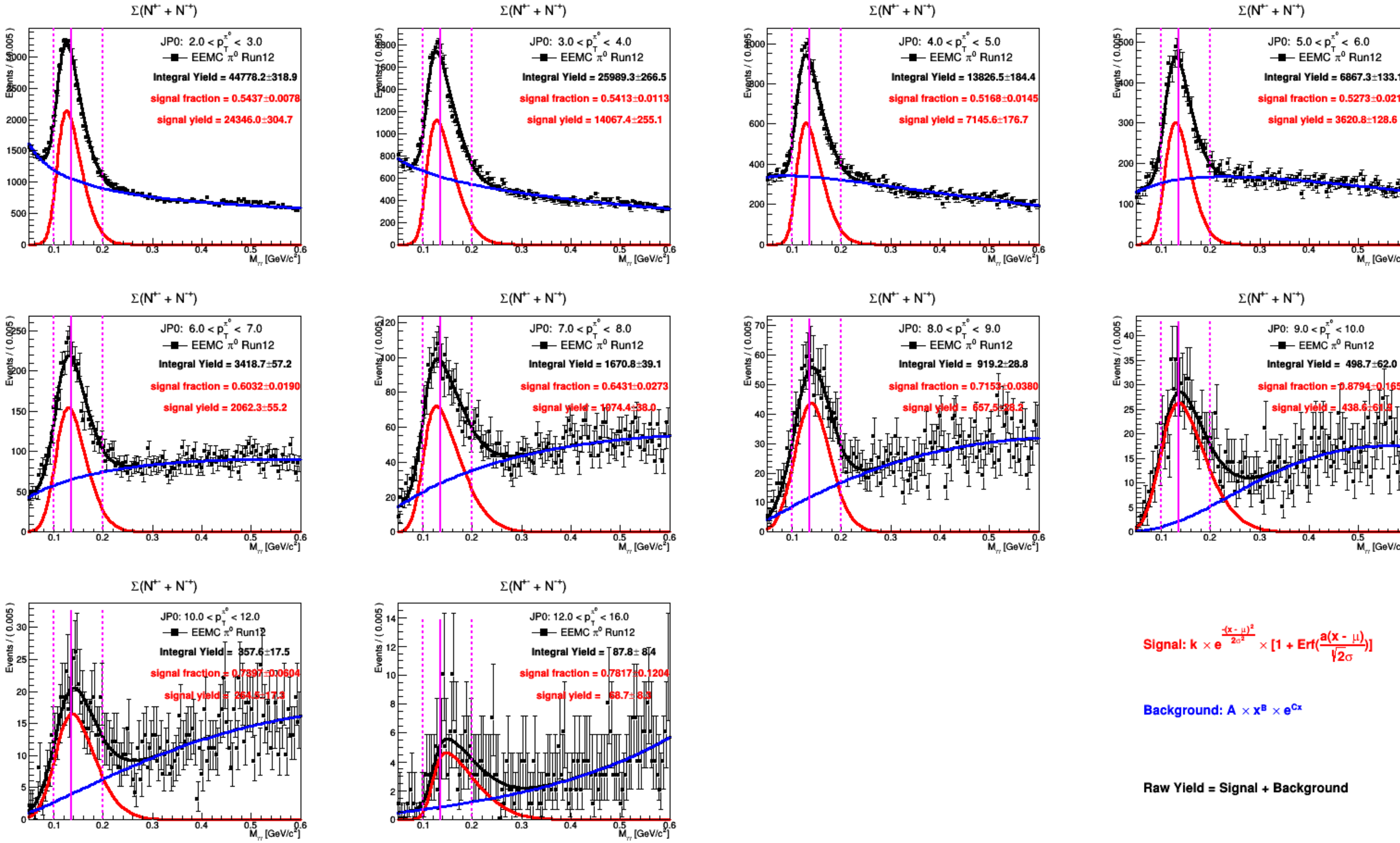


Signal: $k \times e^{-\frac{(x-\mu)^2}{2\sigma^2}} \times [1 + \mathrm{Erf}(\frac{a(x-\mu)}{\sqrt{2}\sigma})]$

Background: $A \times x^B \times e^{Cx}$

Raw Yield = Signal + Background

$$A_{LL} = \frac{\sum P_Y P_B[(N^{++} + N^{--}) - R_3 \boxed{(N^{+-} + N^{-+})}]}{\sum P_Y^2 P_B^2[(N^{++} + N^{--}) + R_3 \boxed{(N^{+-} + N^{-+})}]}$$

* The extended likelihood formalism in RooFit

# Asymmetry Analysis -- Estimate signal fraction within peak region

No indication of the polarization status dependence of the signal fraction is found. The polarization status independence is also found for other asymmetry types and variables.

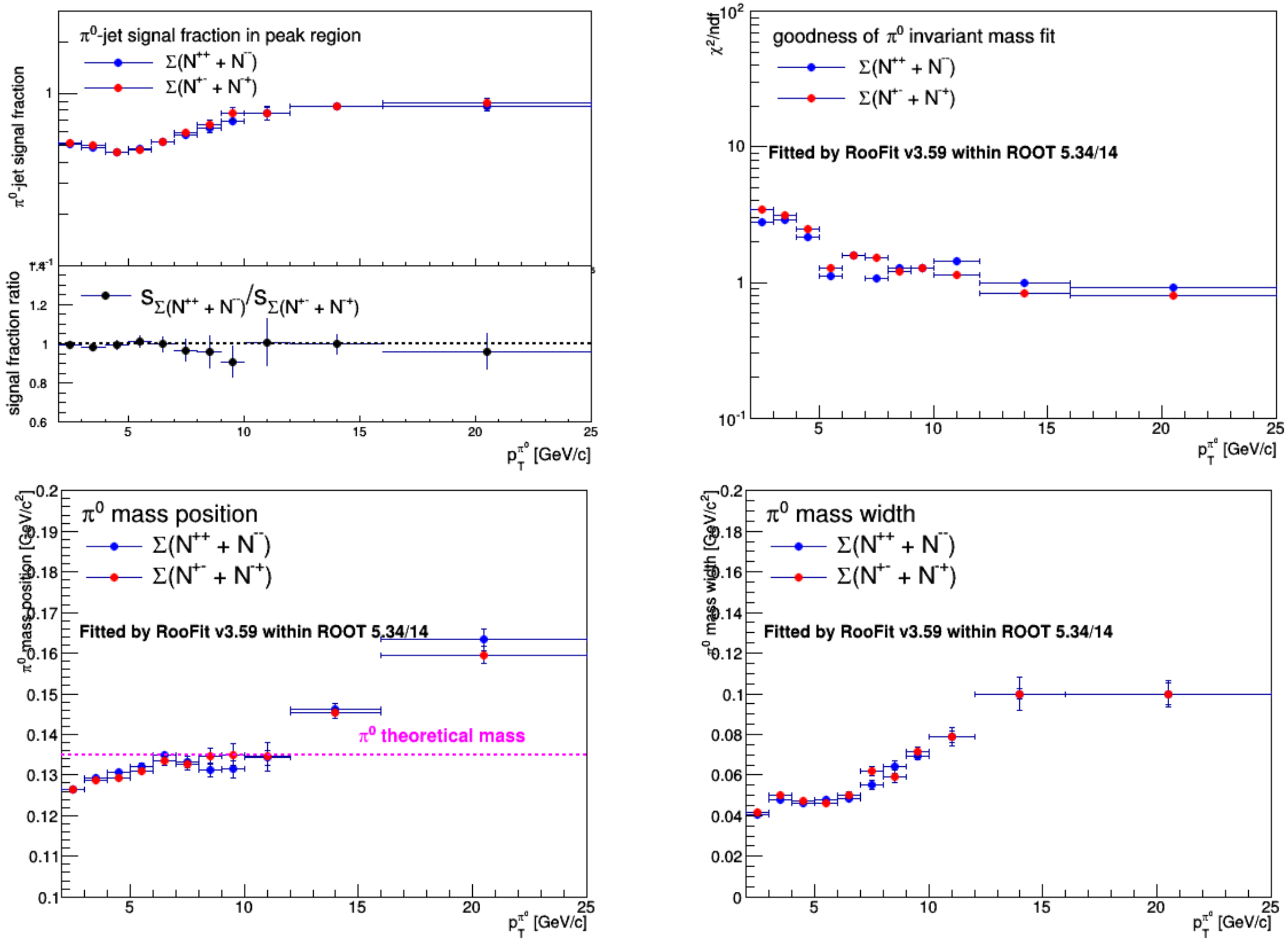


The mass peak position from the fit does not correspond exactly to the $\pi^0$ theoretical mass value, which probably be explained by energy smearing effects, calibration, etc.

# Asymmetry Analysis -- Estimate signal fraction within peak region

The average of the two different-polarization-status signal fractions is used for the estimate of the signal fraction within the peak region.

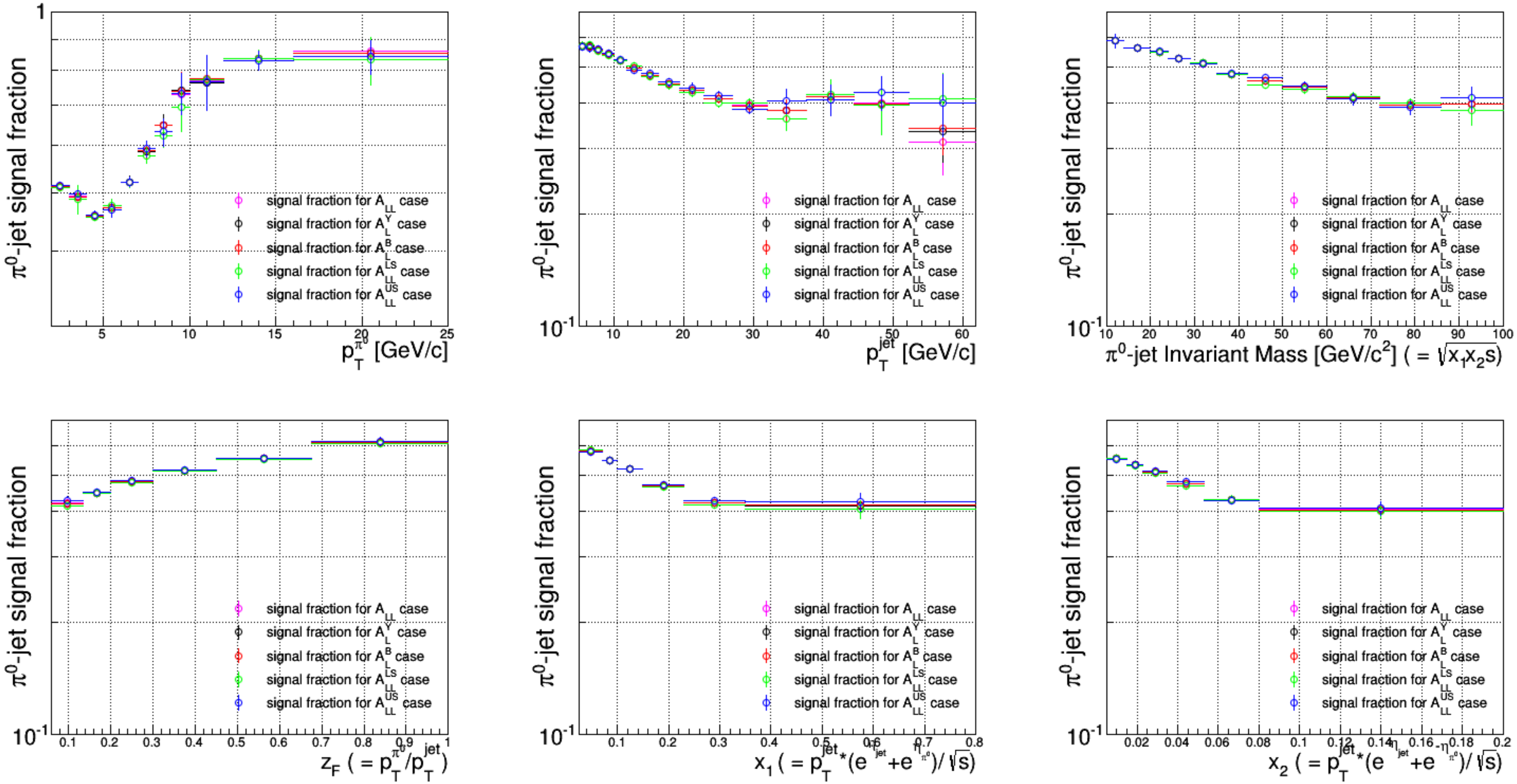


It seems that the signal fractions are mostly consistent within uncertainties among different asymmetry types.

# Asymmetry Results -- Longitudinal double asymmetry, $A_{LL}$

## Raw longitudinal double asymmetry, $A_{LL}^{S+B}$:

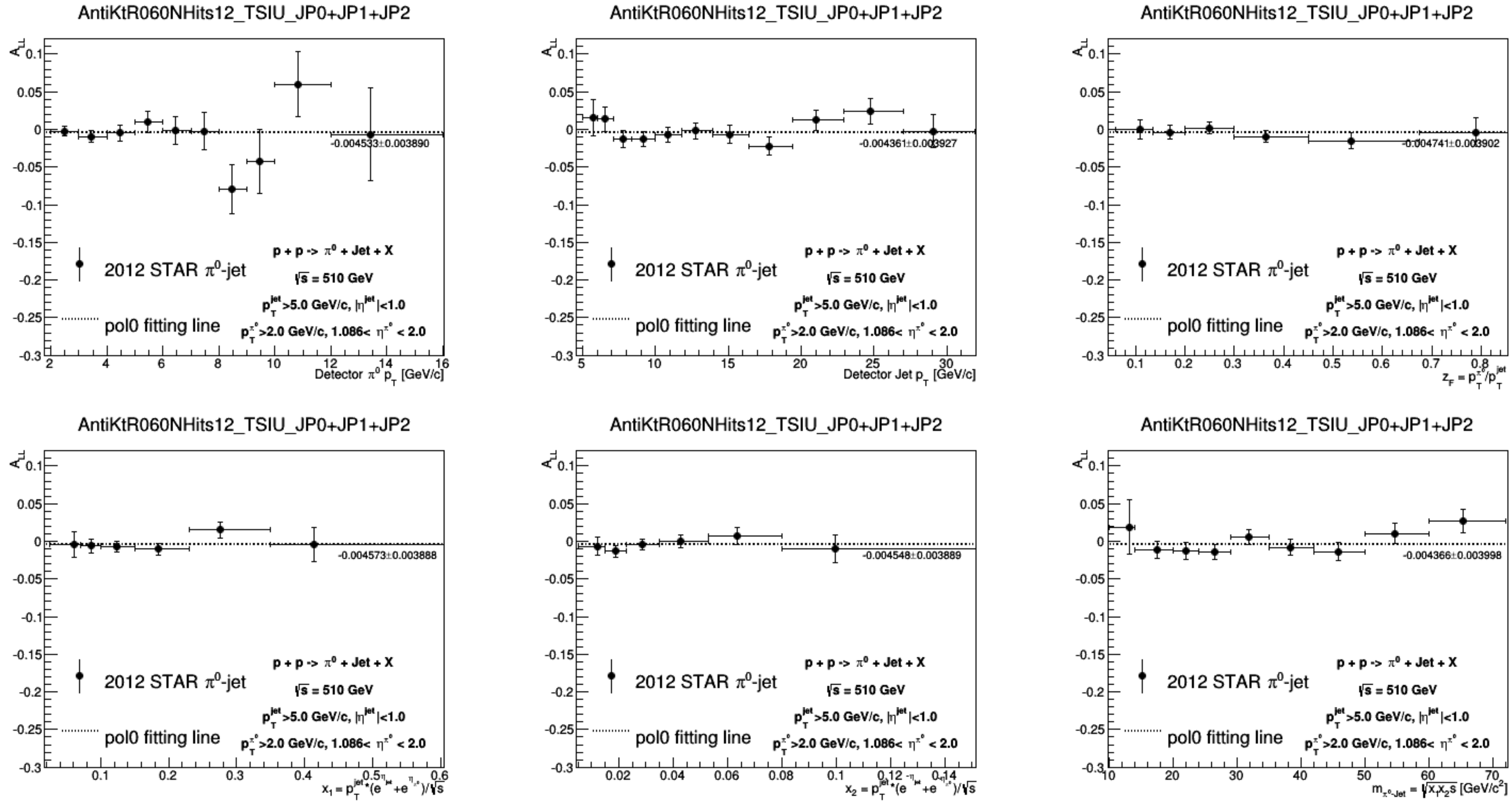


| *Raw $A_{LL}$ | $p_T^{\pi 0}$ | $p_T^{jet}$ | $z_F$ | $x_1$ | $x_2$ | $M_{\pi 0\text{-jet}}$ |
|---|---|---|---|---|---|---|
| $A_{LL}^{S+B}$ | -0.004533±0.003890 | -0.004361±0.003927 | -0.004741±0.00902 | -0.004573±0.003888 | -0.004548±0.003889 | -0.004366±0.003998 |

* Fit to a constant.

# Asymmetry Results -- Longitudinal double asymmetry, $A_{LL}$

## Corrected longitudinal double asymmetry, $A_{LL}{}^{S}$:

Error bar: Statistics errors
Box: systematics errors

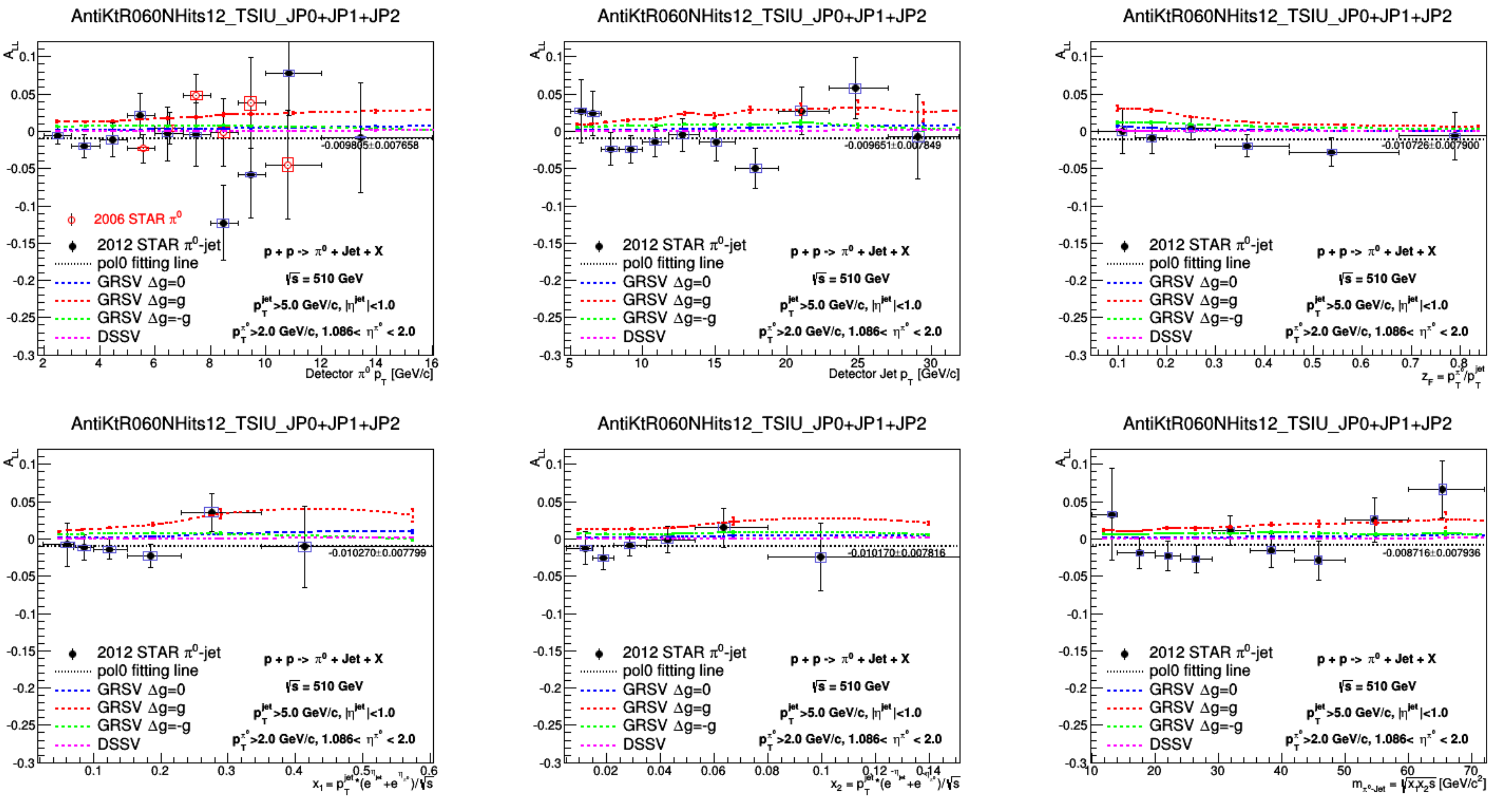


| *Corr. $A_{LL}$ | $p_T{}^{\pi 0}$ | $p_T{}^{jet}$ | $z_F$ | $x_1$ | $x_2$ | $M_{\pi 0\text{-jet}}$ |
|---|---|---|---|---|---|---|
| $A_{LL}{}^{S}$ | -0.009805±0.007658 | -0.009651±0.007849 | -0.010726±0.007900 | -0.010270±0.007799 | -0.010170±0.007816 | -0.008716±0.007936 |

* Fit to a constant.

# Asymmetry Results -- Longitudinal double asymmetry, $A_{LL}$

**A_LL vs. p_{T}^{#pi^{0}}:**

| Bin | Low | High | <p_T> | A_LL | dA_LL_stat | dA_LL_sys |
|---|---|---|---|---|---|---|
| 1 | 2.0 | 3.0 | 2.477875 | -0.005158 | 0.011690 | 0.004264 |
| 2 | 3.0 | 4.0 | 3.448977 | -0.019854 | 0.015468 | 0.004614 |
| 3 | 4.0 | 5.0 | 4.448042 | -0.011590 | 0.022705 | 0.005325 |
| 4 | 5.0 | 6.0 | 5.451194 | 0.021290 | 0.029868 | 0.005023 |
| 5 | 6.0 | 7.0 | 6.454747 | -0.003572 | 0.036436 | 0.004125 |
| 6 | 7.0 | 8.0 | 7.457299 | -0.004303 | 0.042654 | 0.003177 |
| 7 | 8.0 | 9.0 | 8.452913 | -0.122992 | 0.050320 | 0.005912 |
| 8 | 9.0 | 10.0 | 9.453567 | -0.057934 | 0.057999 | 0.003131 |
| 9 | 10.0 | 12.0 | 10.832187 | 0.077844 | 0.056371 | 0.004824 |
| 10 | 12.0 | 16.0 | 13.423045 | -0.008143 | 0.073828 | 0.000899 |

**A_LL vs. z_{F}^{#pi^{0}-jet}:**

| Bin | Low | High | <z_F> | A_LL | dA_LL_stat | dA_LL_sys |
|---|---|---|---|---|---|---|
| 1 | 0.0600 | 0.1350 | 0.108632 | 0.000328 | 0.030173 | 0.006225 |
| 2 | 0.1350 | 0.2000 | 0.169016 | -0.009145 | 0.020763 | 0.005567 |
| 3 | 0.2000 | 0.3000 | 0.248632 | 0.003762 | 0.015032 | 0.004862 |
| 4 | 0.3000 | 0.4500 | 0.364551 | -0.019310 | 0.014802 | 0.004261 |
| 5 | 0.4500 | 0.6750 | 0.537633 | -0.027959 | 0.019537 | 0.003645 |
| 6 | 0.6750 | 1.0000 | 0.789070 | -0.006301 | 0.031695 | 0.002848 |

**A_LL vs. invM^{#pi^{0}-jet}:**

| Bin | Low | High | <invM> | A_LL | dA_LL_stat | dA_LL_sys |
|---|---|---|---|---|---|---|
| 1 | 10.0 | 14.0 | 13.152270 | 0.033091 | 0.061613 | 0.003418 |
| 2 | 14.0 | 20.0 | 17.533341 | -0.018854 | 0.020404 | 0.003610 |
| 3 | 20.0 | 24.0 | 22.044551 | -0.022551 | 0.020000 | 0.003811 |
| 4 | 24.0 | 29.0 | 26.454476 | -0.026609 | 0.018635 | 0.004179 |
| 5 | 29.0 | 35.0 | 31.854768 | 0.011297 | 0.019496 | 0.004439 |
| 6 | 35.0 | 42.0 | 38.319995 | -0.015220 | 0.022677 | 0.005059 |
| 7 | 42.0 | 50.0 | 45.780600 | -0.028512 | 0.026192 | 0.005515 |
| 8 | 50.0 | 60.0 | 54.589254 | 0.025015 | 0.029715 | 0.005913 |
| 9 | 60.0 | 72.0 | 65.324841 | 0.066392 | 0.038722 | 0.006752 |

**A_LL vs. p_{T}^{jet}:**

| Bin | Low | High | <p_T> | A_LL | dA_LL_stat | dA_LL_sys |
|---|---|---|---|---|---|---|
| 1 | 5.0 | 6.0 | 5.707359 | 0.026945 | 0.042181 | 0.003482 |
| 2 | 6.0 | 7.1 | 6.556493 | 0.023625 | 0.029485 | 0.003481 |
| 3 | 7.1 | 8.4 | 7.795629 | -0.023481 | 0.021406 | 0.003656 |
| 4 | 8.4 | 10.0 | 9.196479 | -0.024140 | 0.018764 | 0.003891 |
| 5 | 10.0 | 11.8 | 10.870230 | -0.014376 | 0.019558 | 0.004188 |
| 6 | 11.8 | 13.9 | 12.786308 | -0.004766 | 0.022183 | 0.004613 |
| 7 | 13.9 | 16.4 | 15.107659 | -0.014597 | 0.024691 | 0.005023 |
| 8 | 16.4 | 19.4 | 17.817471 | -0.049685 | 0.027339 | 0.005624 |
| 9 | 19.4 | 22.9 | 21.014896 | 0.027481 | 0.031998 | 0.005995 |
| 10 | 22.9 | 27.0 | 24.727643 | 0.057564 | 0.041279 | 0.006647 |
| 11 | 27.0 | 31.9 | 29.092652 | -0.006814 | 0.056865 | 0.007015 |

**A_LL vs. x1^{#pi^{0}-jet}:**

| Bin | Low | High | <x_{1}> | A_LL | dA_LL_stat | dA_LL_sys |
|---|---|---|---|---|---|---|
| 1 | 0.0250 | 0.0700 | 0.061146 | -0.007499 | 0.028958 | 0.003233 |
| 2 | 0.0700 | 0.1000 | 0.086190 | -0.011639 | 0.016599 | 0.003721 |
| 3 | 0.1000 | 0.1500 | 0.123580 | -0.013871 | 0.013240 | 0.004170 |
| 4 | 0.1500 | 0.2300 | 0.184125 | -0.022709 | 0.015790 | 0.005110 |
| 5 | 0.2300 | 0.3500 | 0.275002 | 0.035817 | 0.025284 | 0.006190 |
| 6 | 0.3500 | 0.8000 | 0.413820 | -0.010244 | 0.054336 | 0.006365 |

**A_LL vs. x2^{#pi^{0}-jet}:**

| Bin | Low | High | <x_{2}> | A_LL | dA_LL_stat | dA_LL_sys |
|---|---|---|---|---|---|---|
| 1 | 0.0050 | 0.0150 | 0.012401 | -0.012467 | 0.021751 | 0.003633 |
| 2 | 0.0150 | 0.0230 | 0.019055 | -0.025618 | 0.015495 | 0.003945 |
| 3 | 0.0230 | 0.0350 | 0.028621 | -0.008288 | 0.014338 | 0.004352 |
| 4 | 0.0350 | 0.0530 | 0.042642 | -0.000858 | 0.017407 | 0.004987 |
| 5 | 0.0530 | 0.0800 | 0.063792 | 0.015101 | 0.026357 | 0.005975 |
| 6 | 0.0800 | 0.2000 | 0.099657 | -0.024614 | 0.045235 | 0.006686 |

**The systematic uncertainty are much smaller than the statistical uncertainty.**

# Asymmetry Results -- Longitudinal single-spin asymmetry, $A_L^Y$

Raw longitudinal single-spin asymmetry, $A_L^Y$:

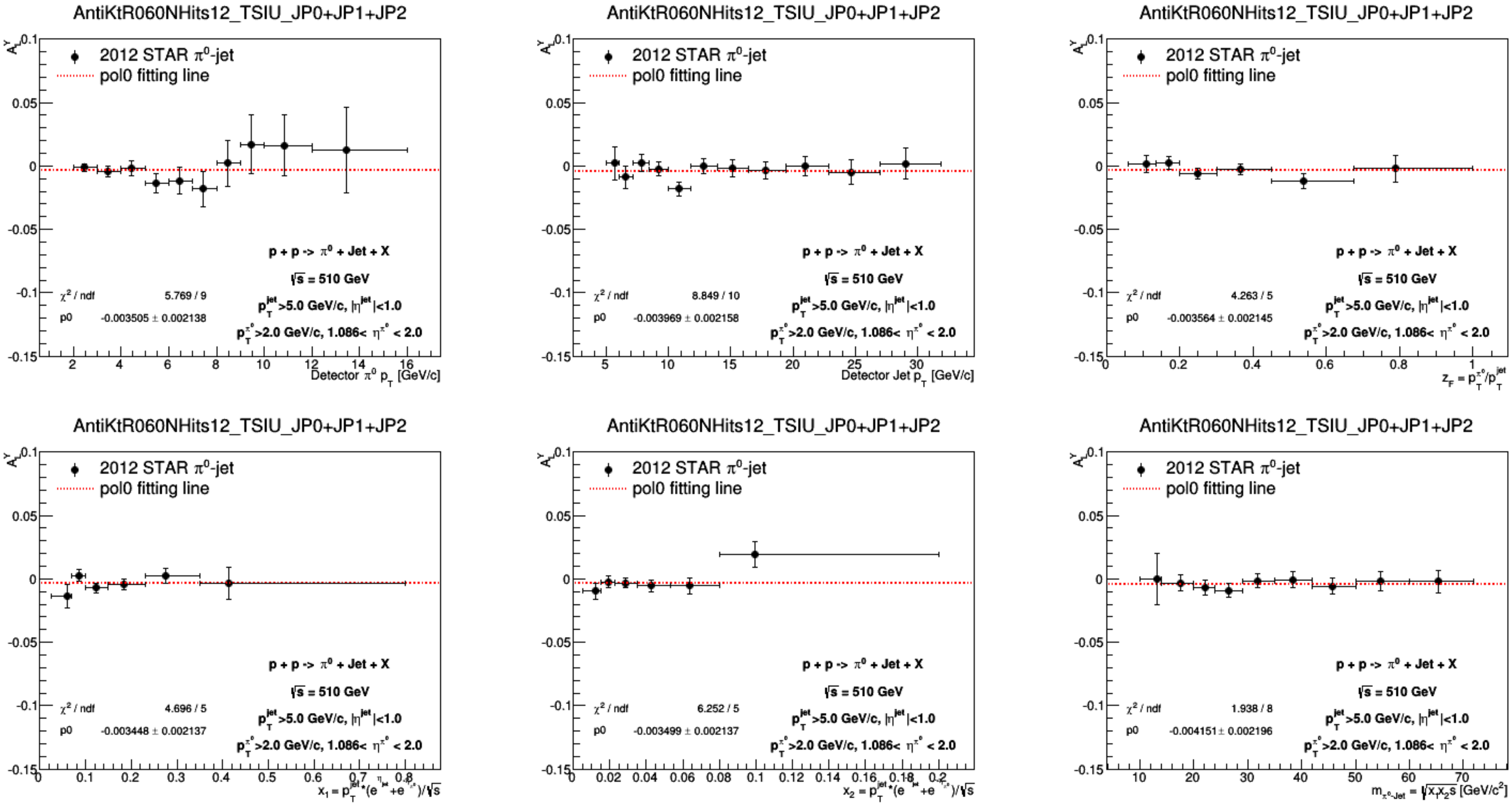


| *Raw $A_L^Y$ | $p_T^{\pi 0}$ | $p_T^{jet}$ | $z_F$ | $x_1$ | $x_2$ | $M_{\pi 0\text{-jet}}$ |
|---|---|---|---|---|---|---|
| $A_L^Y$ | -0.003505±0.002138 | -0.003969±0.002158 | -0.003564±0.002145 | -0.003448±0.002137 | -0.003499±0.002137 | -0.004151±0.002196 |

* Fit to a constant.

# Asymmetry Results -- Longitudinal single-spin asymmetry, $A_L^Y$

Error bar: Statistics errors
Box: systematics errors

## Corrected longitudinal single-spin asymmetry, $A_L^Y$:

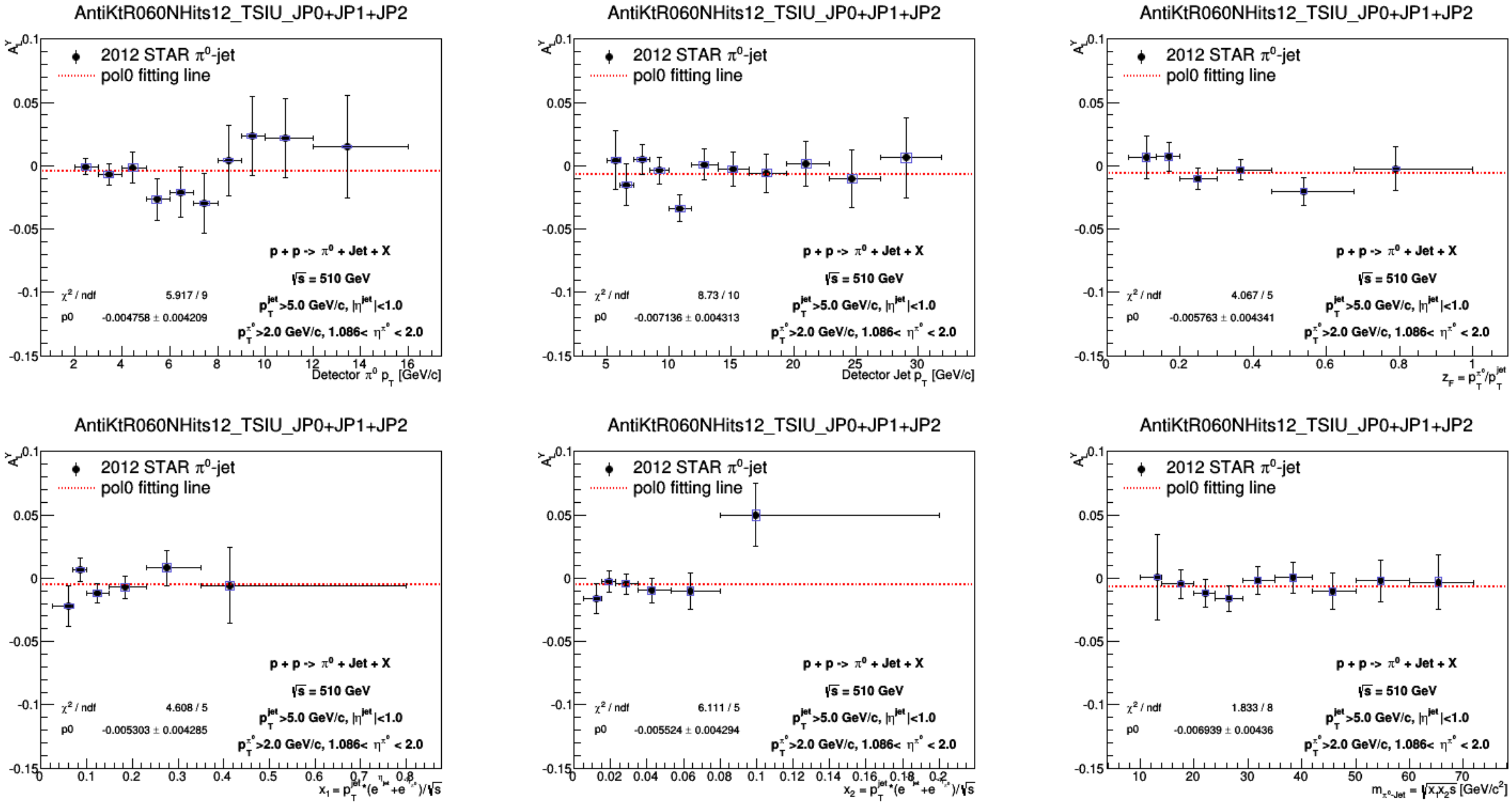


| *Corr. $A_L^Y$ | $p_T^{\pi 0}$ | $p_T^{jet}$ | $z_F$ | $x_1$ | $x_2$ | $M_{\pi 0\text{-jet}}$ |
|---|---|---|---|---|---|---|
| $A_L^Y$ | -0.004758±0.004209 | -0.007136±0.004313 | -0.005763±0.004341 | -0.005303±0.004285 | -0.005524±0.004294 | -0.006939±0.004360 |

* Fit to a constant.

# Asymmetry Results -- Longitudinal single-spin asymmetry, $A_L^B$

Raw longitudinal single-spin asymmetry, $A_L^B$:

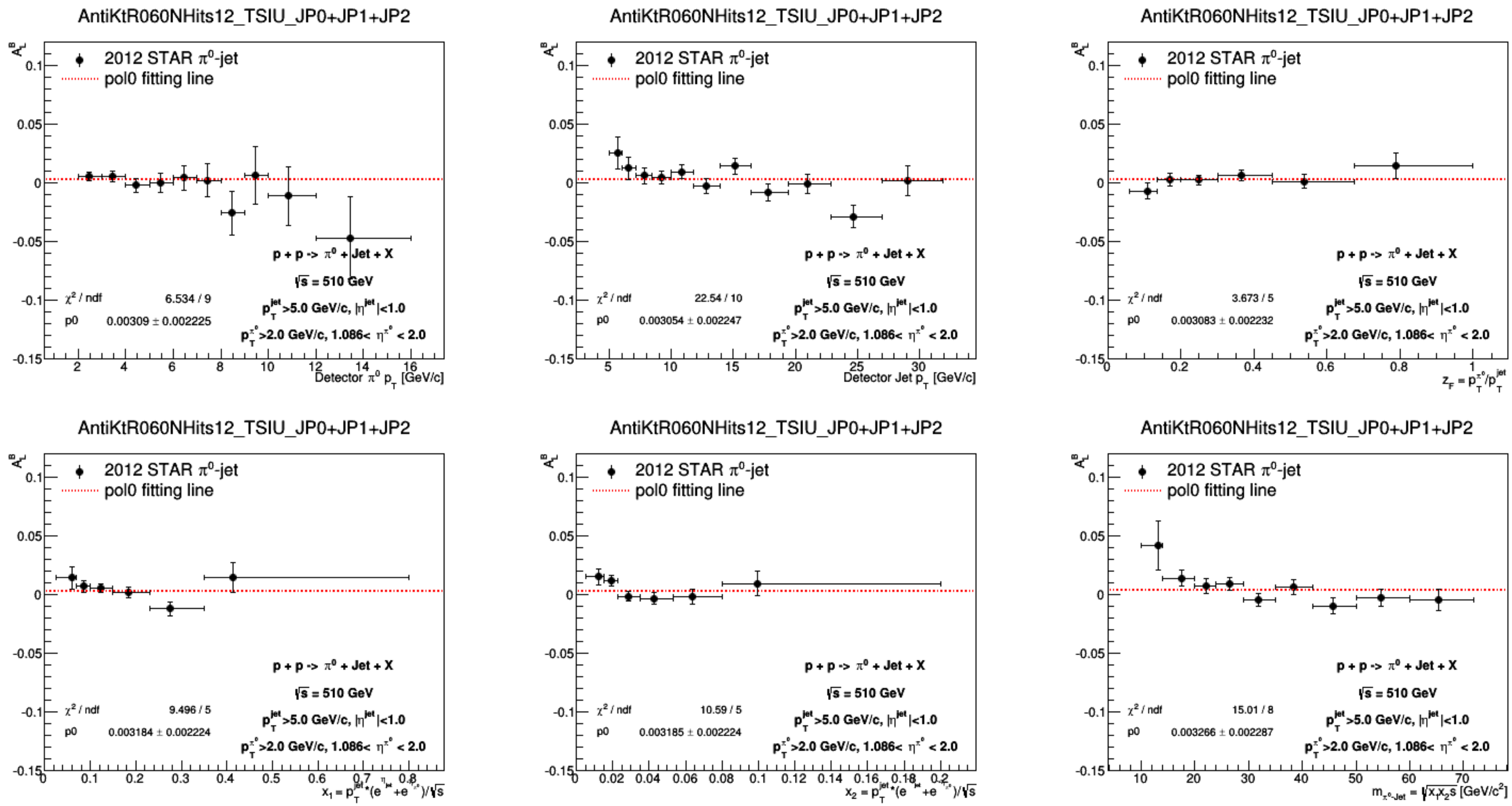


| *Raw $A_L^B$ | $p_T^{\pi 0}$ | $p_T^{jet}$ | $z_F$ | $x_1$ | $x_2$ | $M_{\pi 0\text{-jet}}$ |
|---|---|---|---|---|---|---|
| $A_L^B$ | 0.003090±0.002225 | 0.003054±0.002247 | 0.003083±0.002232 | 0.003184±0.002224 | 0.003185±0.002224 | 0.003266±0.002287 |

* Fit to a constant.

# Asymmetry Results -- Longitudinal single-spin asymmetry, $A_L^B$

Error bar: Statistics errors
Box: systematics errors

## Corrected longitudinal single-spin asymmetry, $A_L^B$:

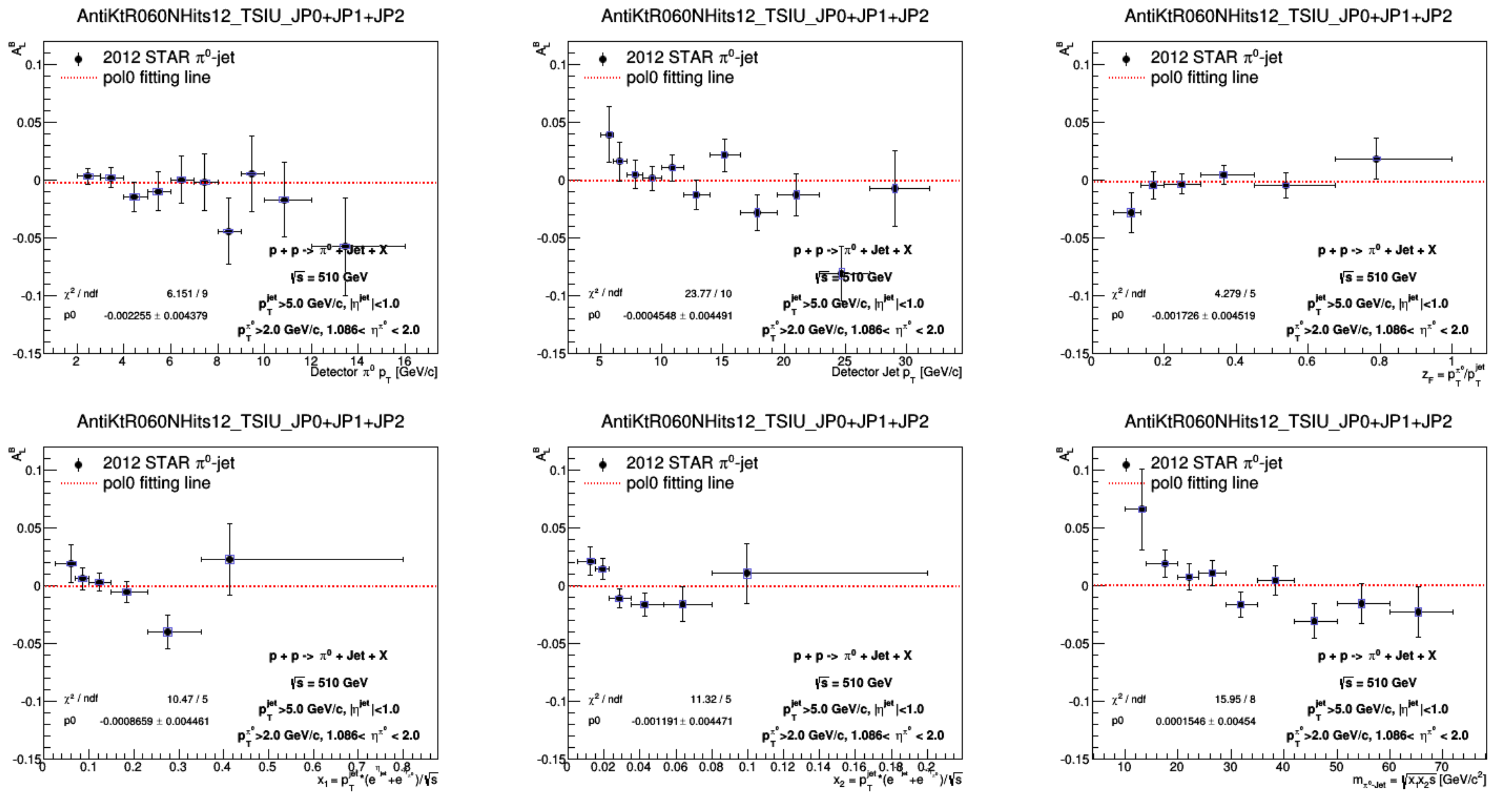


| *Corr. $A_L^B$ | $p_T^{\pi 0}$ | $p_T^{jet}$ | $z_F$ | $x_1$ | $x_2$ | $M_{\pi 0\text{-jet}}$ |
|---|---|---|---|---|---|---|
| $A_L^B$ | -0.002255±0.004379 | -0.000455±0.004491 | -0.001726±0.004519 | -0.000866±0.004461 | -0.001191±0.004471 | 0.000155±0.004540 |

* Fit to a constant.

# Asymmetry Results -- Like-sign longitudinal double asymmetry, $A_{LL}^{LS}$

## Raw like-sign longitudinal double asymmetry, $A_{LL}^{LS}$:

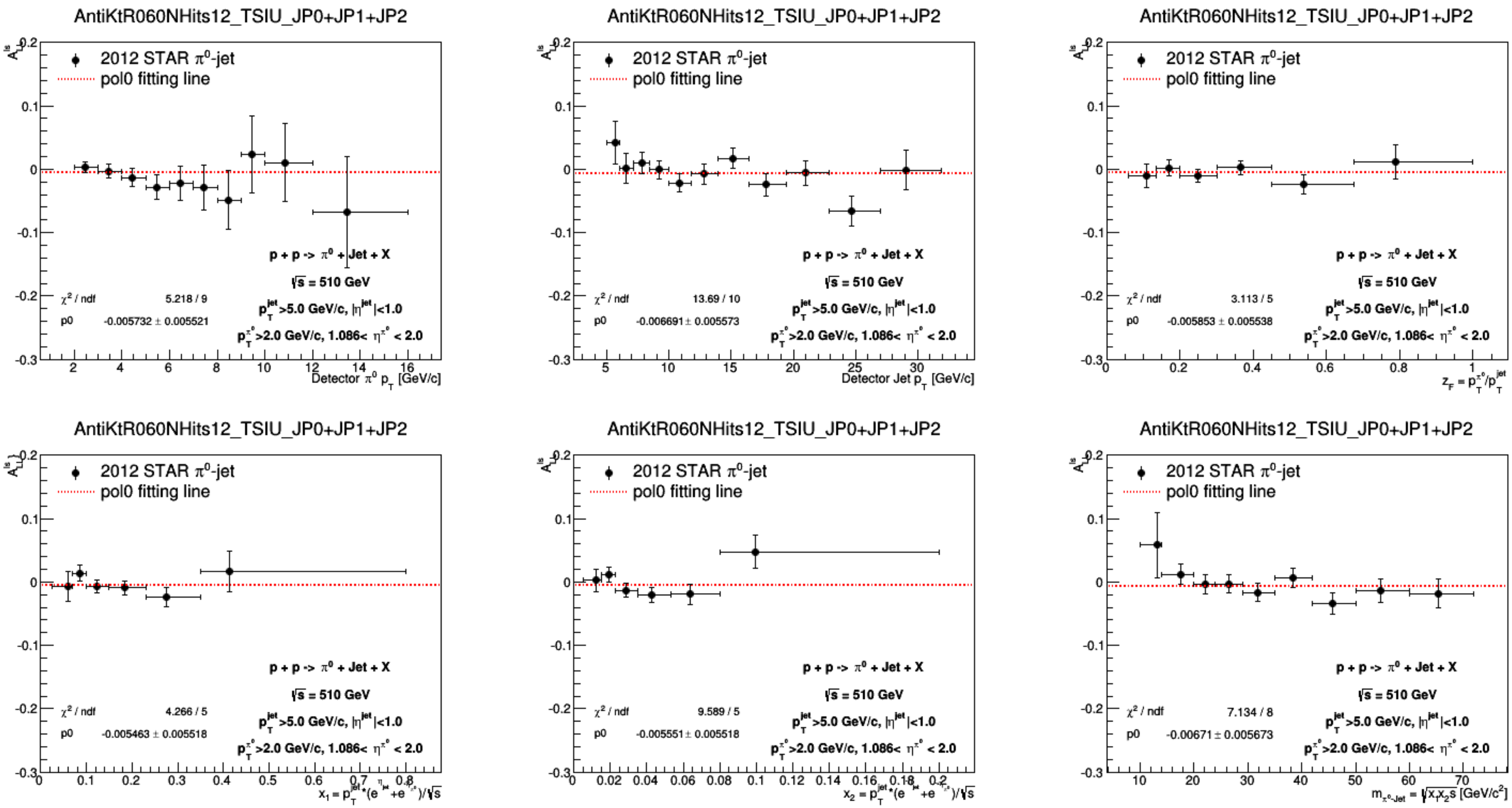


| *Raw $A_{LL}^{LS}$ | $p_T^{\pi 0}$ | $p_T^{jet}$ | $z_F$ | $x_1$ | $x_2$ | $M_{\pi 0\text{-jet}}$ |
|---|---|---|---|---|---|---|
| $A_{LL}^{LS}$ | -0.005732±0.005521 | -0.006691±0.005573 | -0.005853±0.005538 | -0.005463±0.005518 | -0.005551±0.005518 | -0.006710±0.005673 |

* Fit to a constant.

# Asymmetry Results -- Like-sign longitudinal double asymmetry, $A_{LL}^{LS}$

Corrected like-sign longitudinal double asymmetry, $A_{LL}^{LS}$:

Error bar: Statistics errors
Box: systematics errors

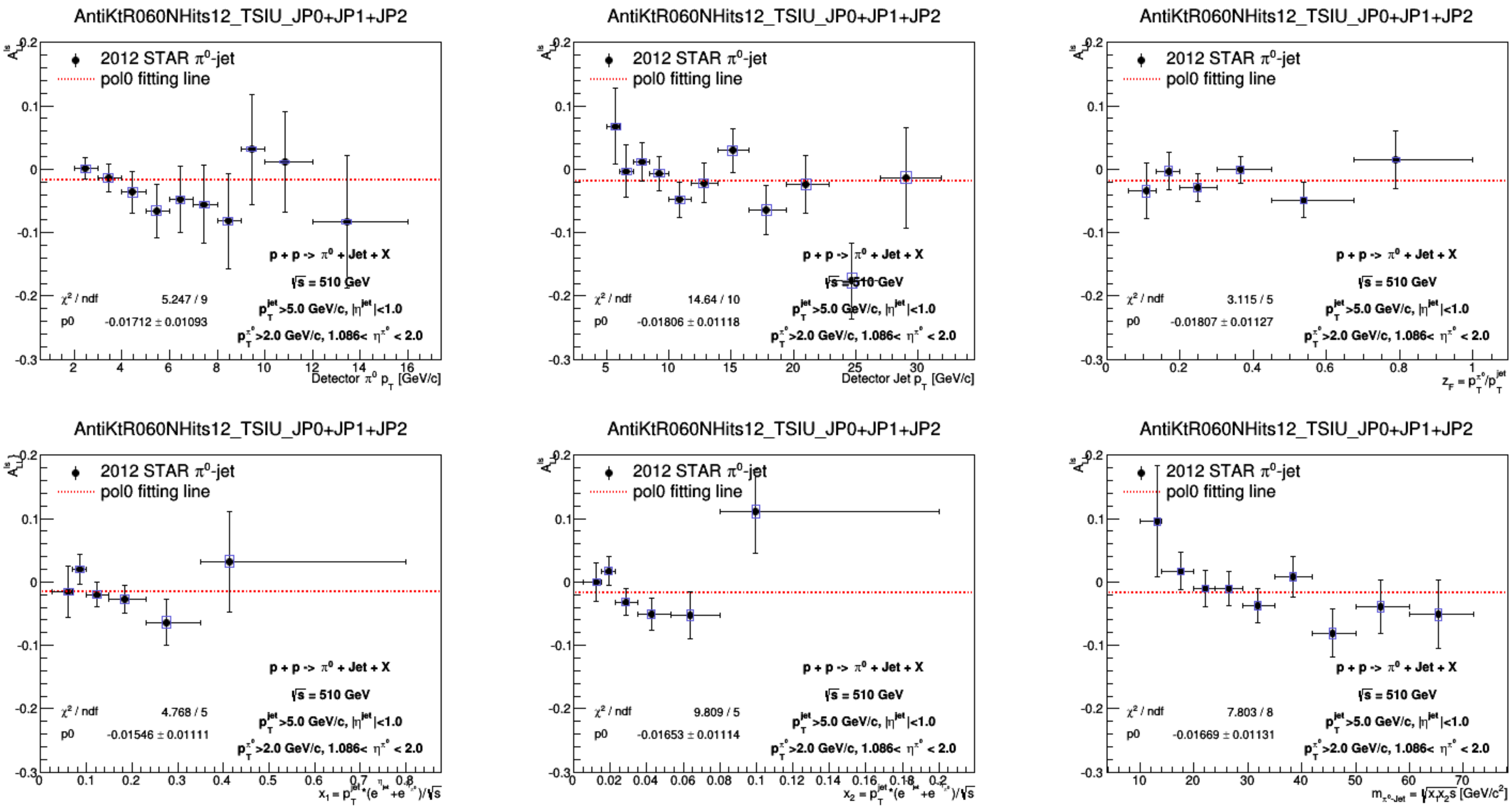


| *Corr. $A_{LL}^{LS}$ | $p_T^{\pi 0}$ | $p_T^{jet}$ | $z_F$ | $x_1$ | $x_2$ | $M_{\pi 0\text{-jet}}$ |
|---|---|---|---|---|---|---|
| $A_{LL}^{LS}$ | -0.017120±0.01093 | -0.018060±0.011180 | -0.018070±0.011270 | -0.015460±0.011110 | -0.016530±0.011140 | -0.016690±0.011310 |

* Fit to a constant.

# Asymmetry Results -- Unlike-sign longitudinal double asymmetry, $A_{LL}^{US}$

## Raw unlike-sign longitudinal double asymmetry, $A_{LL}^{US}$:

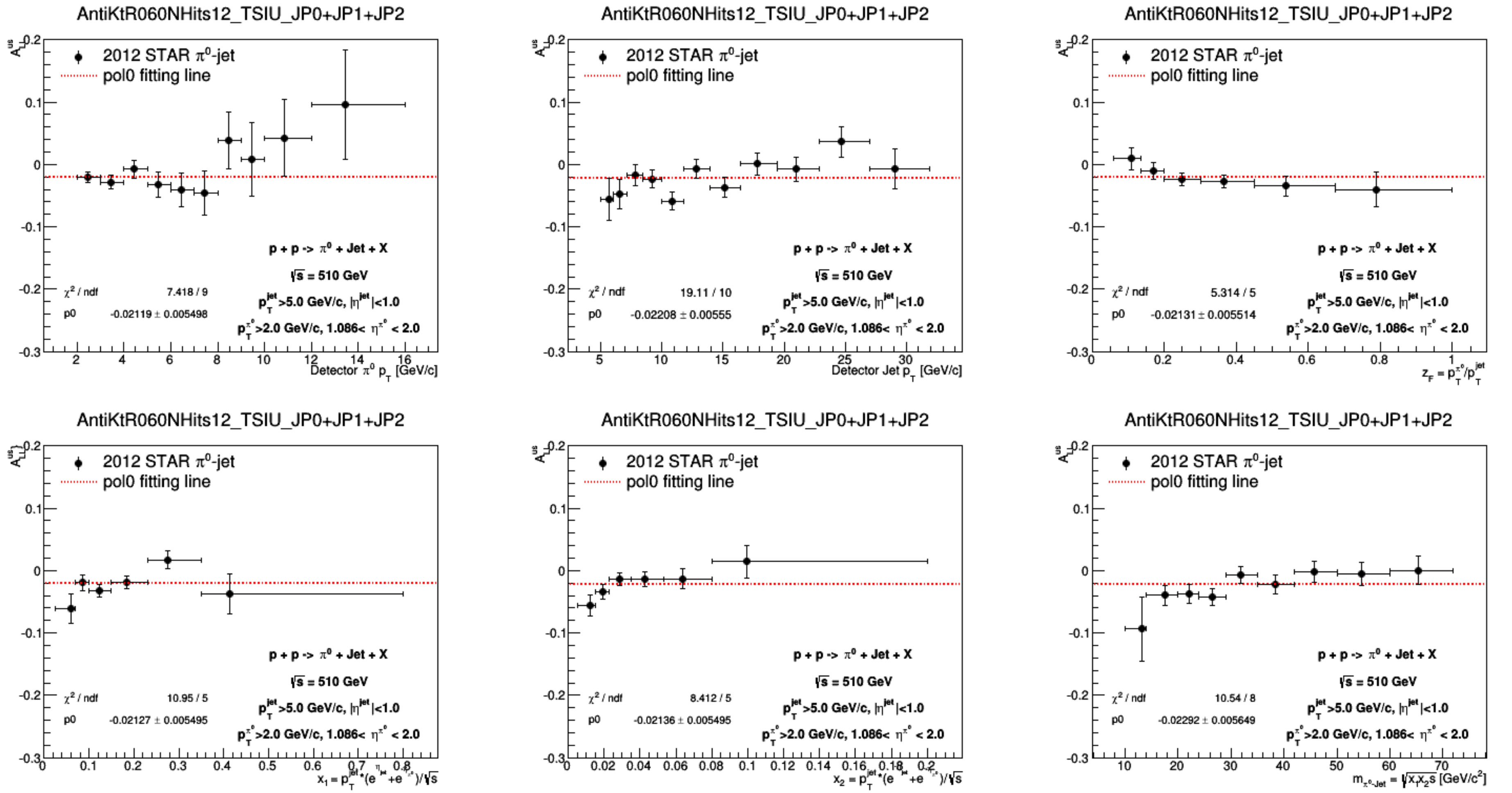


| *Raw $A_{LL}^{US}$ | $p_T^{\pi 0}$ | $p_T^{jet}$ | $z_F$ | $x_1$ | $x_2$ | $M_{\pi 0\text{-jet}}$ |
|---|---|---|---|---|---|---|
| $A_{LL}^{US}$ | -0.021190±0.005498 | -0.02208±0.005550 | -0.021310±0.005514 | -0.02127±0.005495 | -0.02136±0.005495 | -0.02292±0.005649 |

* Fit to a constant.

# Asymmetry Results -- Unlike-sign longitudinal double asymmetry, $A_{LL}^{US}$

Error bar: Statistics errors
Box: systematics errors

Corrected unlike-sign longitudinal double asymmetry, $A_{LL}^{US}$:

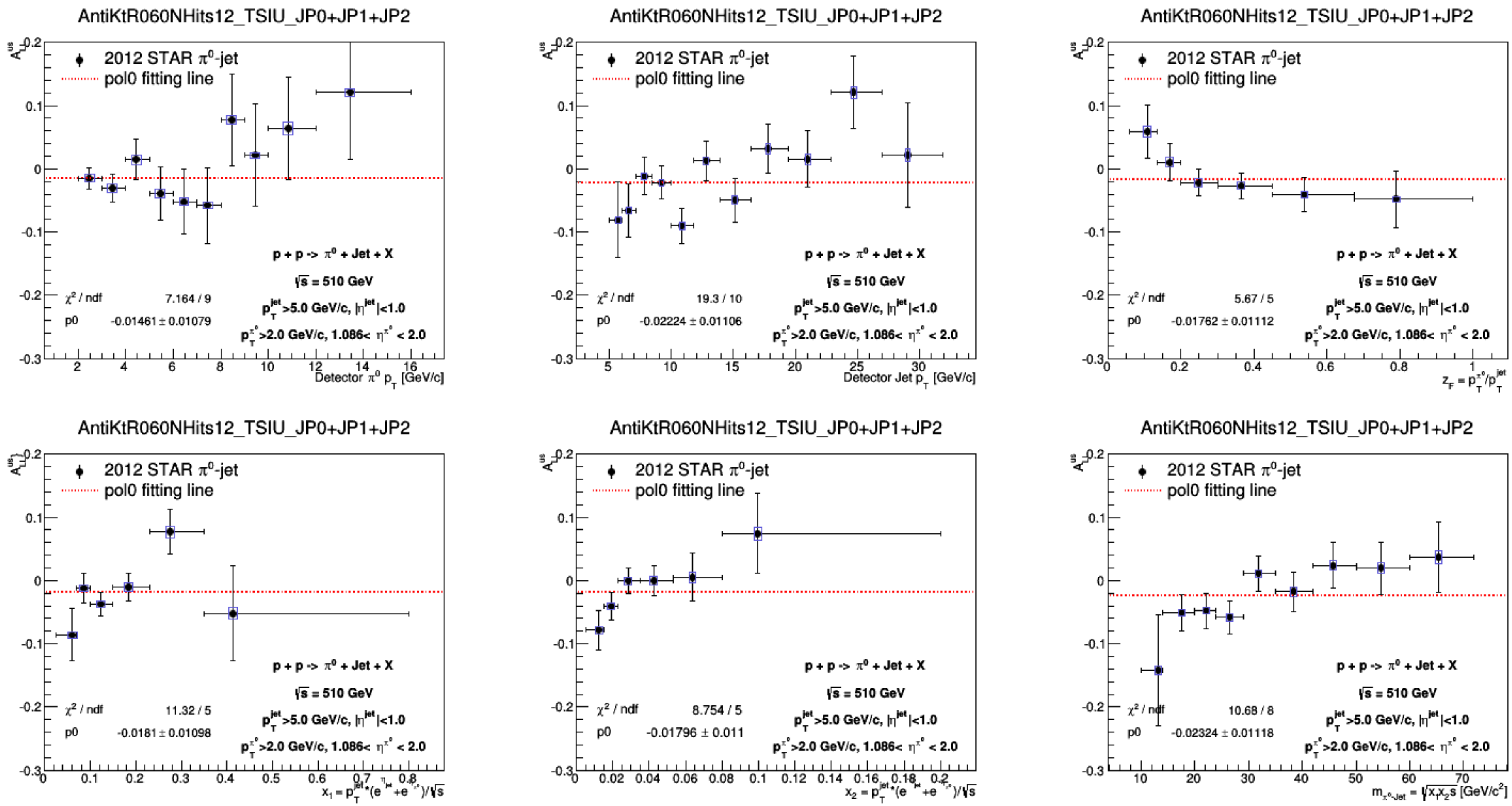


| *Corr. $A_{LL}^{US}$ | $p_T^{\pi 0}$ | $p_T^{jet}$ | $z_F$ | $x_1$ | $x_2$ | $M_{\pi 0\text{-jet}}$ |
|---|---|---|---|---|---|---|
| $A_{LL}^{US}$ | -0.01461±0.01079 | -0.02224±0.01106 | -0.01762±0.01112 | -0.01810±0.01098 | -0.01796±0.011 | -0.02324±0.01118 |

* Fit to a constant.

# Asymmetry Results -- False asymmetries

| Variable bin | Asymmetry type | Deviation from the mean in the constant fit | |
|---|---|---|---|
| | | Raw | Corrected |
| $p_T^{\pi 0}$ | $A_L^Y$ | 1.64 | 1.13 |
| | $A_L^B$ | 1.39 | 0.51 |
| | $A_{LL}^{LS}$ | 1.04 | 1.57 |
| | $A_{LL}^{US}$ | 3.85 | 1.35 |
| $p_T^{jet}$ | $A_L^Y$ | 1.84 | 1.65 |
| | $A_L^B$ | 1.36 | 0.10 |
| | $A_{LL}^{LS}$ | 1.20 | 1.62 |
| | $A_{LL}^{US}$ | 3.98 | 2.01 |
| $z_F$ | $A_L^Y$ | 1.66 | 1.33 |
| | $A_L^B$ | 1.38 | 0.38 |
| | $A_{LL}^{LS}$ | 1.06 | 1.60 |
| | $A_{LL}^{US}$ | 3.86 | 1.58 |
| $x_1$ | $A_L^Y$ | 1.61 | 1.24 |
| | $A_L^B$ | 1.43 | 0.19 |
| | $A_{LL}^{LS}$ | 0.99 | 1.39 |
| | $A_{LL}^{US}$ | 3.87 | 1.65 |
| $x_2$ | $A_L^Y$ | 1.64 | 1.29 |
| | $A_L^B$ | 1.43 | 0.27 |
| | $A_{LL}^{LS}$ | 1.00 | 1.48 |
| | $A_{LL}^{US}$ | 3.89 | 1.63 |
| $M_{\pi 0\text{-jet}}$ | $A_L^Y$ | 1.89 | 1.59 |
| | $A_L^B$ | 1.43 | 0.03 |
| | $A_{LL}^{LS}$ | 1.18 | 1.48 |
| | $A_{LL}^{US}$ | 4.06 | 2.08 |

# Asymmetry Results -- Longitudinal double asymmetry, $A_{LL}$

Error bar: Statistics errors
Box: systematics errors

## Corrected longitudinal double asymmetry, $A_{LL}^{S}$:

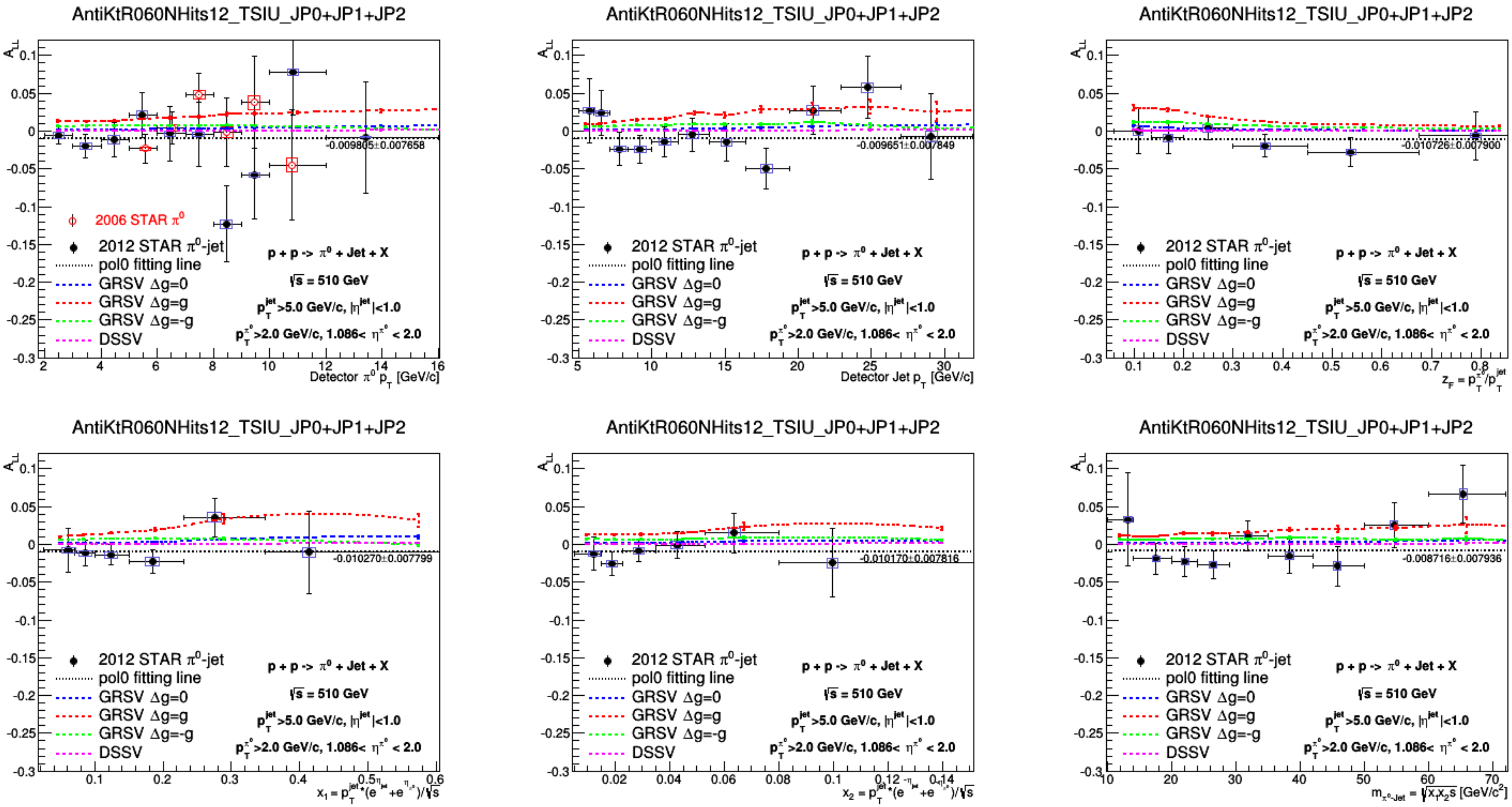


| *Corr. $A_{LL}$ | $p_T^{\pi 0}$ | $p_T^{jet}$ | $z_F$ | $x_1$ | $x_2$ | $M_{\pi 0\text{-jet}}$ |
|---|---|---|---|---|---|---|
| $A_{LL}^{S}$ | -0.009805±0.007658 | -0.009651±0.007849 | -0.010726±0.007900 | -0.010270±0.007799 | -0.010170±0.007816 | -0.008716±0.007936 |

* Fit to a constant.

# Summary and Outlook

Summary:

1. Background asymmetry corrections have been done for estimation of the real signal asymmetry.
2. The statistical and systematic uncertainties have been estimated.
3. The false asymmetries are consistent to zero within two sigma except for the raw unlike-sign longitudinal double asymmetry.
4. Theoretical curves were updated with higher iterations, and seems agree with the data.

Outlook:

1. Request for the preliminary results!

**Thanks!**

# Backup Slides

# Background Asymmetry Estimations – Low mass region

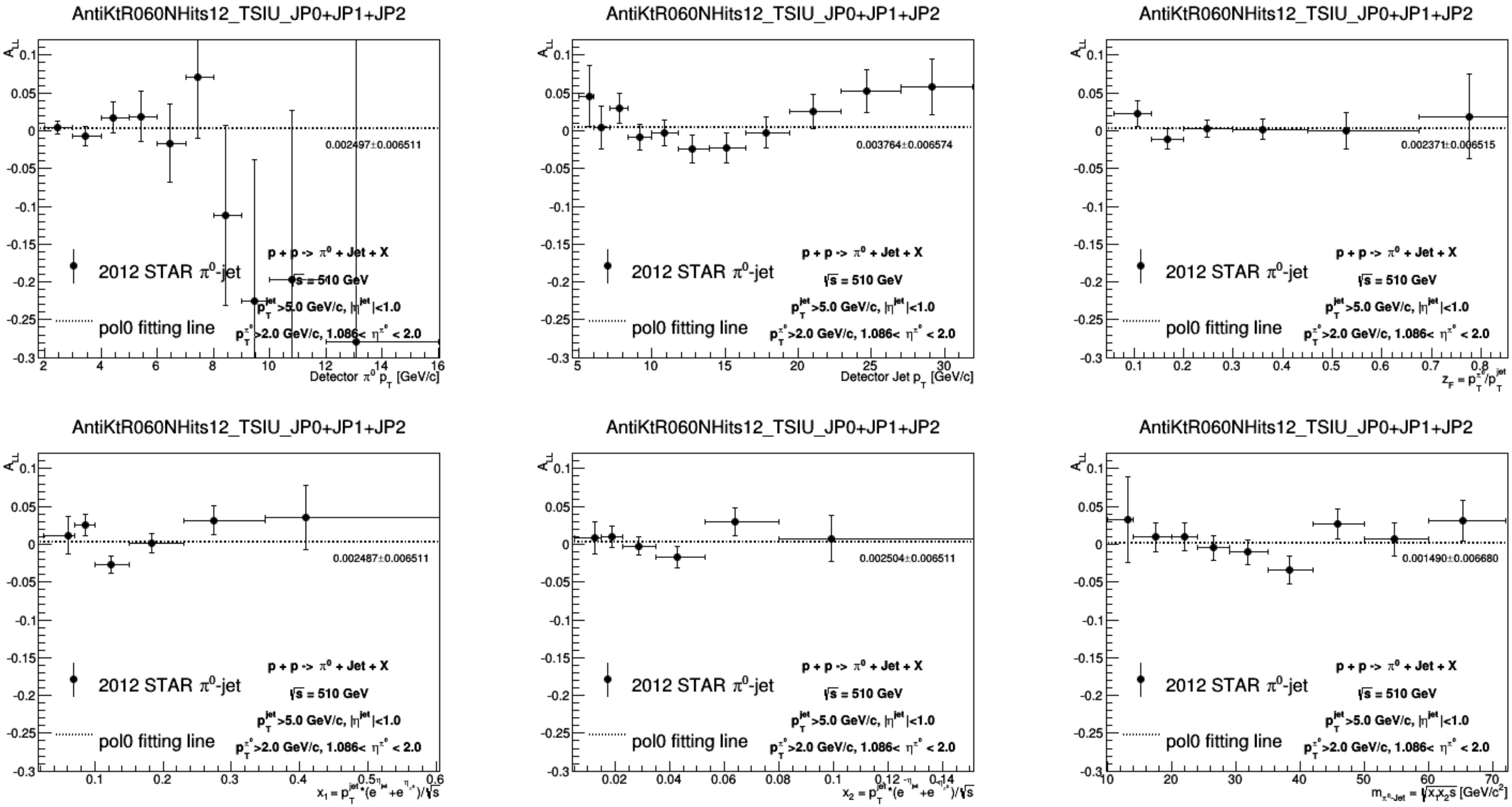

# Background Asymmetry Estimations – Low mass region

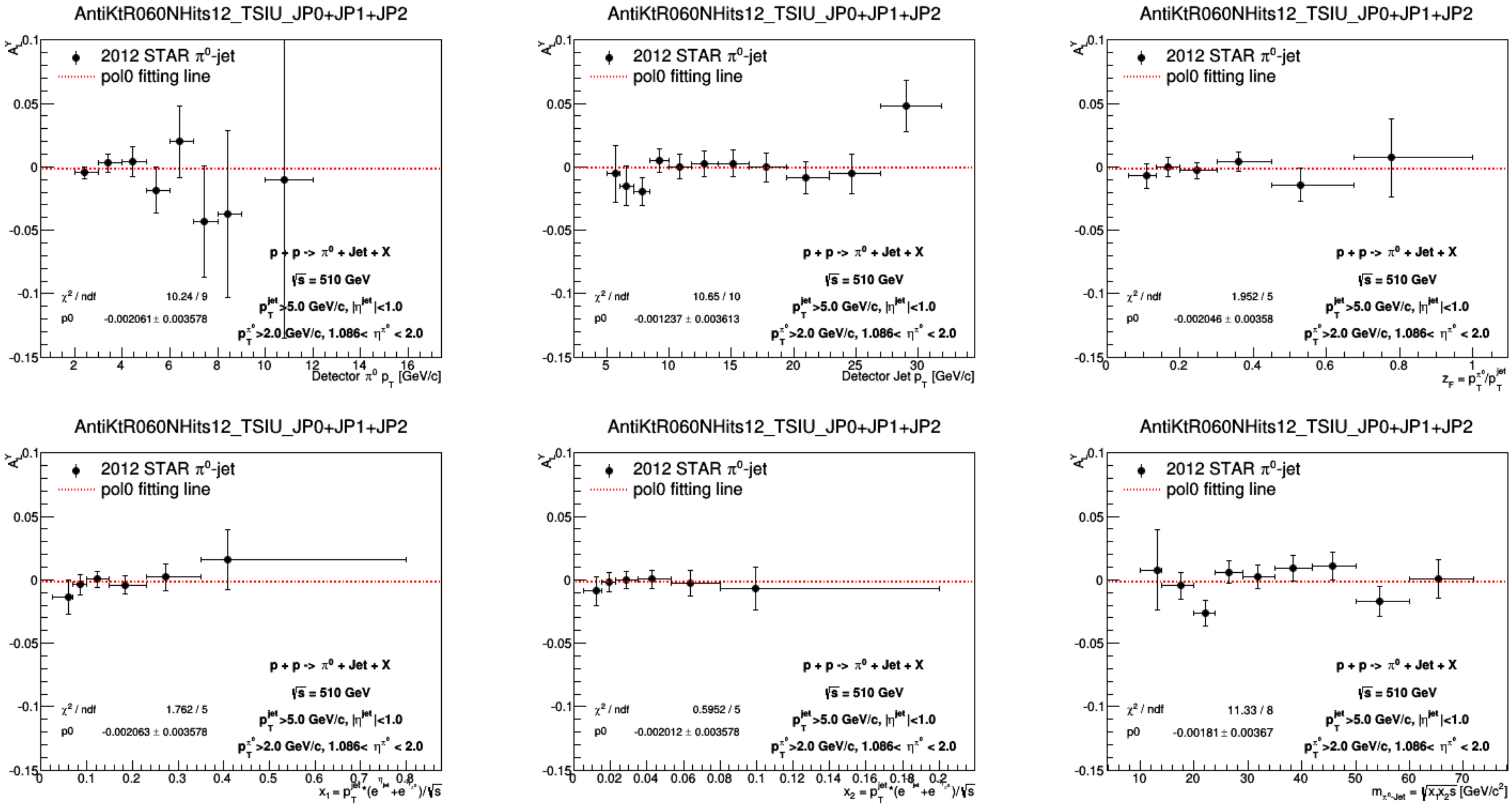

# Background Asymmetry Estimations – Low mass region

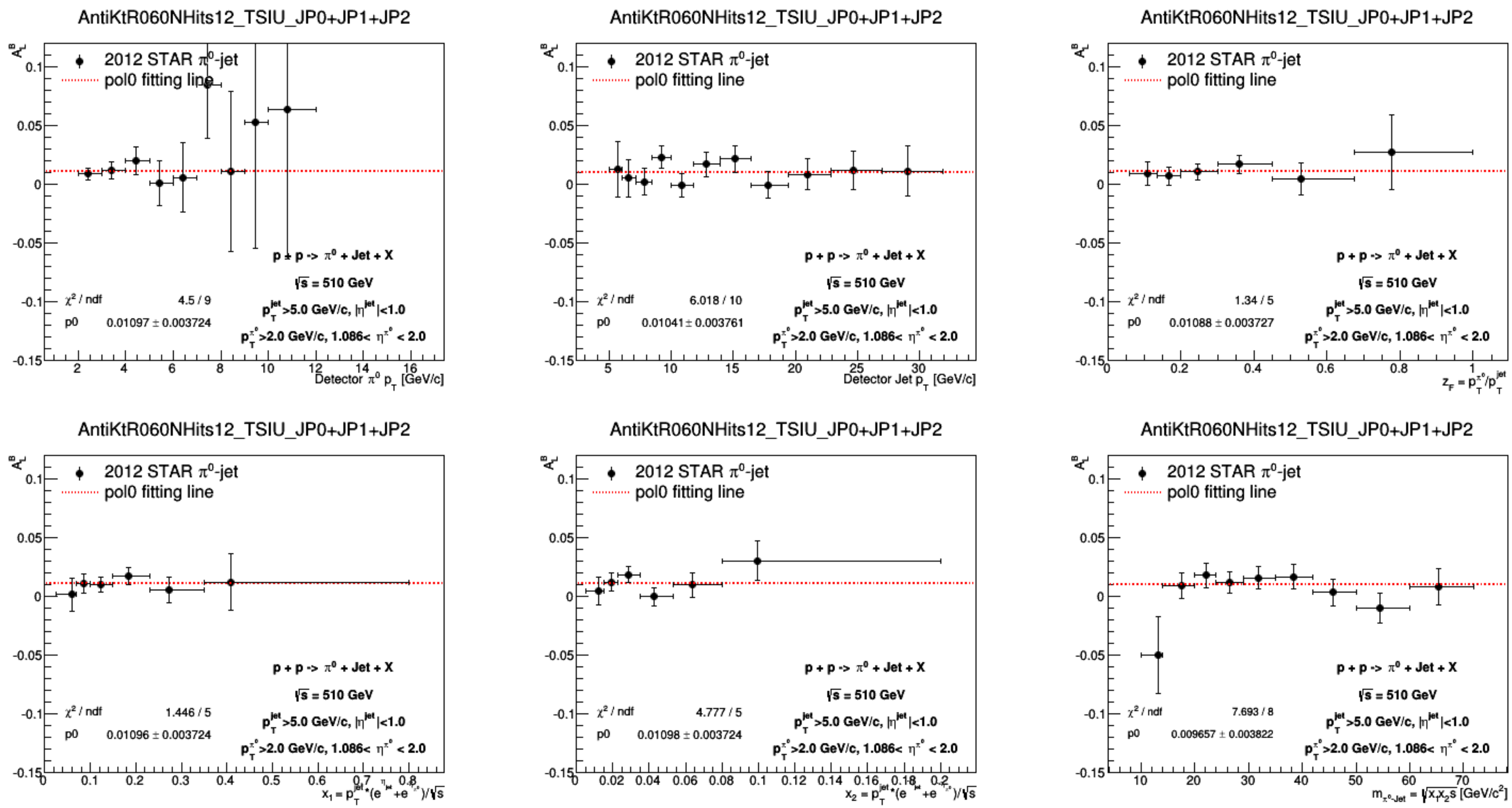

# Background Asymmetry Estimations – Low mass region

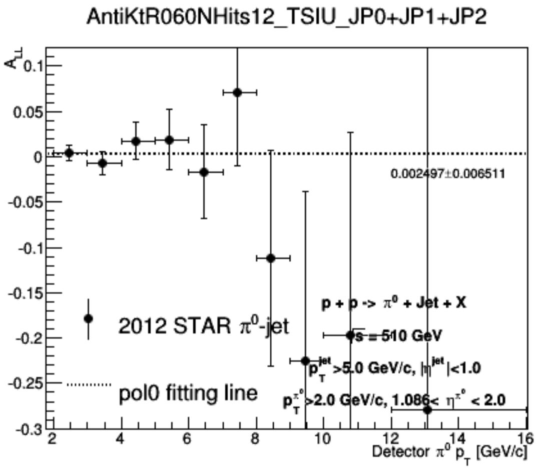


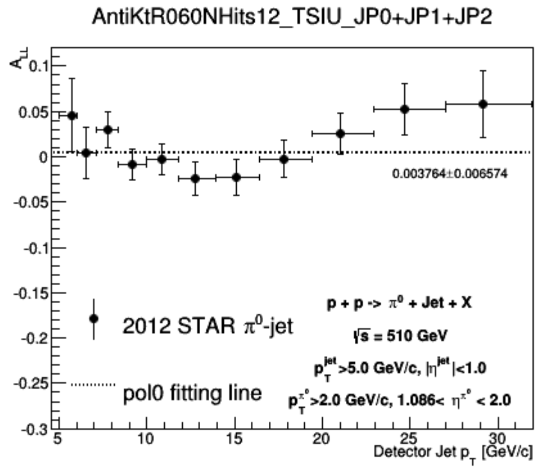


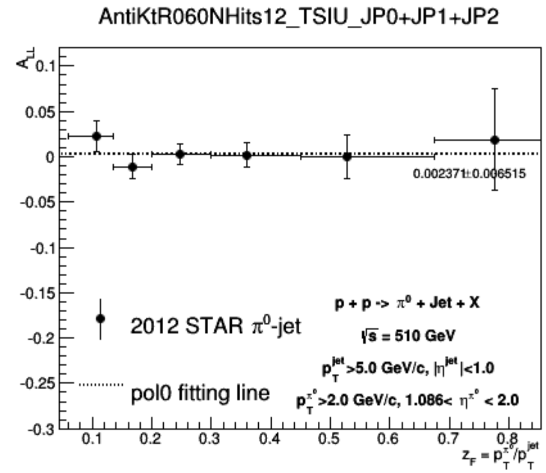


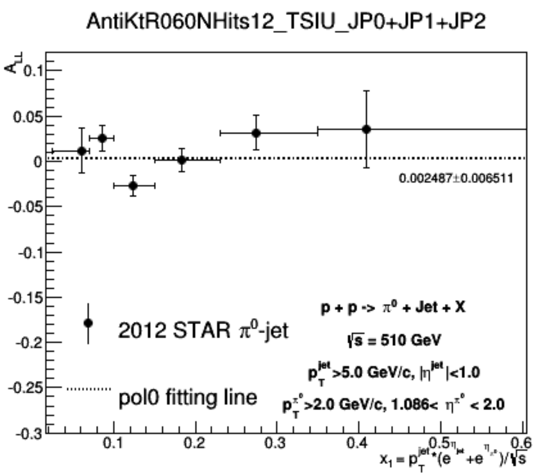


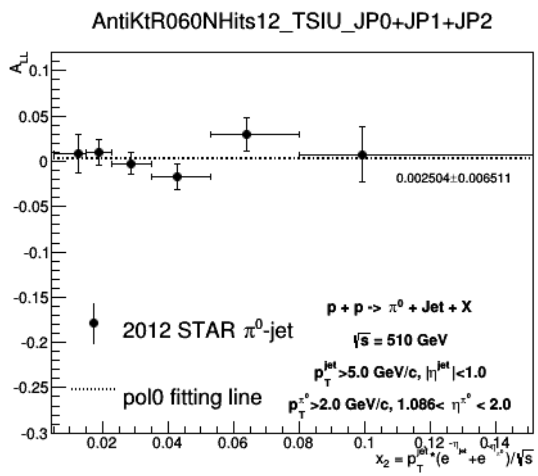


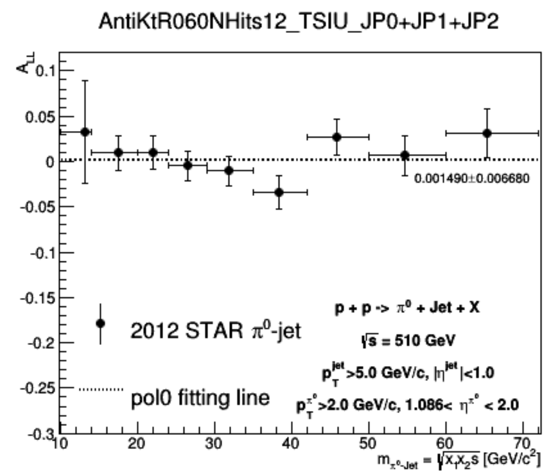

# Background Asymmetry Estimations – Low mass region

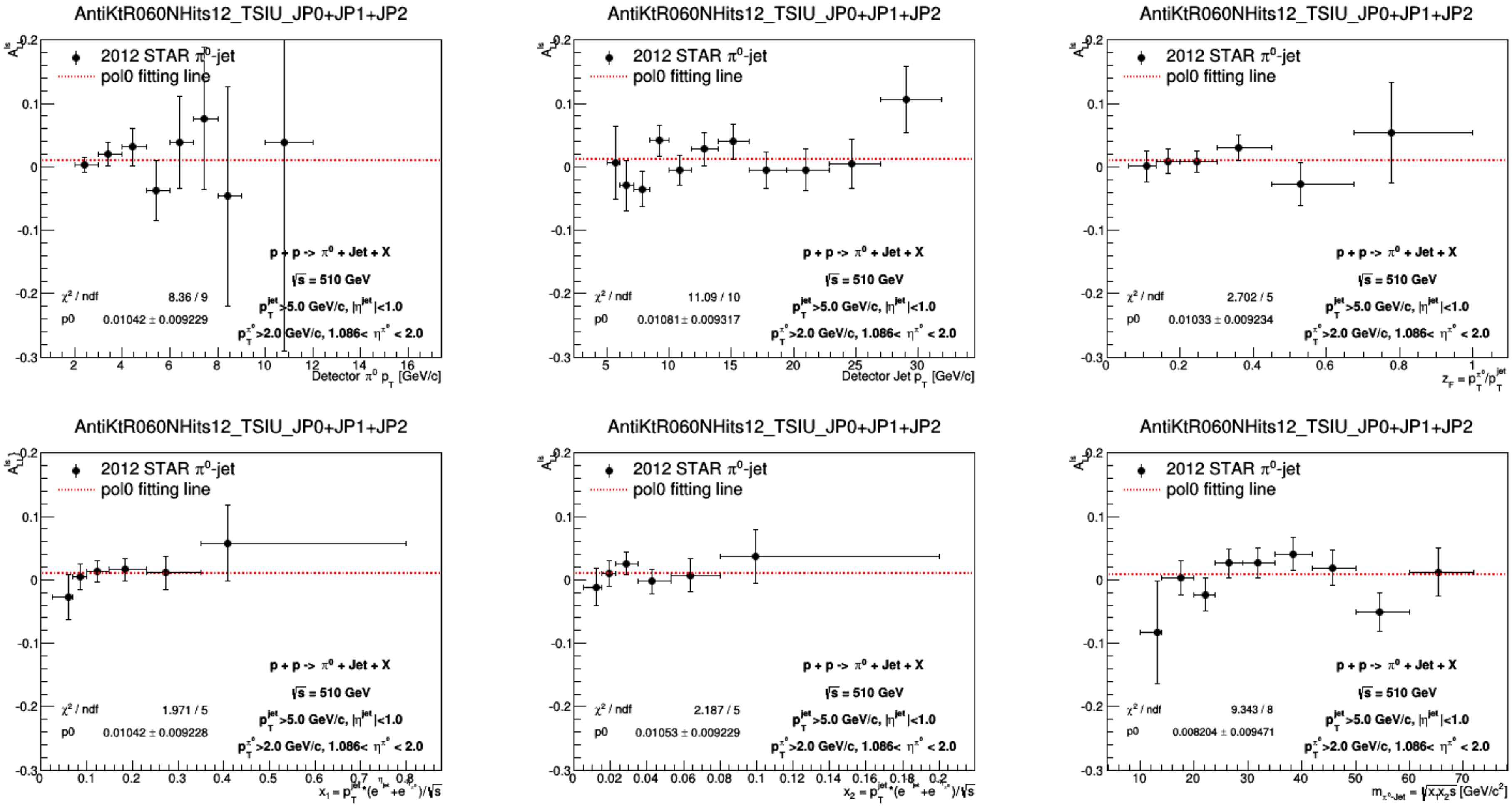

# Background Asymmetry Estimations – High mass region

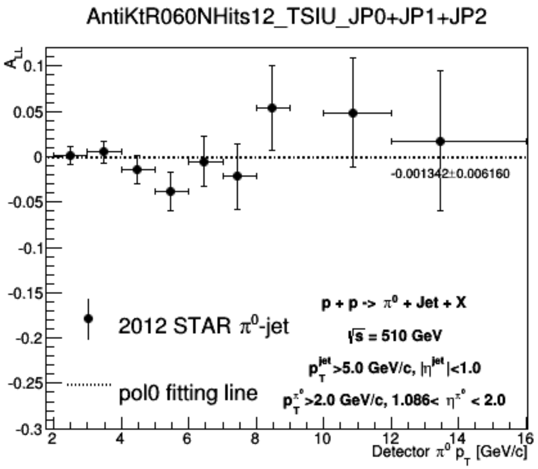


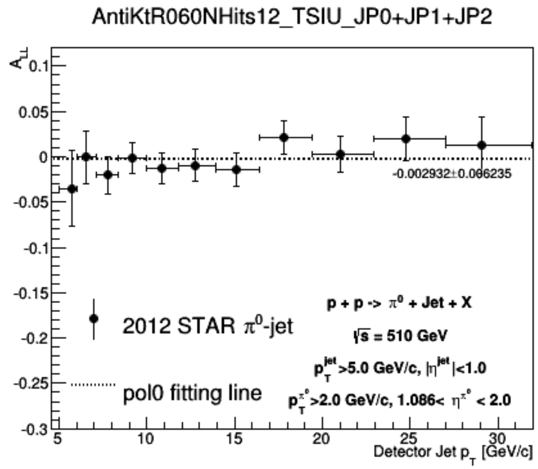


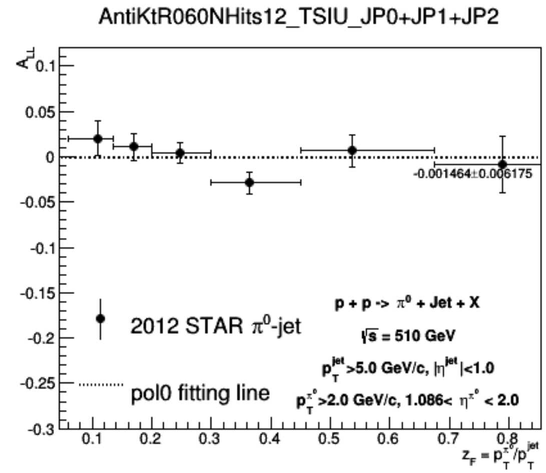


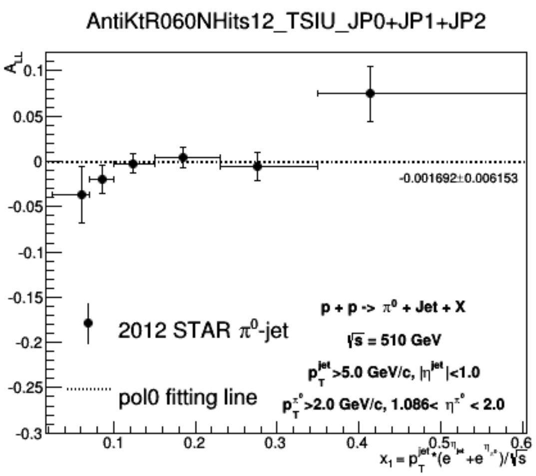


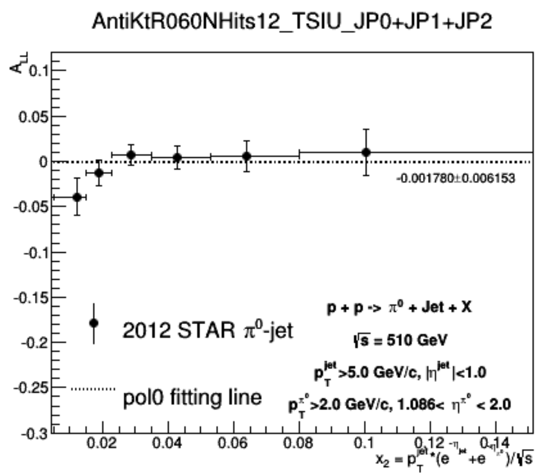


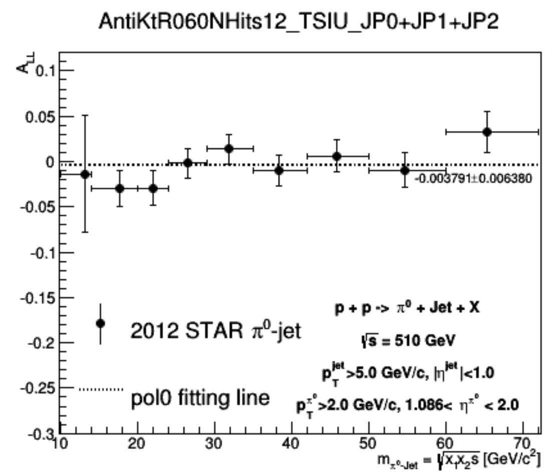

# Background Asymmetry Estimations – High mass region

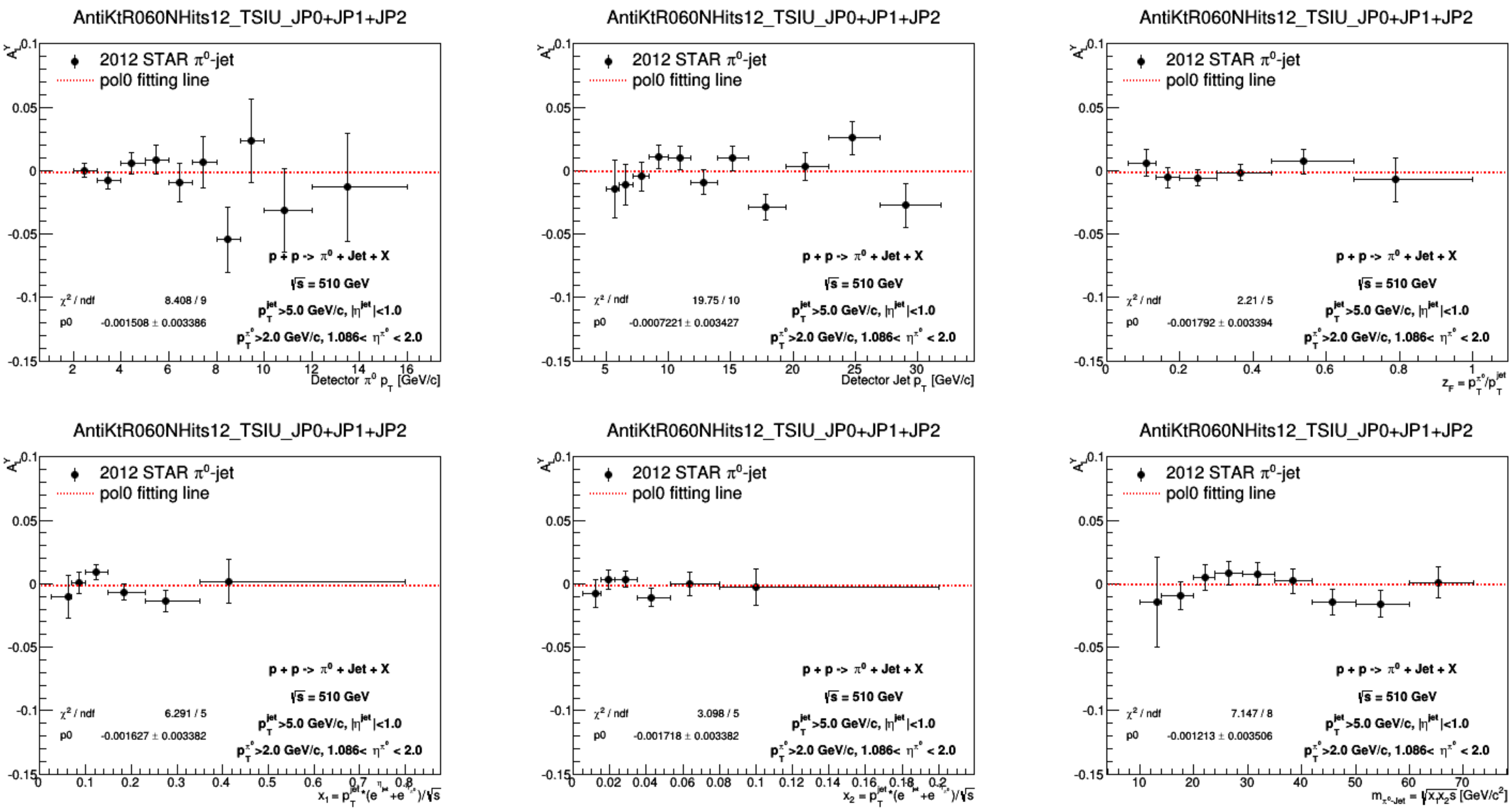

# Background Asymmetry Estimations – High mass region

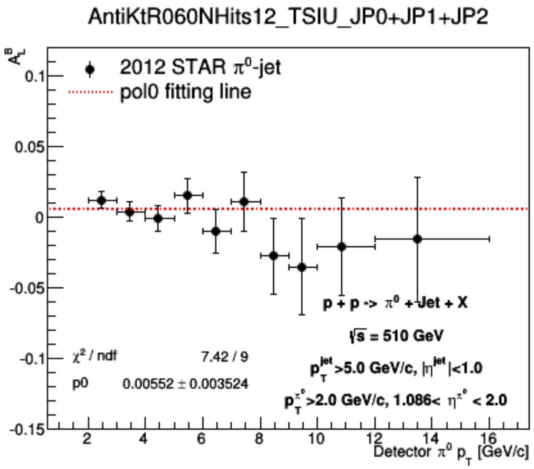


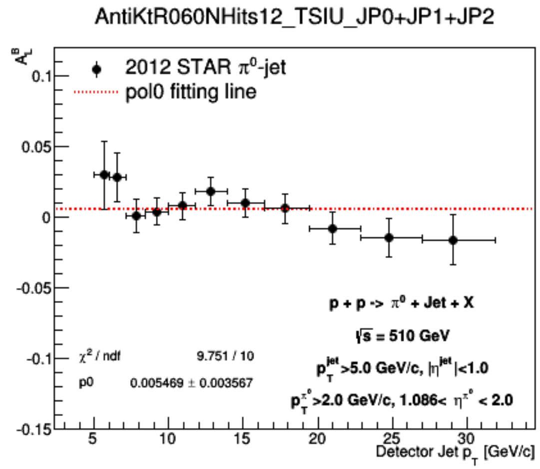


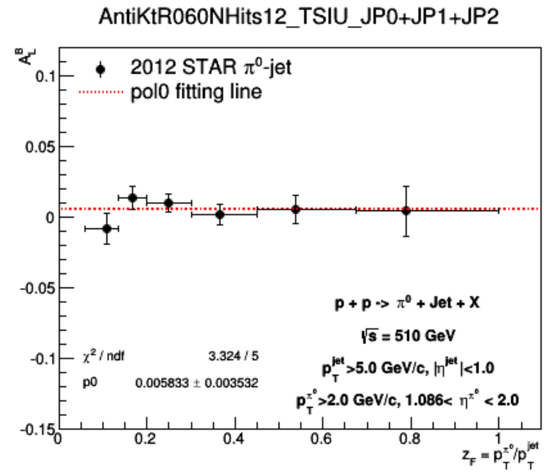


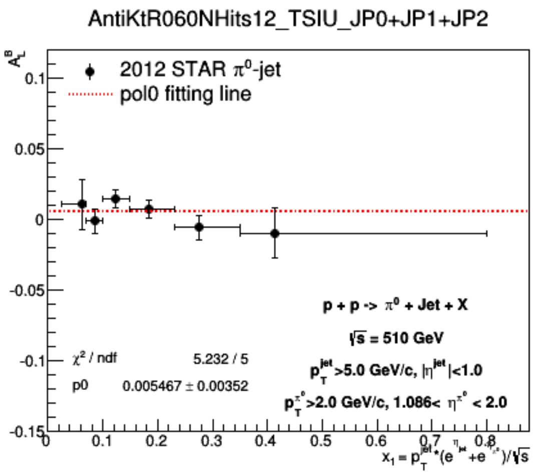


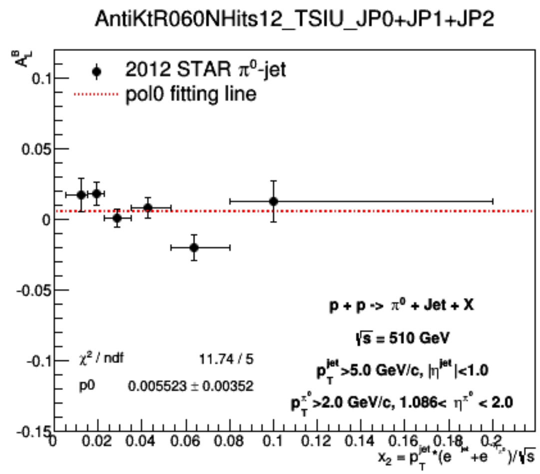


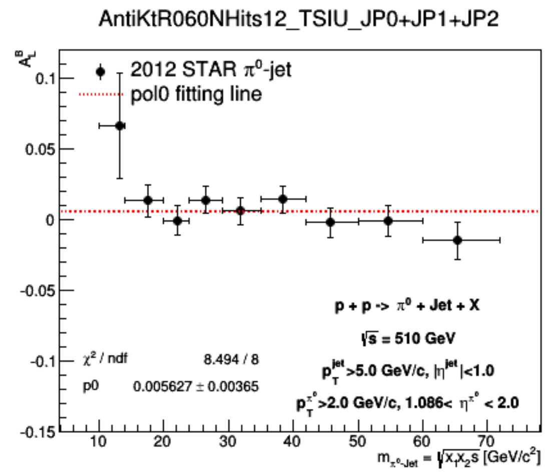

# Background Asymmetry Estimations – High mass region

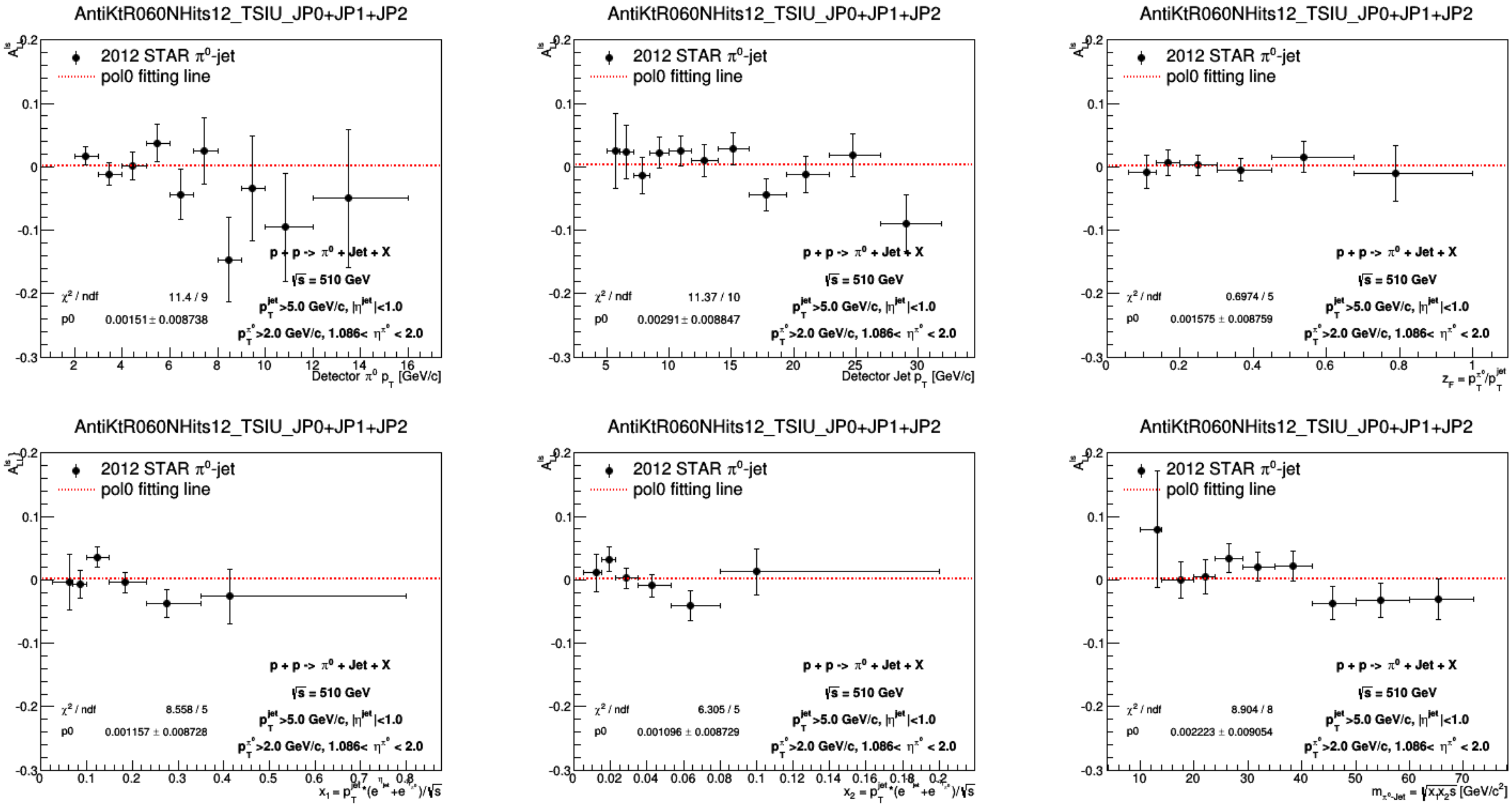

# Background Asymmetry Estimations – High mass region

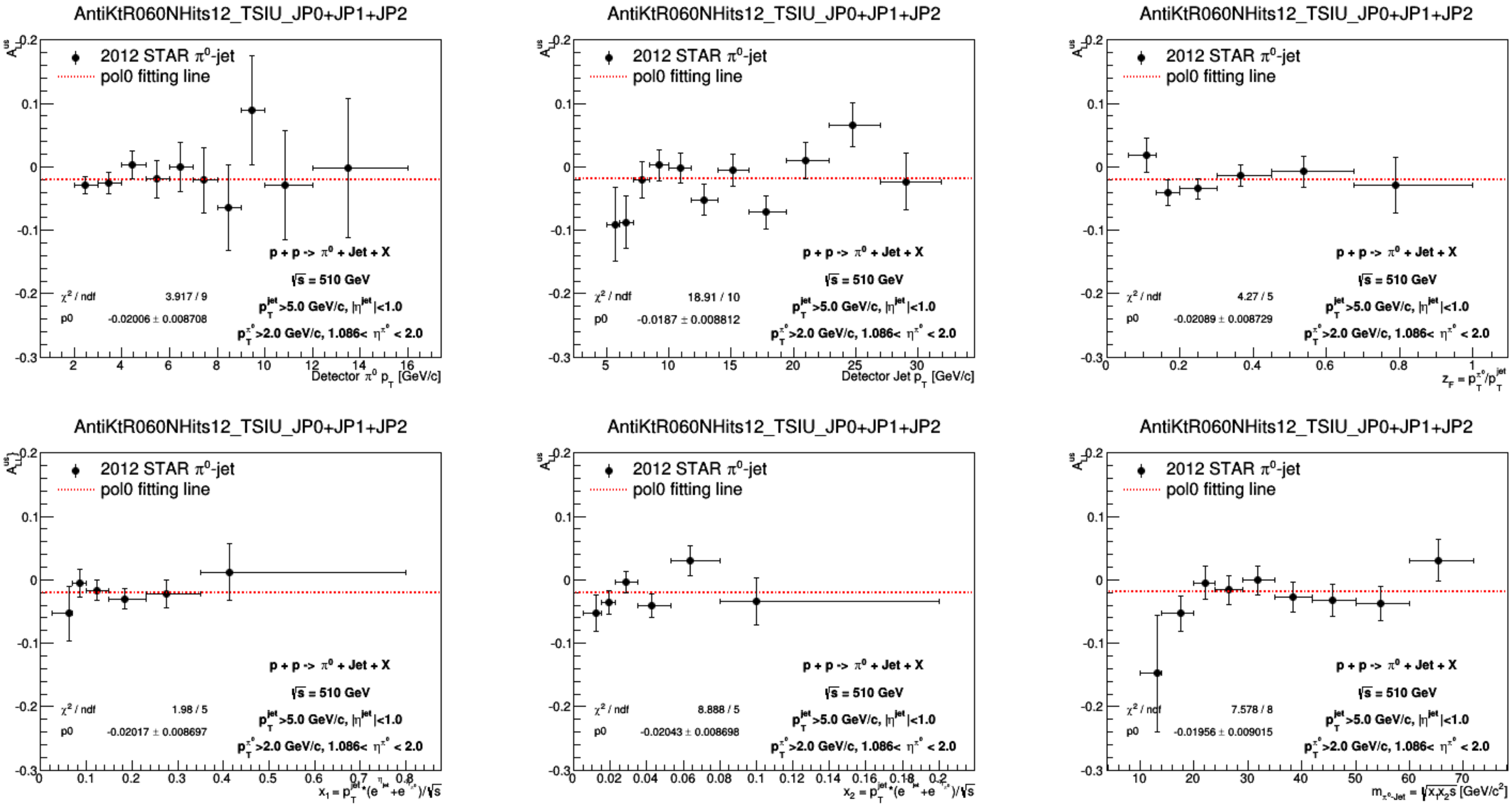

# Estimate signal fraction via sig.+bkg. fit -- $p_T^{\pi 0}$ bin

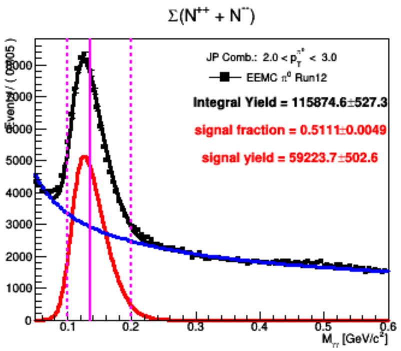


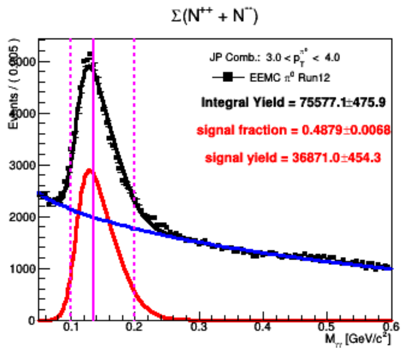


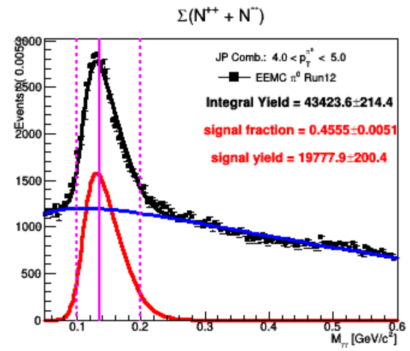


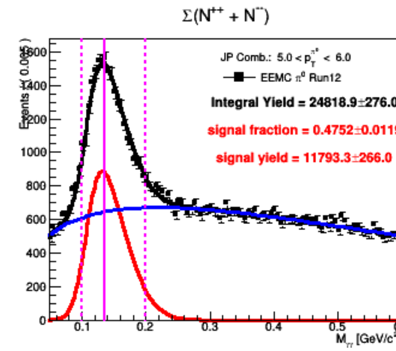


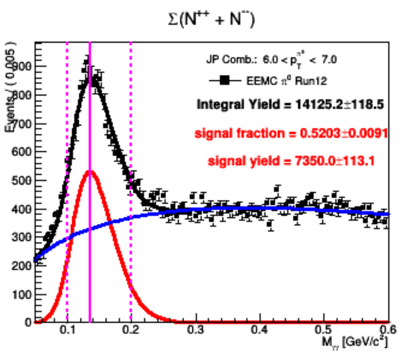


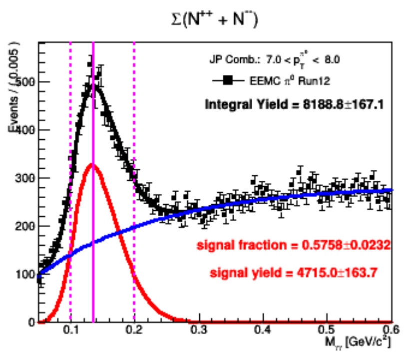


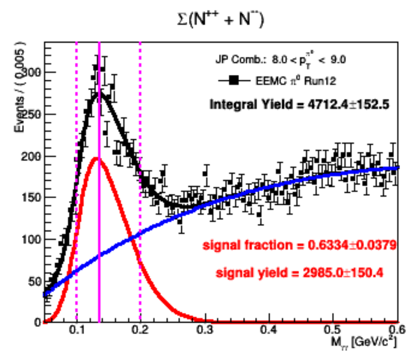


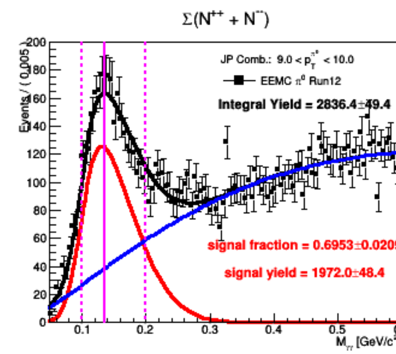


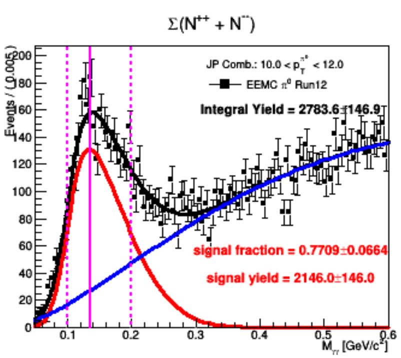


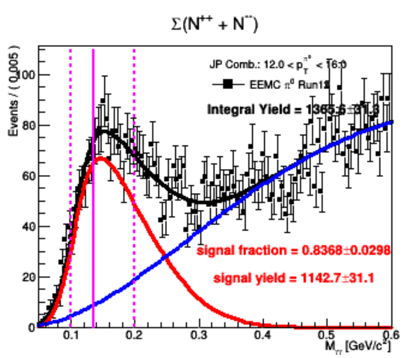


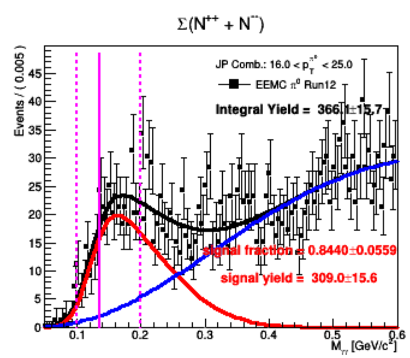


Signal: $k \times e^{\frac{-(x-\mu)^2}{2\sigma^2}} \times [1 + \mathrm{Erf}(\frac{a(x-\mu)}{\sqrt{2}\sigma})]$

Background: $A \times x^B \times e^{Cx}$

Raw Yield = Signal + Background

# Estimate $\pi^0$-jet signal fraction via sig.+bkg. fit -- $p_T^{\pi0}$ bin

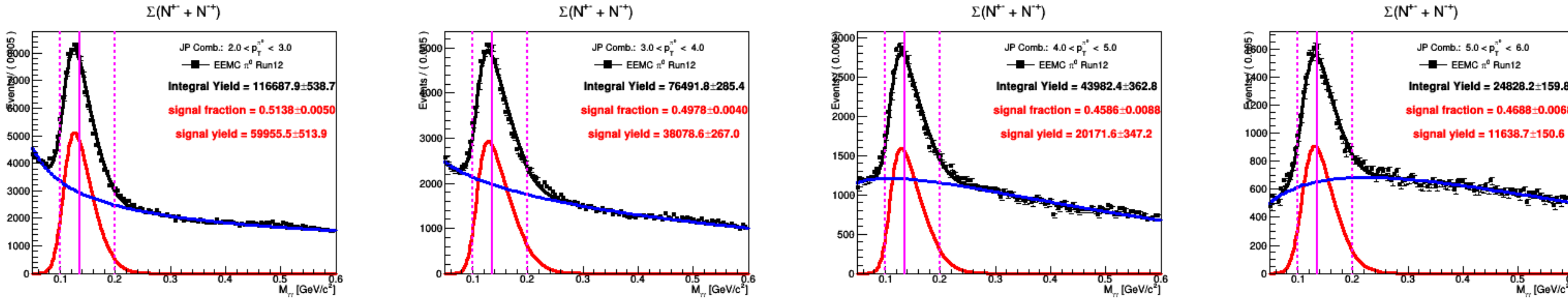


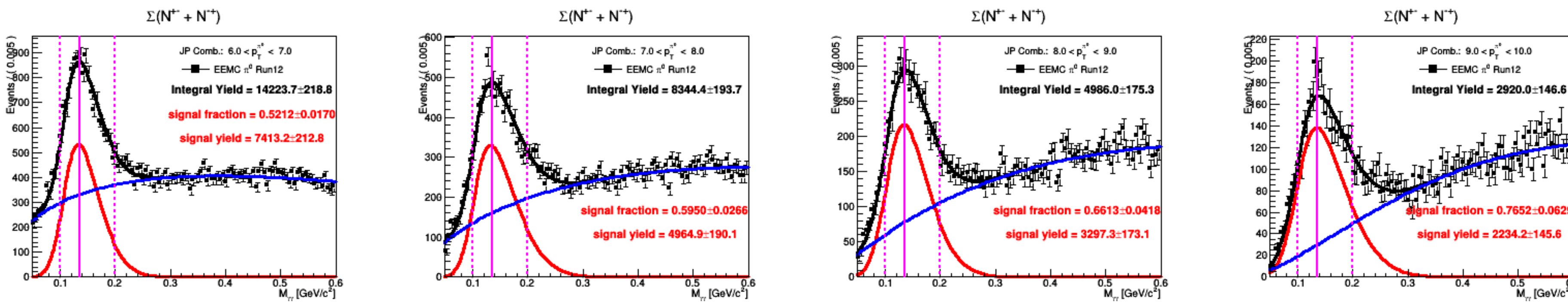


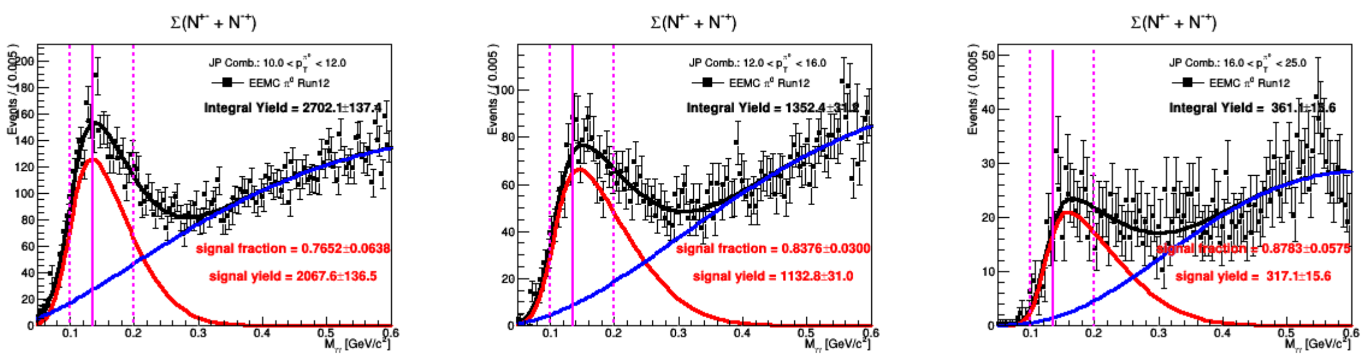


Signal: $k \times e^{\frac{-(x-\mu)^2}{2\sigma^2}} \times [1 + \mathrm{Erf}(\frac{a(x-\mu)}{\sqrt{2}\sigma})]$

Background: $A \times x^B \times e^{Cx}$

Raw Yield = Signal + Background

# Estimate $\pi^0$-jet signal fraction via sig.+bkg. fit -- $p_T^{\pi 0}$ bin

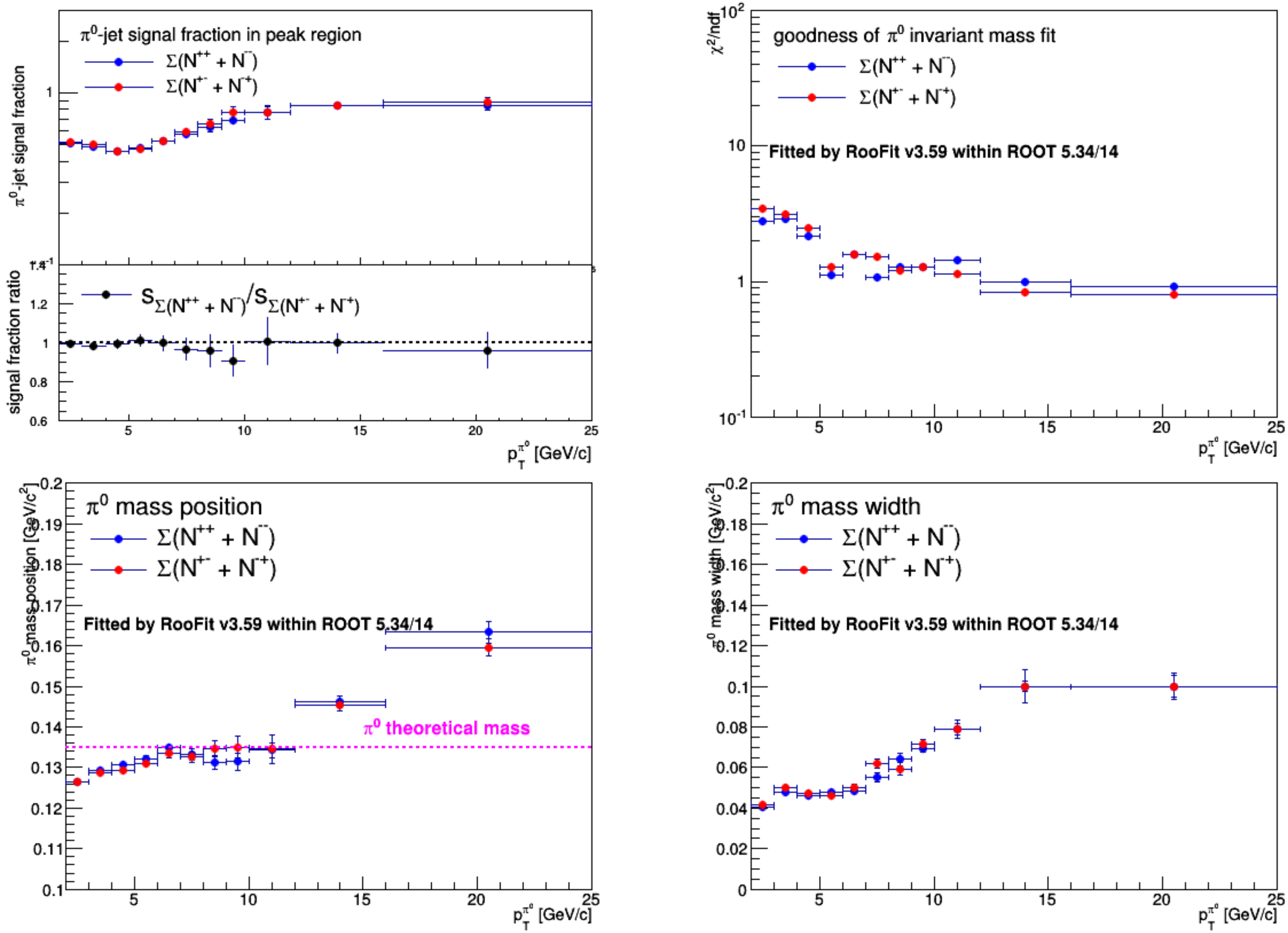

# Estimate $\pi^0$-jet signal fraction via sig.+bkg. fit -- $p_T^{jet}$ bin

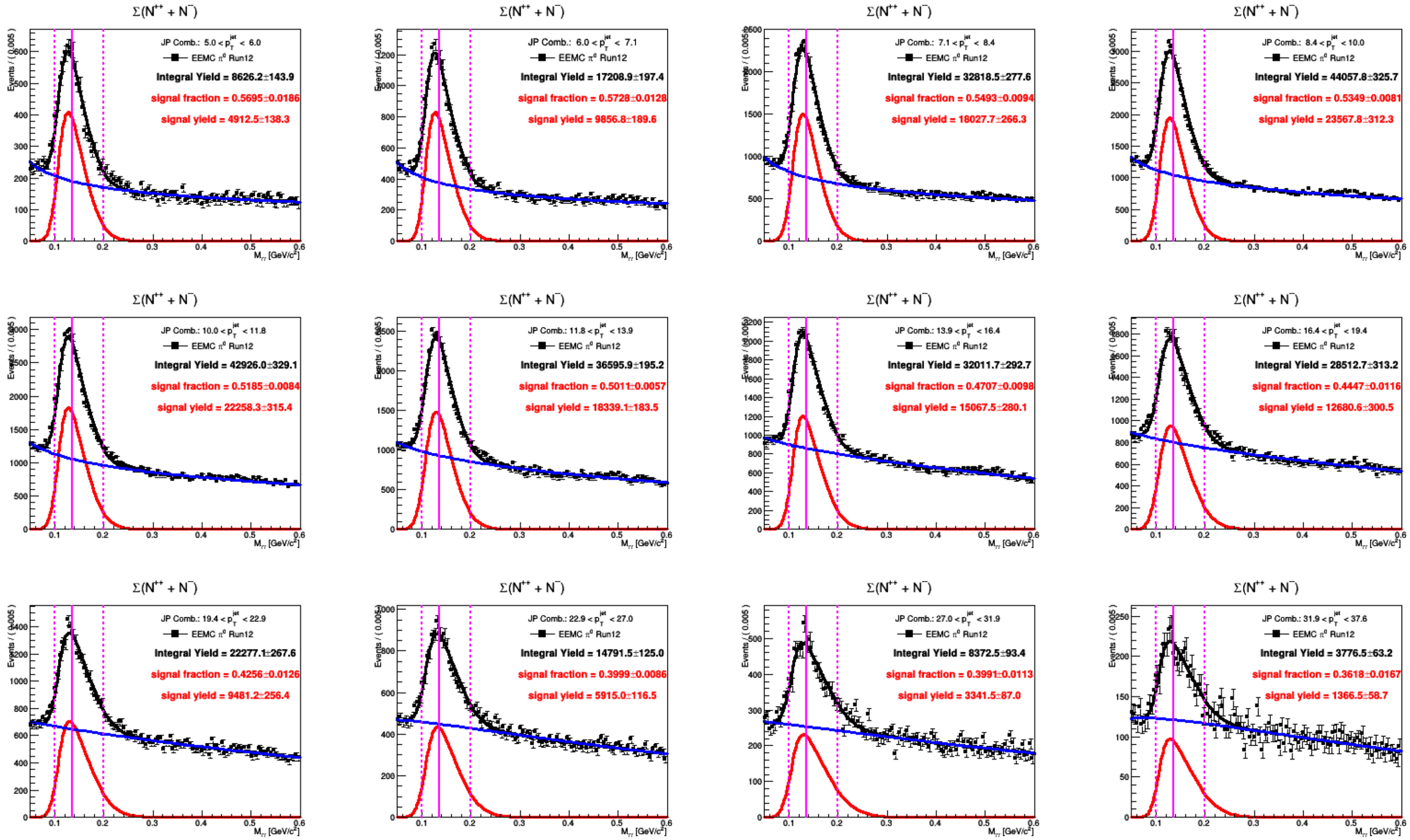


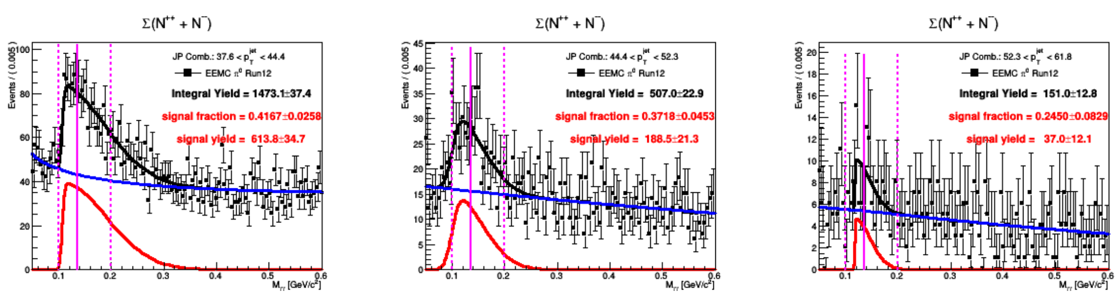


Signal: $k \times e^{\frac{-(x-\mu)^2}{2\sigma^2}} \times [1 + \mathrm{Erf}(\frac{a(x-\mu)}{\sqrt{2}\sigma})]$

Background: $A \times x^B \times e^{Cx}$

Raw Yield = Signal + Background

# Estimate $\pi^0$-jet signal fraction via sig.+bkg. fit -- $p_T^{jet}$ bin

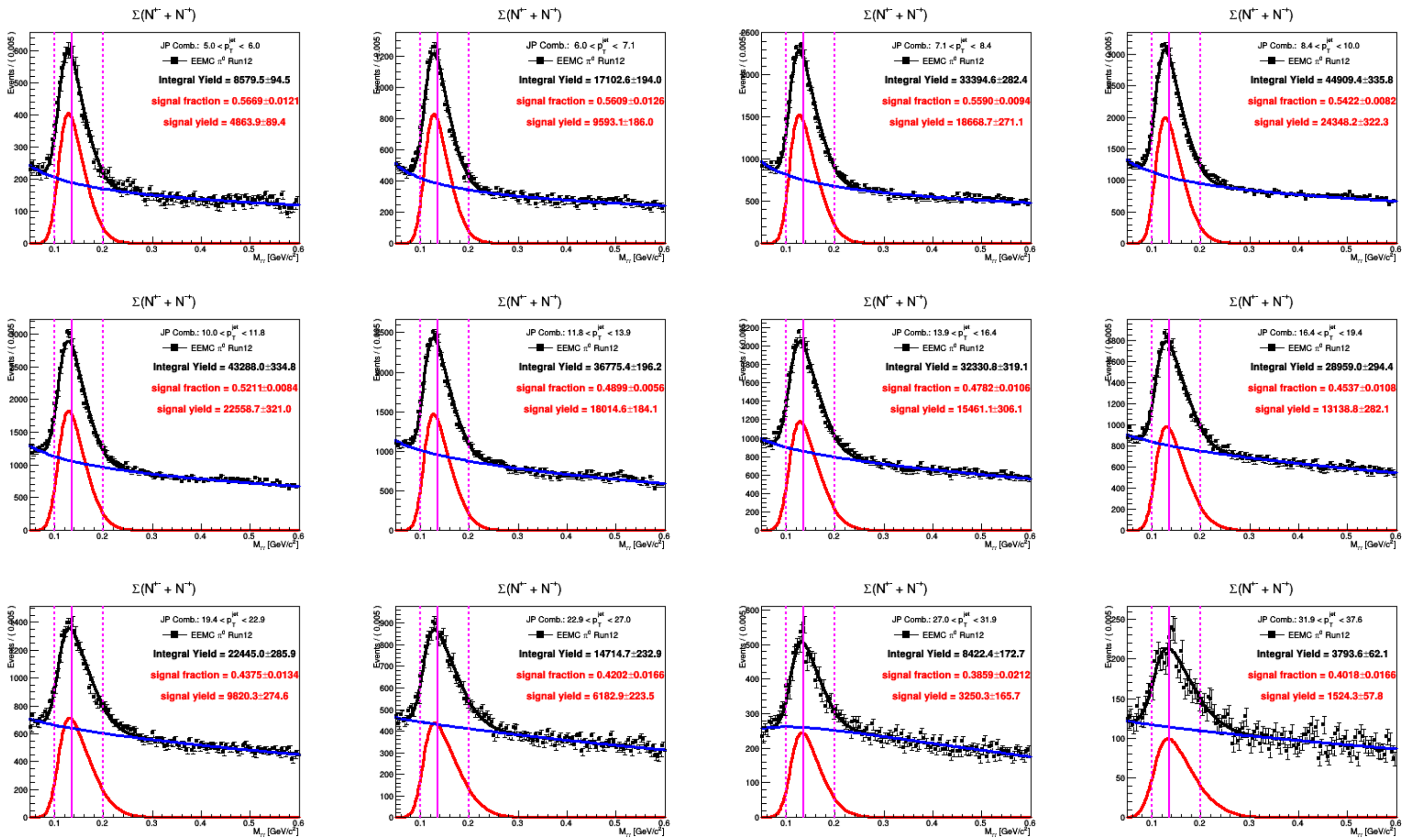


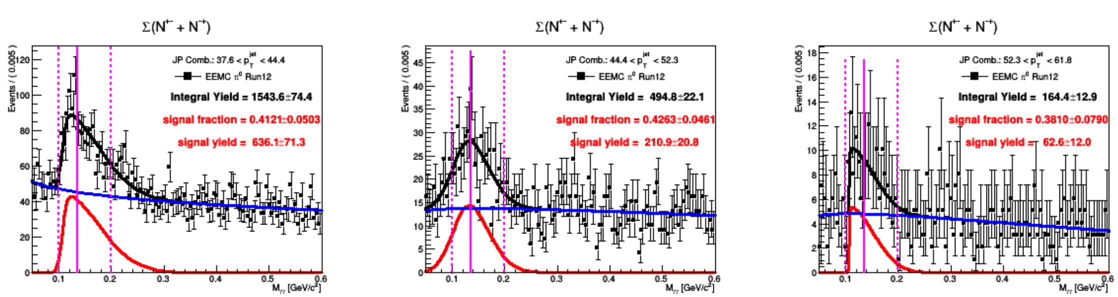


Signal: $k \times e^{-\frac{(x-\mu)^2}{2\sigma^2}} \times [1 + \mathrm{Erf}(\frac{a(x-\mu)}{\sqrt{2}\sigma})]$

Background: $A \times x^B \times e^{Cx}$

Raw Yield = Signal + Background

# Estimate $\pi^0$-jet signal fraction via sig.+bkg. fit -- $p_T^{jet}$ bin

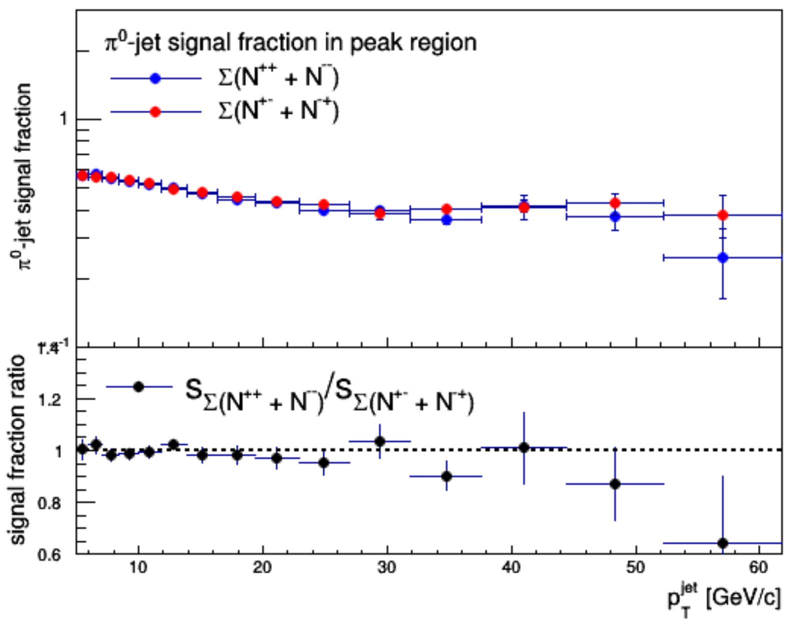


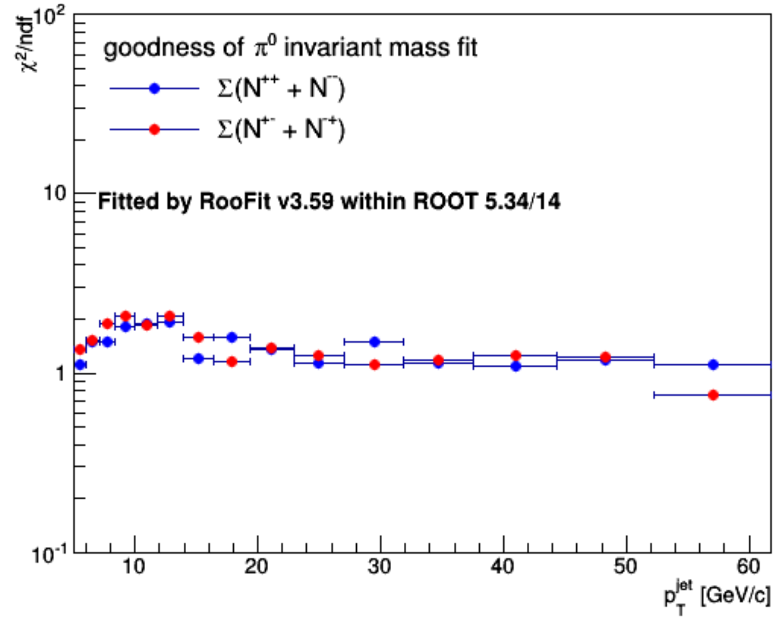


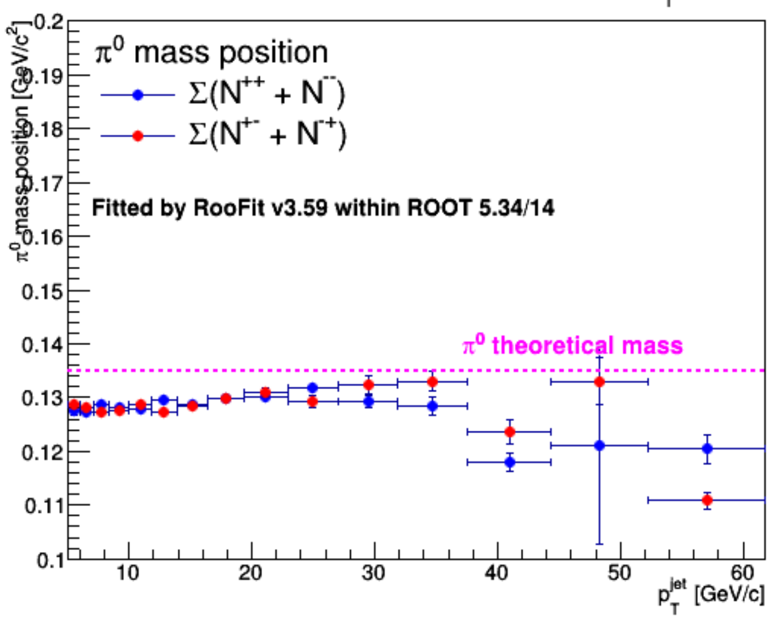


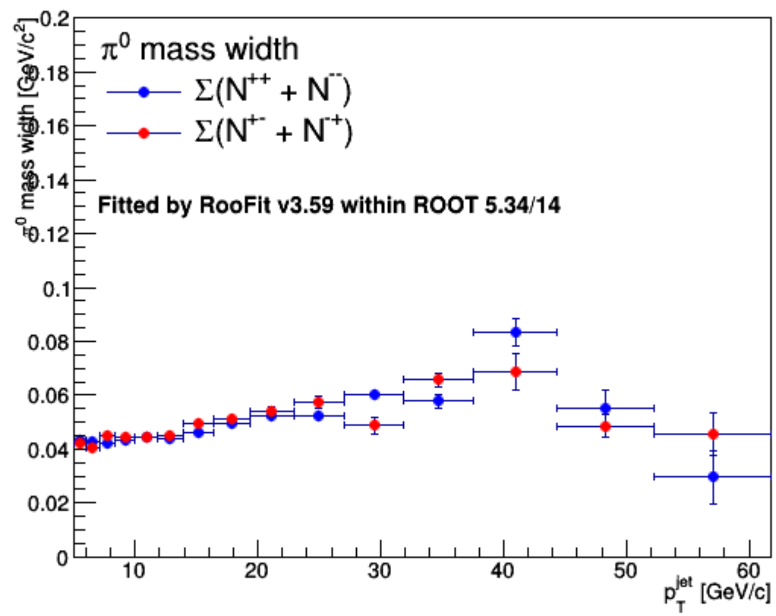

# Estimate $\pi^0$-jet signal fraction via sig.+bkg. fit -- $z_F$ bin

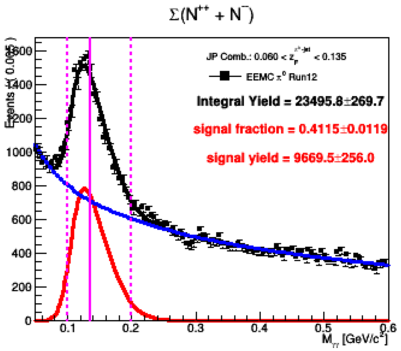


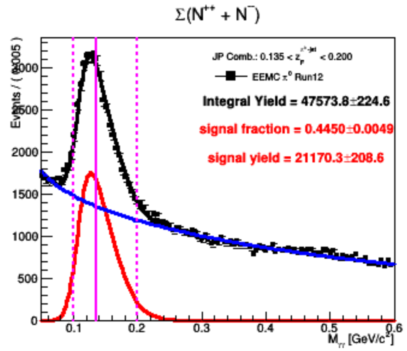


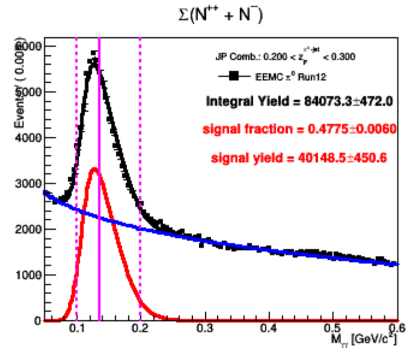


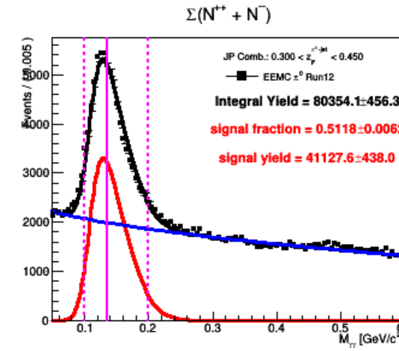


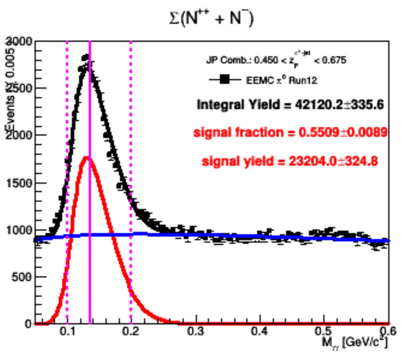


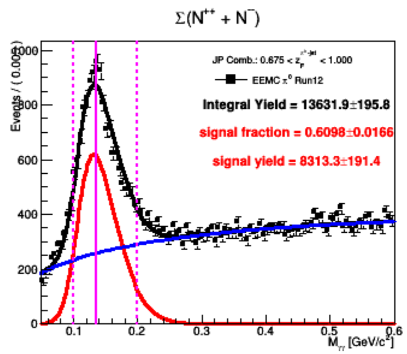


**Signal:** $k \times e^{\frac{-(x-\mu)^2}{2\sigma^2}} \times [1 + \mathrm{Erf}(\frac{a(x-\mu)}{\sqrt{2}\sigma})]$

**Background:** $A \times x^B \times e^{Cx}$

**Raw Yield = Signal + Background**

# Estimate $\pi^0$-jet signal fraction via sig.+bkg. fit -- $z_F$ bin

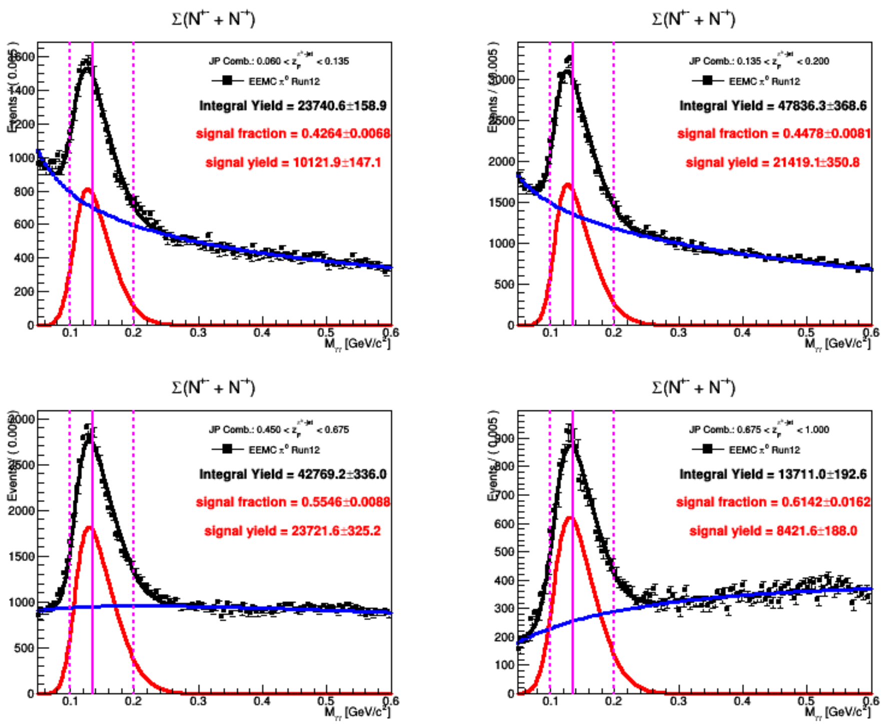


Signal: $k \times e^{\frac{-(x-\mu)^2}{2\sigma^2}} \times [1 + \mathrm{Erf}(\frac{a(x-\mu)}{\sqrt{2}\sigma})]$

Background: $A \times x^B \times e^{Cx}$

Raw Yield = Signal + Background

# Estimate $\pi^0$-jet signal fraction via sig.+bkg. fit -- $z_F$ bin

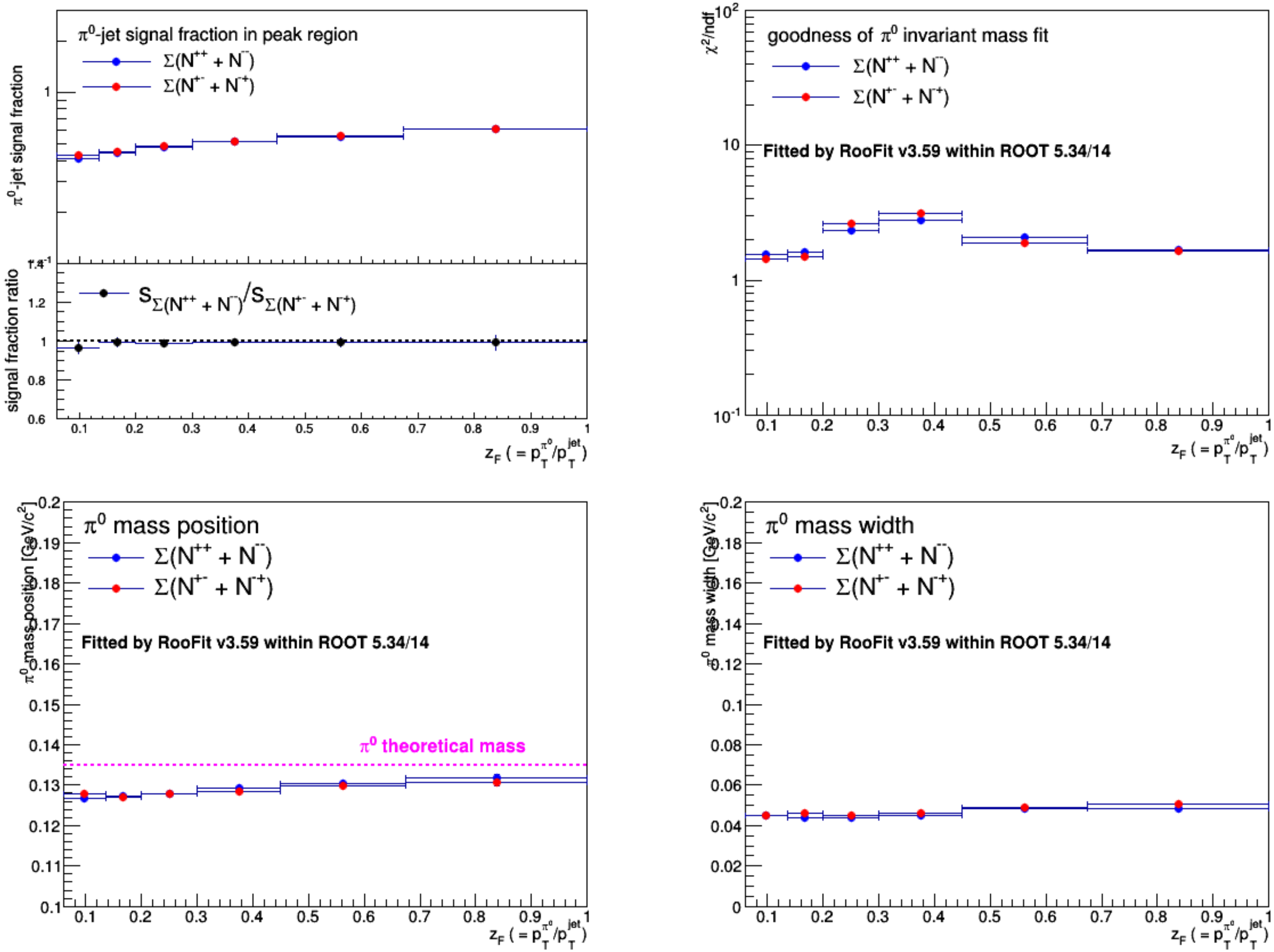

# Estimate $\pi^0$-jet signal fraction via sig.+bkg. fit -- $x_1$ bin

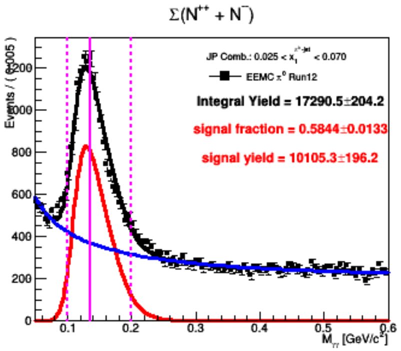


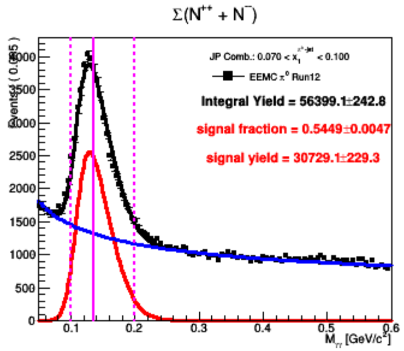


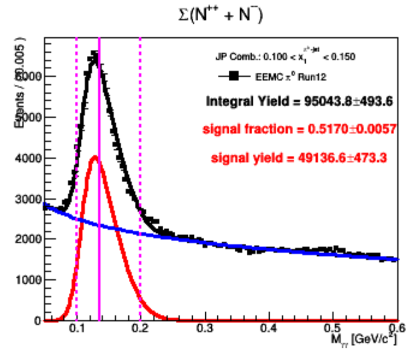


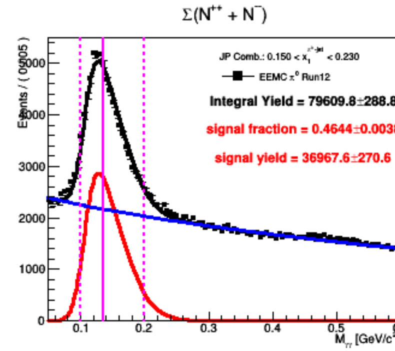


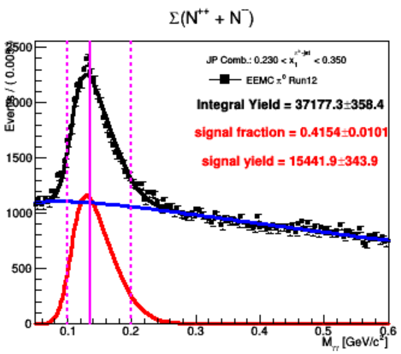


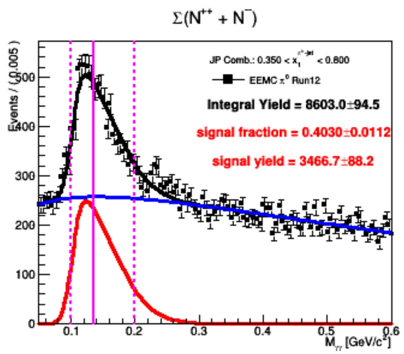


**Signal:** $k \times e^{\frac{-(x-\mu)^2}{2\sigma^2}} \times [1 + \mathrm{Erf}(\frac{a(x-\mu)}{\sqrt{2}\sigma})]$

**Background:** $A \times x^B \times e^{Cx}$

**Raw Yield = Signal + Background**

# Estimate $\pi^0$-jet signal fraction via sig.+bkg. fit -- $x_1$ bin

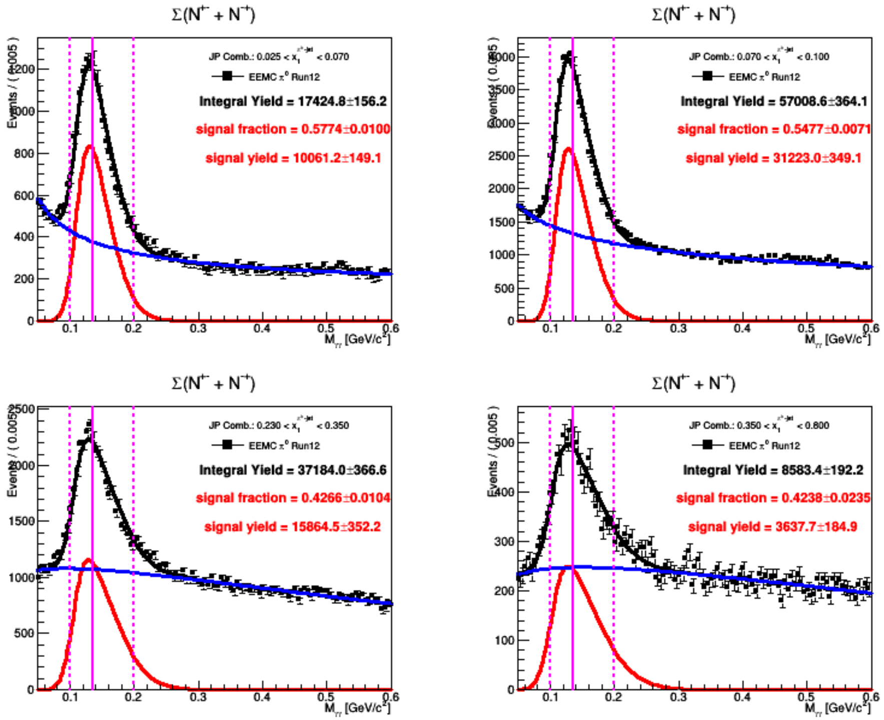


Signal: $k \times e^{\frac{-(x-\mu)^2}{2\sigma^2}} \times [1 + Erf(\frac{a(x-\mu)}{\sqrt{2}\sigma})]$

Background: $A \times x^B \times e^{Cx}$

Raw Yield = Signal + Background

# Estimate $\pi^0$-jet signal fraction via sig.+bkg. fit -- $x_1$ bin

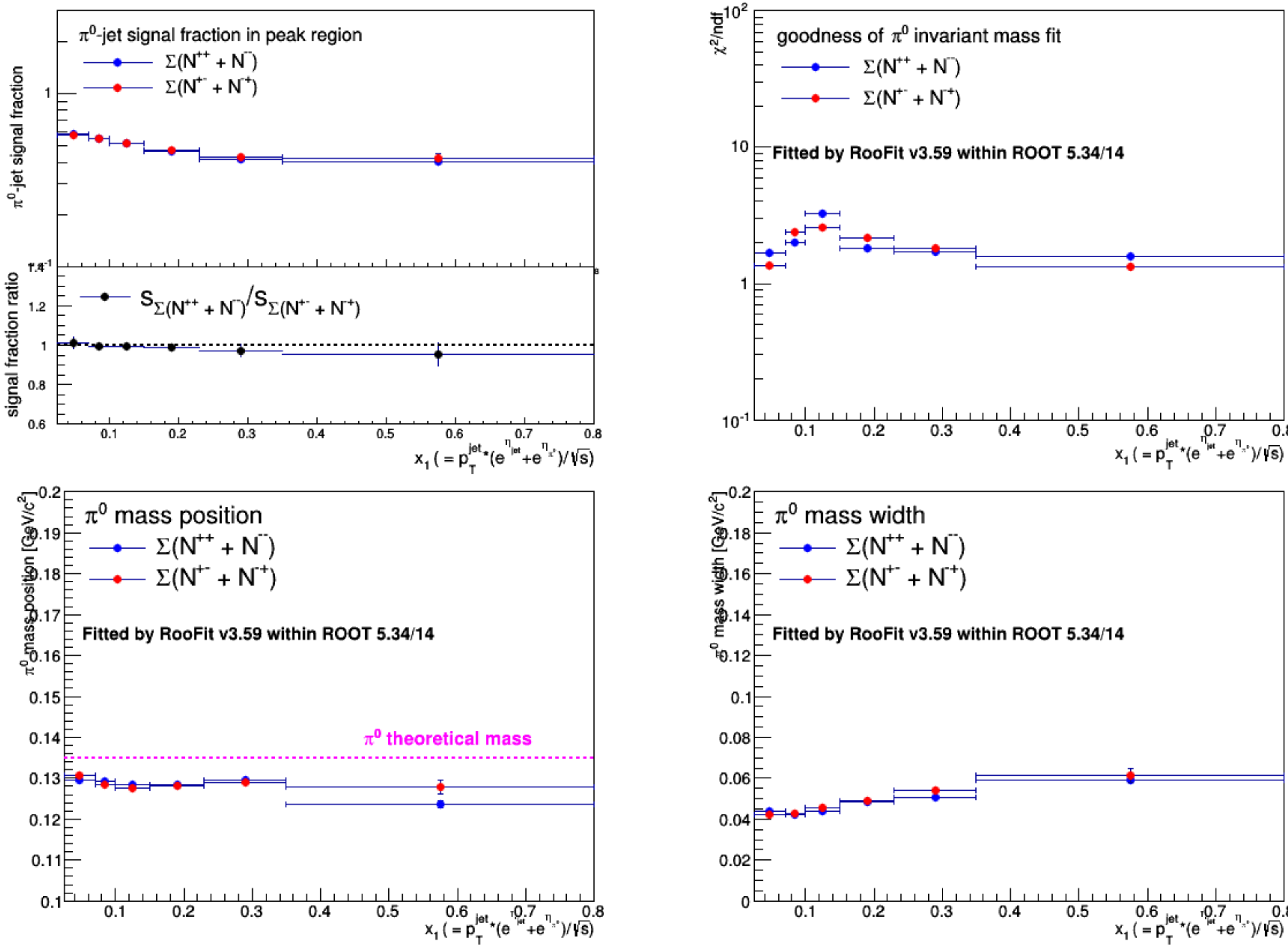

# Estimate $\pi^0$-jet signal fraction via sig.+bkg. fit -- $x_2$ bin

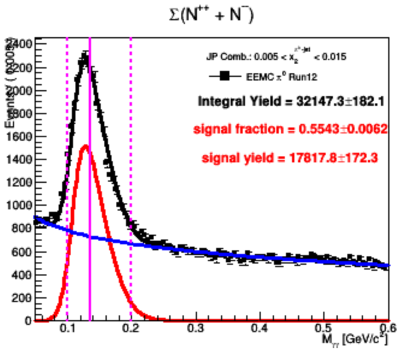


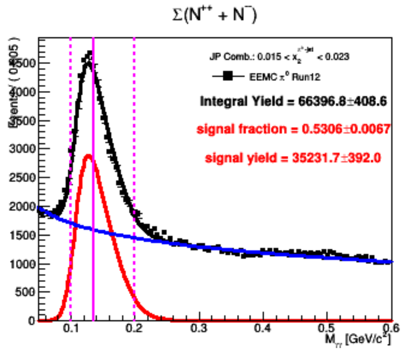


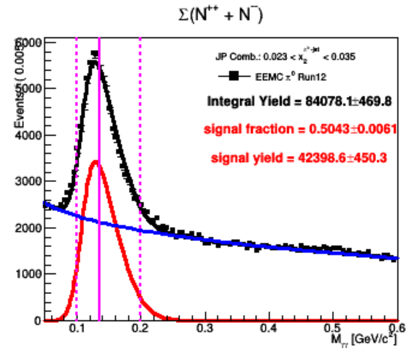


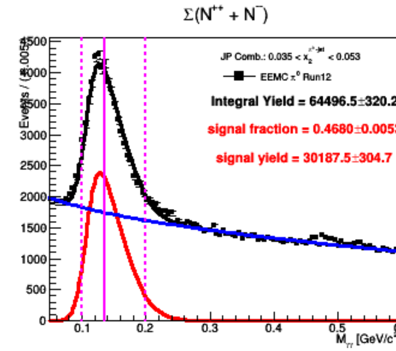


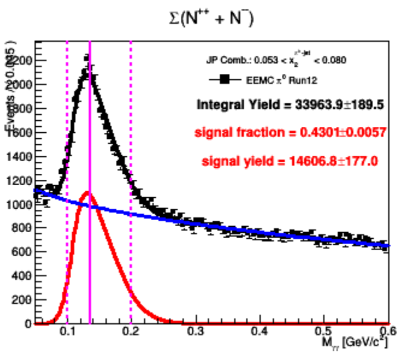


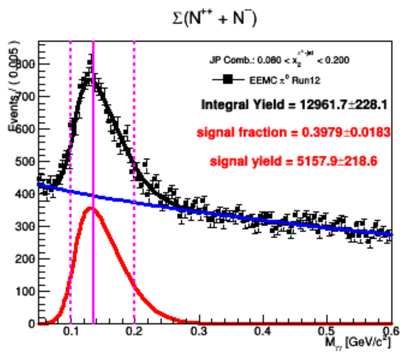


**Signal:** $k \times e^{\frac{-(x-\mu)^2}{2\sigma^2}} \times [1 + \mathrm{Erf}(\frac{a(x-\mu)}{\sqrt{2}\sigma})]$

**Background:** $A \times x^B \times e^{Cx}$

**Raw Yield = Signal + Background**

# Estimate $\pi^0$-jet signal fraction via sig.+bkg. fit -- $x_2$ bin

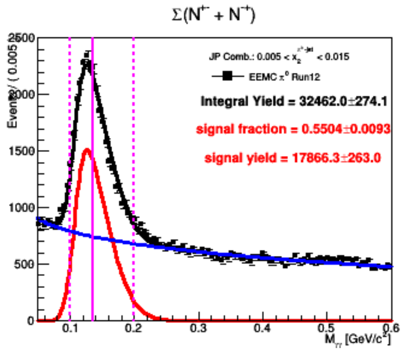


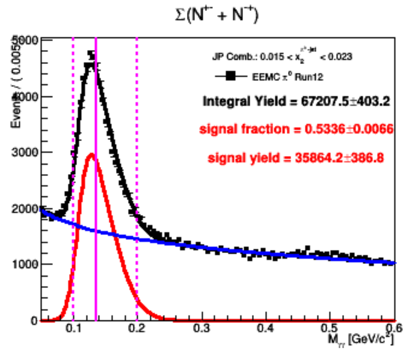


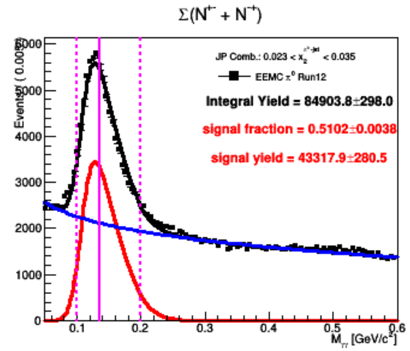


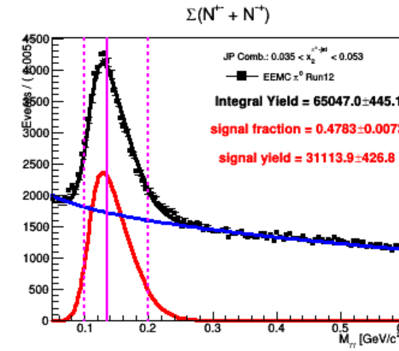


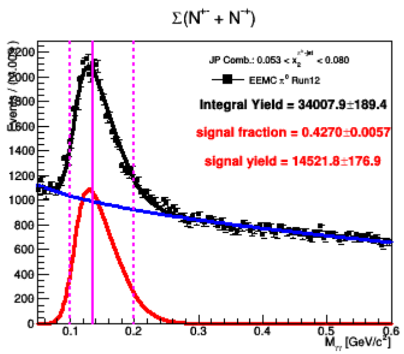


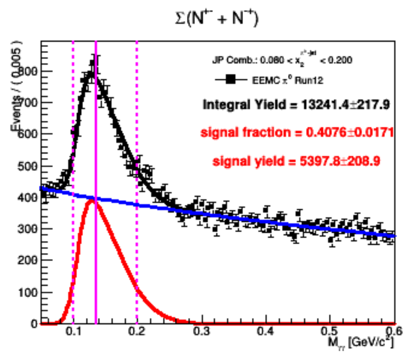


**Signal:** $k \times e^{\frac{-(x-\mu)^2}{2\sigma^2}} \times [1 + \mathrm{Erf}(\frac{a(x-\mu)}{\sqrt{2}\sigma})]$

**Background:** $A \times x^B \times e^{Cx}$

**Raw Yield = Signal + Background**

# Estimate $\pi^0$-jet signal fraction via sig.+bkg. fit -- $x_2$ bin

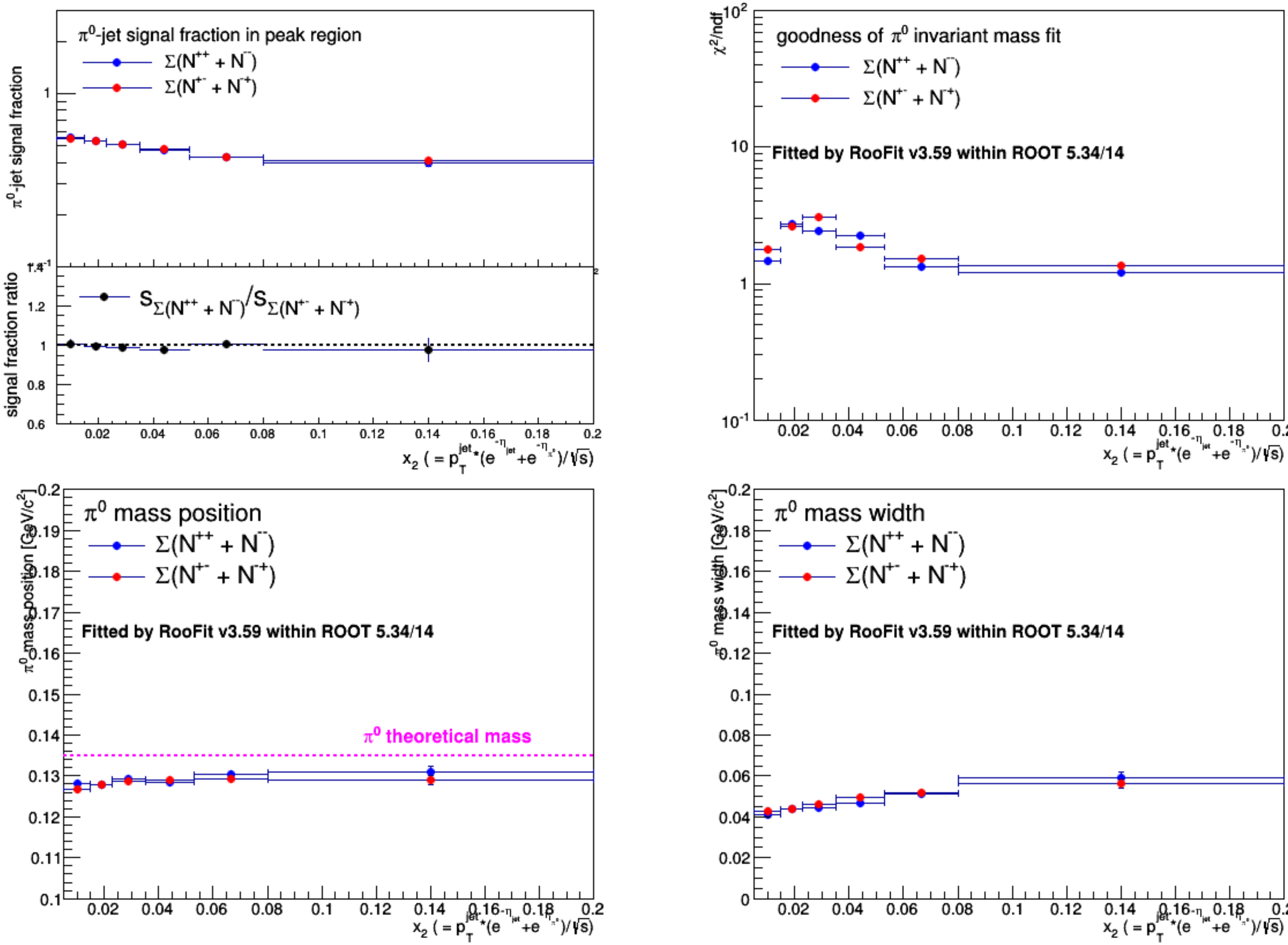

# Estimate $\pi^0$-jet signal fraction via sig.+bkg. fit -- invariant mass bin

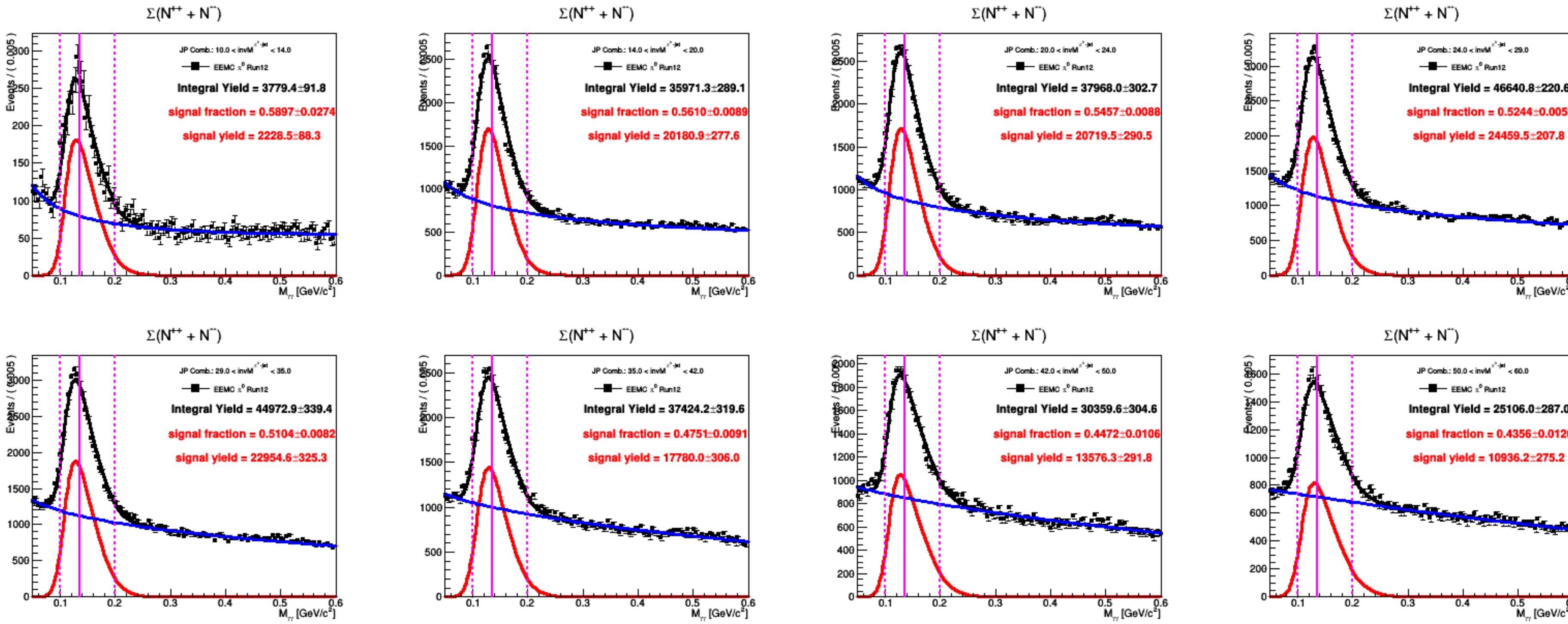


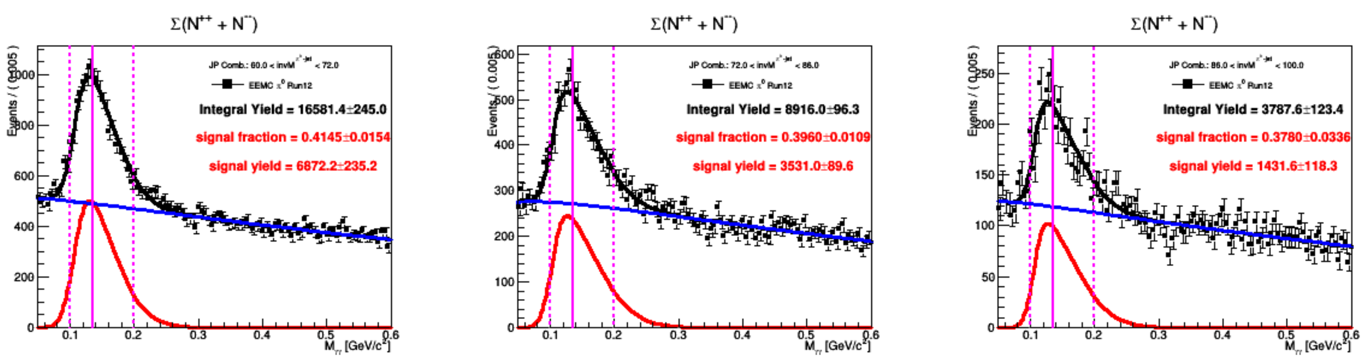


Signal: $k \times e^{\frac{-(x-\mu)^2}{2\sigma^2}} \times [1 + \mathrm{Erf}(\frac{a(x-\mu)}{\sqrt{2}\sigma})]$

Background: $A \times x^B \times e^{Cx}$

Raw Yield = Signal + Background

# Estimate $\pi^0$-jet signal fraction via sig.+bkg. fit -- invariant mass bin

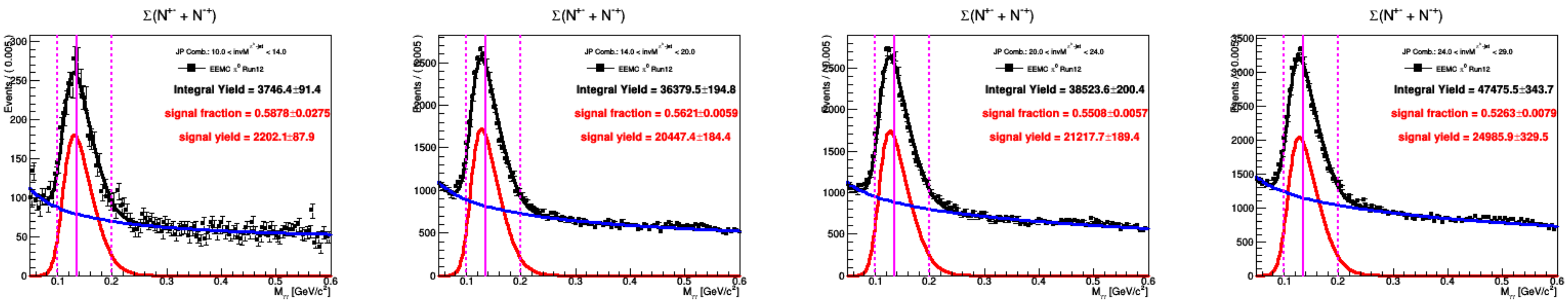


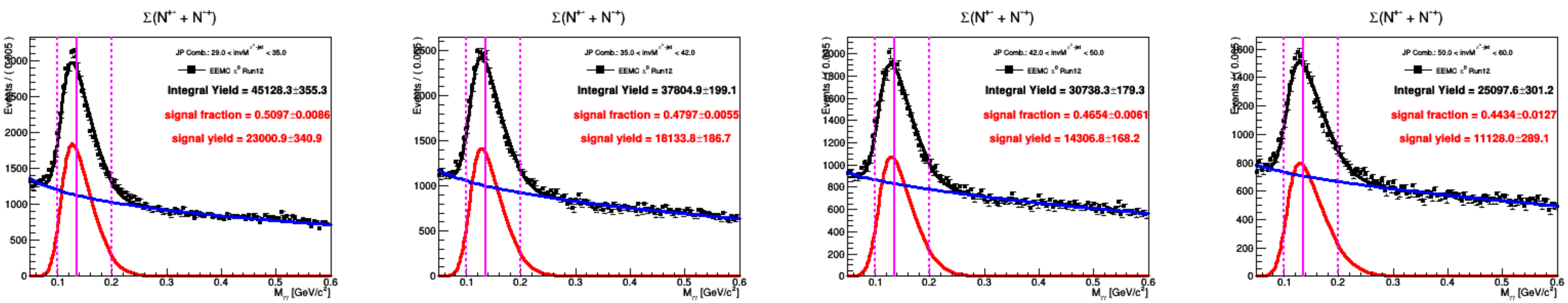


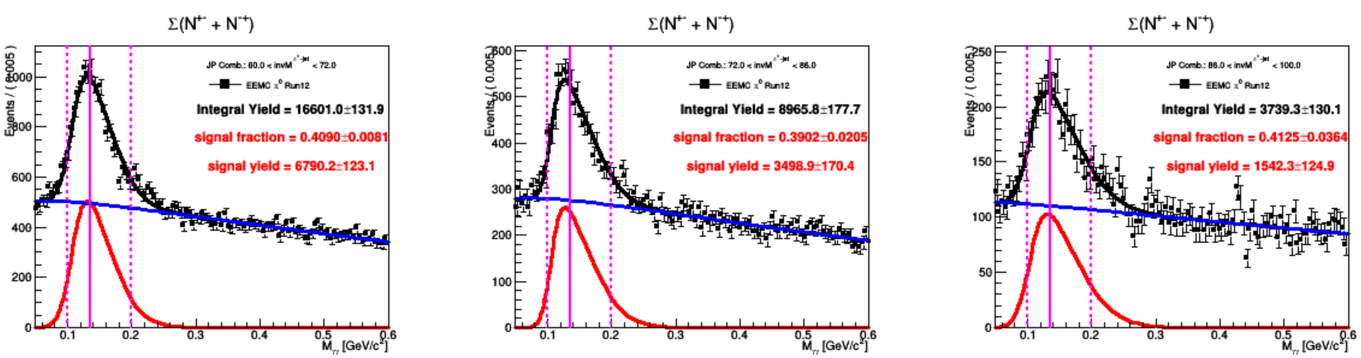


Signal: $k \times e^{\frac{-(x-\mu)^2}{2\sigma^2}} \times [1 + \mathrm{Erf}(\frac{a(x-\mu)}{\sqrt{2}\sigma})]$

Background: $A \times x^B \times e^{Cx}$

Raw Yield = Signal + Background

# Estimate $\pi^0$-jet signal fraction via sig.+bkg. fit -- invariant mass bin

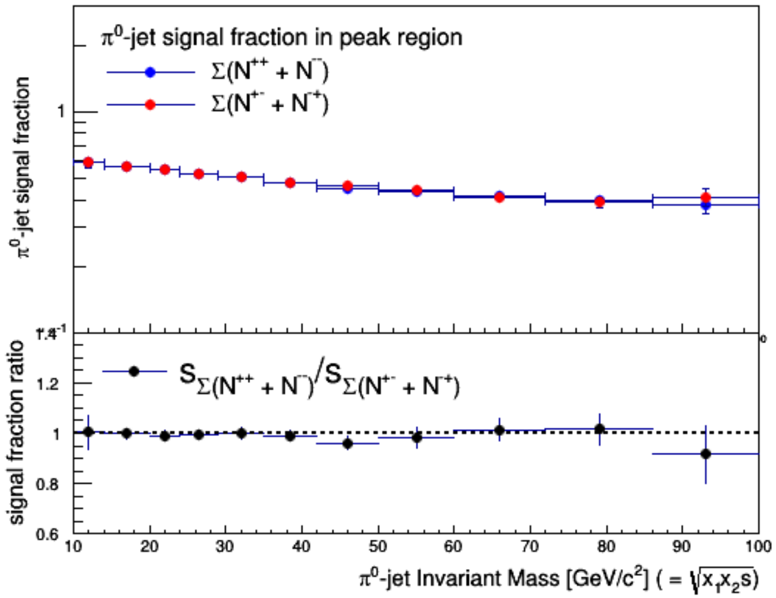


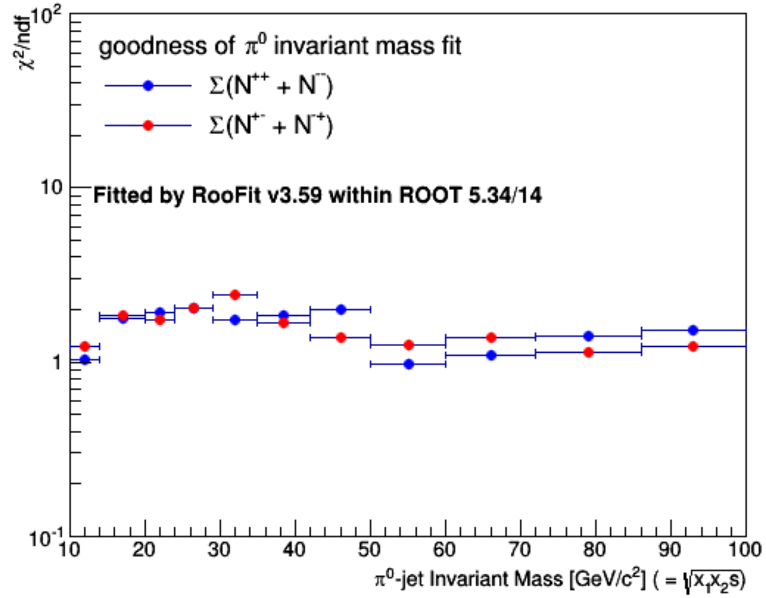


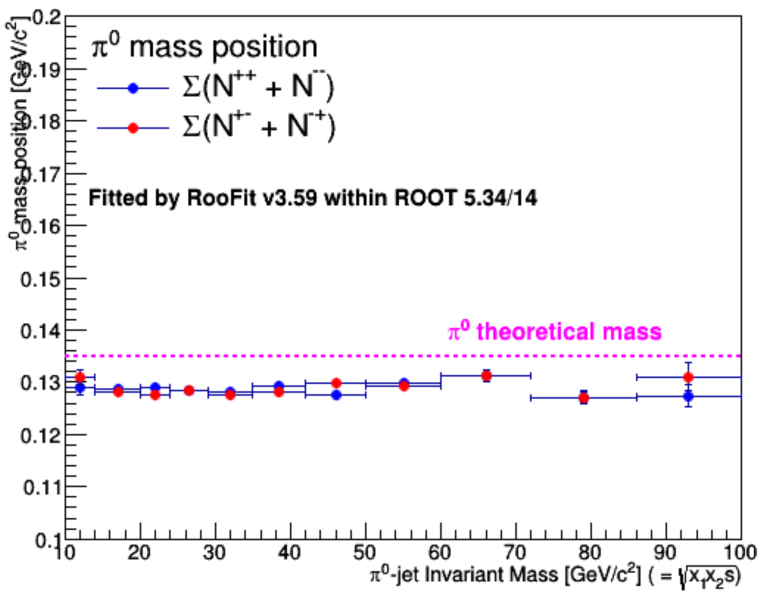


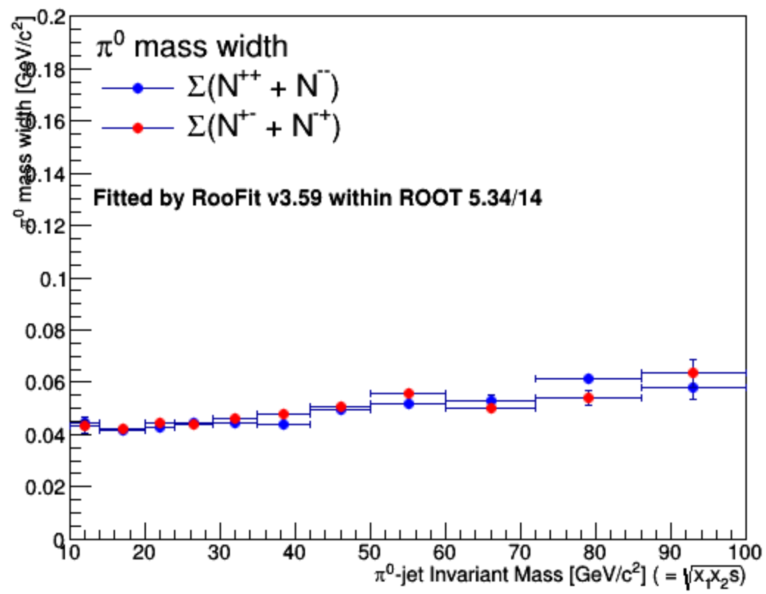

# Motivation – $\pi^0$-jet $A_{LL}$ measurements

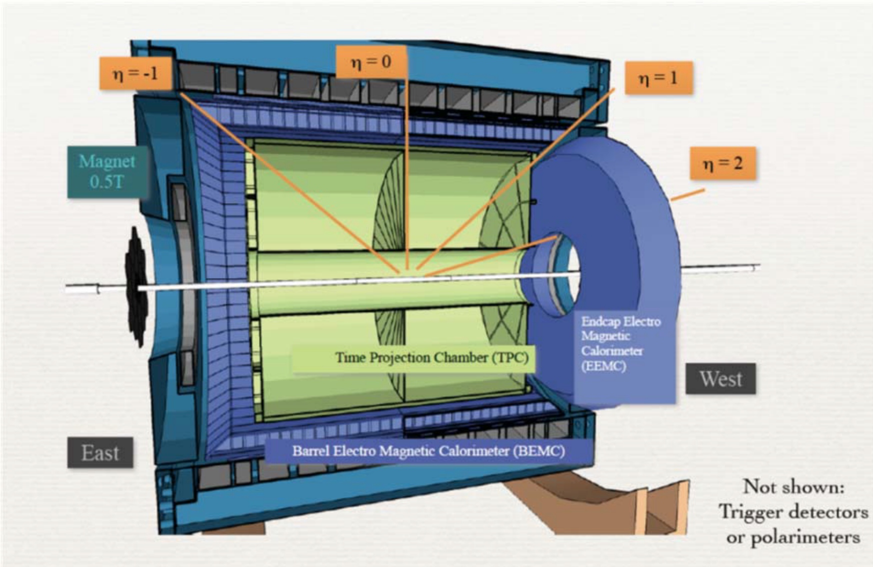


Compared to the di-jet correlation measurements, the forward $\pi^0$ – barrel jet coincidence measurements have benefit of extending into the forward region ($1.08 < \eta_{det} < 2.0$ with EEMC coverage).

This extension covers a wider cosθ, and therefore can probe Δg(x) over a wider x range.

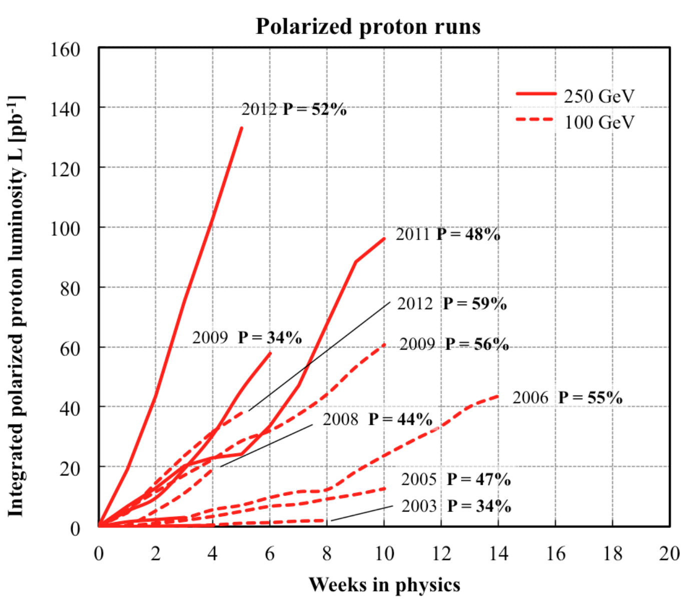


## $\pi^0$-jet coincidence event:

anti-kT jet finding algorithm
Jet: barrel region (BEMC+TPC), JP0/JP1/JP2 trigger

TSIU $\pi^0$ reconstruction algorithm
$\pi^0$: forward region (EEMC), JP0/JP1/JP2 trigger

$\pi^0$ and jet are restricted to back-to-back with $|\Delta\phi| > 2.0$

Statistics enough? The Run 12 data would be OK.

# Asymmetry Analysis -- Variable definitions

$A_{\mathrm{LL}}$ was measured as a function of jet or $\pi^0$ $p_{\mathrm{T}}$.
To better determine $\Delta$g, $A_{\mathrm{LL}}$ as a function of x, z or invariant mass $M$ are used.

**Variable definitions:**

$$z = \frac{p_T^{\pi^0}}{p_T^{jet}},$$

$$x_1 = \frac{p_T^{jet}}{\sqrt{s}}\left(e^{\eta_{jet}} + e^{\eta_{\pi^0}}\right), \quad x_2 = \frac{p_T^{jet}}{\sqrt{s}}\left(e^{-\eta_{jet}} + e^{-\eta_{\pi^0}}\right)$$

$$invM_{\pi^0-jet} = \sqrt{x_1 x_2 s}.$$

Pythia simulation: sub-process fraction as a function of $p_{\mathrm{T}}$ and z:

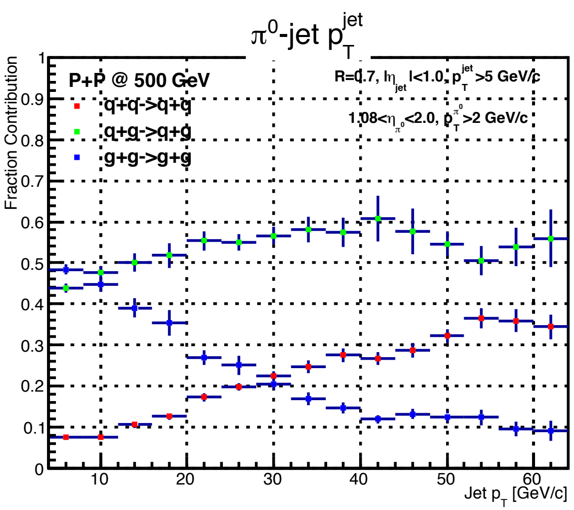


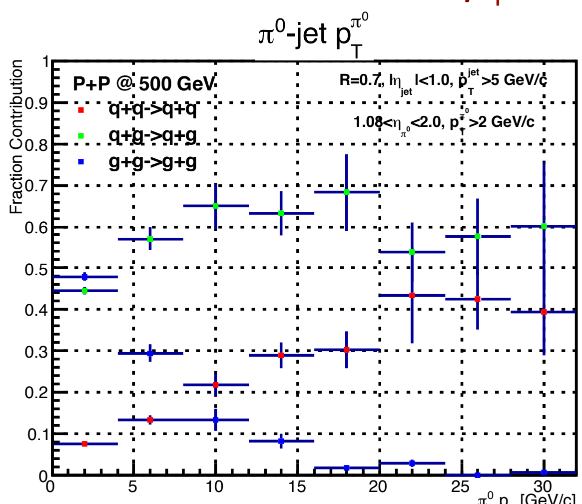


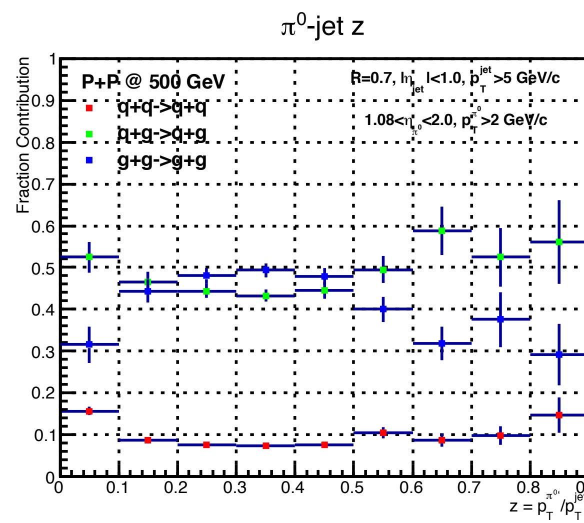

# Asymmetry Analysis -- Variable definitions

## Pythia simulation: kinematic region

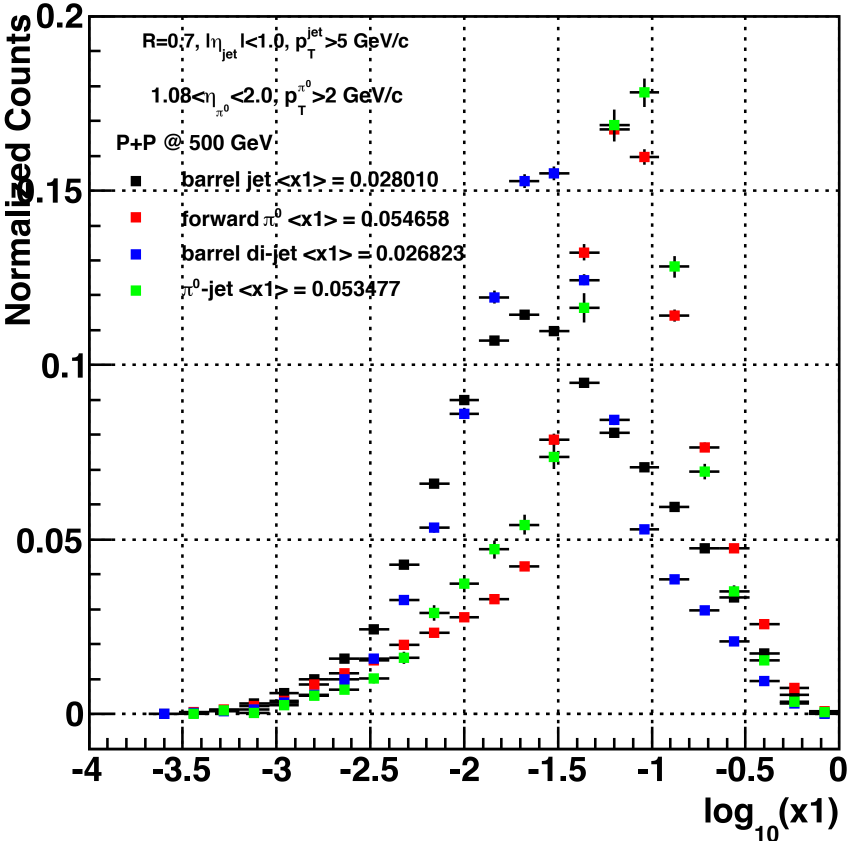


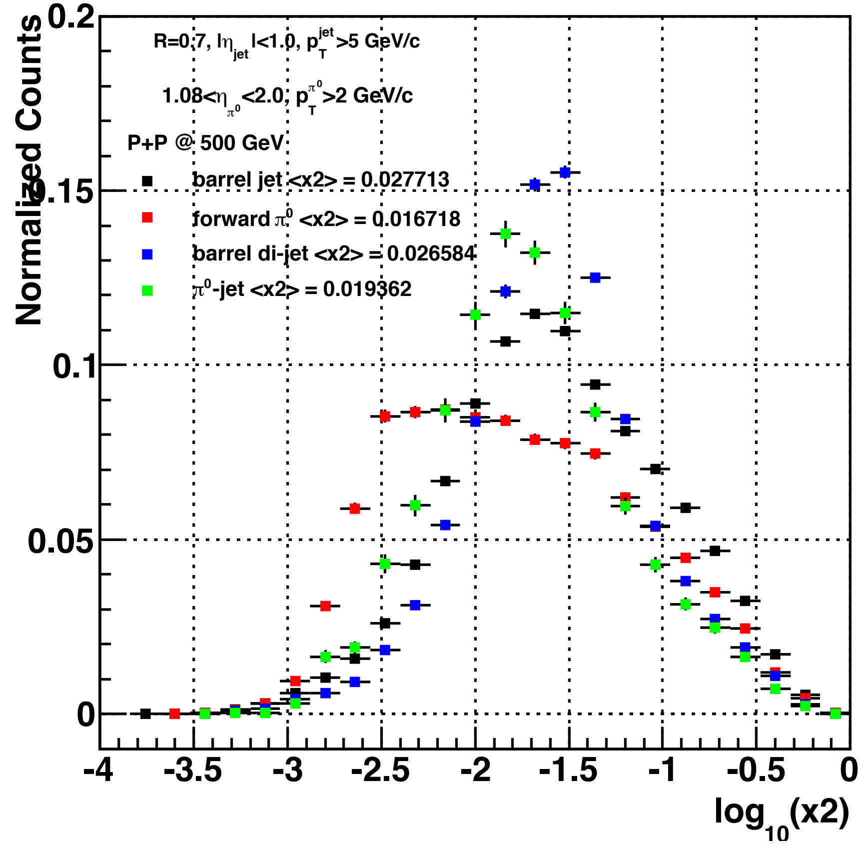


The average $x_2$ (~ 0.019) of the $\pi^0$-jet coincidence measurements is smaller than the one (~ 0.027) of the di-jet measurements as expected.

All the above $x_1$ and $x_2$ distributions are scaled to 1.0 for comparison.

# Asymmetry Analysis -- Run list from Zilong

Ratio of JP0/JP1/JP2 triggered $\pi^0$-jet event to the total analyzed events (~174M events):